INTERACTION OF WATER WITH MALTODEXTRINS AND LACTOSE

Ajay Shah

A thesis submitted to the University of London in fulfilment of the Degree of Doctor of Philosophy

Department of Pharmaceutics, The School of Pharmacy,
29/39 Brunswick Square, London WC1N 1AX

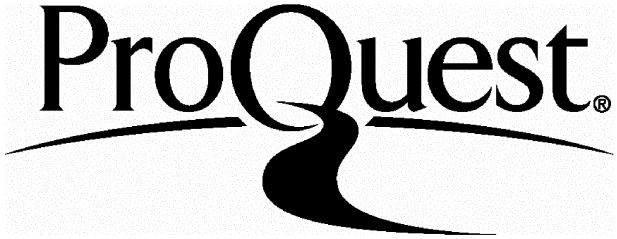

ABSTRACT

The effect of drying on the introduction of amorphous material was investigated using lactose as a model substance. It was found that microwave-vacuum drying of lactose monohydrate and fluid-bed drying of commercial spray-dried lactose did not introduce detectable amounts of amorphous material in to the sample.

The interaction of water with maltodextrins was then investigated. It was found that the maltodextrins undergo a change in physical form from a free-flowing powder through a hard, caked material to a sticky, plasticised material on moisture sorption. It was shown that this change in physical form for the maltodextrins is due to a 'humidity caking mechanism'. Microcalorimetry is able to detect the changes in physical form through broad shoulders/peaks. It was suggested that the broad shoulders/peaks are due to differences in the heat capacity of the materials brought on by water uptake. Following exposure to 75% RH in the DVS, it was found that M150 and M200 were present in a collapsed amorphous state, whereas M040, M100, and M500 were in a non-collapsed amorphous state. Shrinkage of M200 was observed by microscopy further indicating collapse.

A thermodynamic study of the maltodextrin-water interaction found that water sorption in to the maltodextrins occurs in three stages. The first stage involves water that is hydrogen bonded directly to the anhydroglucose units, with a ratio of one water molecule to two anhydroglucose units. This is followed by breaking of some of the original hydrogen bonds and sorption of further water. The final stage results from the changes in physical form occurring in line with the humidity caking mechanism. BET monolayer values were calculated for the maltodextrins. It was found that the "monolayer values" represent the amount of water that is directly bound to the anhydroglucose units. Swelling was also found to occur up to the "monolayer value".

ACKNOWLEDGEMENTS

I would like to acknowledge my supervisor Professor G Buckton for his advice and support during the course of the project, and especially during the more difficult times encountered during the course. I would like to thank Dr S Booth from MSD for his valuable contributions during the regular meetings held.

I would like to thank EPSRC and MSD for funding of the project, and Aeromatic-Fielder Ltd for allowing use of their equipment.

I would like to thank Manuel and Roy for their help and discussions. I would also like to thank Keith, John, and Helen from the department and Dave from the microscopy unit for all their help and kindness. I would like to thank my fellow students in the department for sharing in the ups and downs encountered during the course of the PhD.

I would like to thank my family for all their support during the course of my studies, and particularly during the write-up.

This thesis is dedicated
to my parents to whom
I am eternally grateful

CONTENTS

LIST OF FIGURES

LIST OF TABLES

Chapter 1

Introduction

1.1 BASIC THERMODYNAMIC CONCEPTS

Thermodynamics is the study of the transformation of energy, and can be used to follow the heat changes that occur during a chemical or physical process. In thermodynamics, the world is considered as two parts: the system and the surroundings. The system is the part of interest, such as a reaction vessel. The surroundings are everything outside, and are separated from the system by a boundary. An open system is where both energy and matter can be transferred between the system and surroundings. A closed system is where energy but not matter can be transferred between system and surroundings. An isolated system does not allow transfer of energy or matter between the system and surroundings.

In thermodynamics, the main parameters that define a thermodynamic system are internal energy (U), enthalpy (H), pressure (P), volume (V), temperature (T), entropy (S), and Gibbs free energy (G). These are related by equations (1.1) and (1.2) below.

$$H = U + PV \tag{1.1}$$

$$G = H - TS \tag{1.2}$$

The first law of thermodynamics states that energy cannot be created or destroyed; it can only be transformed from one form to another. The first law is related to the enthalpy change (ΔH) since transformations in energy are usually associated with a change in enthalpy. The energy of a system can then be defined by equation (1.3).

$$\Delta U = Q - W \tag{1.3}$$

Where ΔU is the change in internal energy, Q is the heat absorbed by the system, and W is the work done by the system. Equation (1.1) shows that internal energy (U) and enthalpy (H) are related; the enthalpy change (ΔH) is thus defined as the heat that is

absorbed or evolved when a system changes its thermodynamic state under constant pressure.

Equation (1.3) shows that work (W) and heat (Q) are means of changing the internal energy (U) of a system. If the temperature (T) of the surroundings is higher than the system, then heat will flow into the system. This has the effect of increasing the internal energy (U) of the system. An increase in the temperature (T) of the system has the effect of increasing the motion of molecules in the material, which in turn results in the molecules becoming more disordered than before.

Entropy (S) is a measure of the degree of organisation in the structure. Substances with a highly organised structure with strong inter-atomic bonding tend to have low entropy values. Gases and substances made of large, flexible molecules tend to have larger entropy values. A spontaneous process is one that occurs naturally and does not require work to be done to bring it about, e.g. a hot object cools to the temperature of its surroundings. The second law of thermodynamics states that all spontaneous processes are accompanied by an overall increase in entropy. Processes do not usually occur in isolation, and therefore we have to consider the entropy change of the surroundings as well as the system. The overall change in entropy (ΔS_{total}) is the sum of two terms, the entropy change for the system (ΔS_{system}) and the surroundings (ΔS_{surr}), as shown in equation (1.4) (Atkins, 1994).

$$\Delta S_{total} = \Delta S_{system} + \Delta S_{surr} \qquad (1.4)$$

However, for processes such as crystallisation (which is known to be spontaneous), order is being introduced in to the system causing the entropy to decrease, which is not the favoured direction for ΔS. This discrepancy can be explained by considering the original statement for the second law, where the **overall** entropy change must be positive. Since crystallisation is a highly exothermic process, heat energy is released in to the surroundings. This has the effect of causing a large increase in the entropy of the surroundings, so that the overall entropy change is positive. Strongly exothermic processes are usually spontaneous at room temperature since the release of heat energy

causes a large increase in the entropy of the surroundings, and more than compensates for the decrease in entropy of the system.

1.2 THE CRYSTALLINE STATE

1.2.1 DEFINITION AND DESCRIPTION

A crystalline material is characterised by repetitious spacing of the constituent particles in a regular three-dimensional array. The ordered arrangement of the molecules in the crystal is based on a geometrical arrangement of points in space called a lattice. The regular arrangement of the crystalline solid is responsible for many of the properties of crystals, including a defined melting point, x-ray diffraction, and sharp, well-defined crystal faces (Byrn, 1982).

The unit cell of the crystal must contain the features of the crystal as a whole. It is for this reason that it may not be the simplest collection of molecules that could generate the lattice by infinite repetition. A crystal can be considered to be made up of a series of unit cells repeated an infinite number of times in three-dimensions. There are seven different types of crystal systems: cubic, tetragonal, orthorhombic, rhombohedral, hexagonal, monoclinic, and triclinic. Crystalline materials with different crystal systems will display different shapes when viewed under a microscope. However, the presence of different shapes does not always indicate different crystal systems. During crystallisation, the first event that occurs is formation of a nucleus. If the rate of growth is equal in all directions, then a cubic shape will be formed. However, if the growth is inhibited in one direction, a plate shape will be formed; growth inhibited in two directions will form a needle-like shape. These differences in the outer appearance of the crystal are not due to different crystal systems, but are referred to as the crystal habit (Carstensen, 1993). The differences in crystal habit have practical implications, e.g. during the tabletting process a cubic-like shape material will exhibit better flow in a powder hopper. However, the less cubic-like shaped materials will have a larger surface area leading to improved dissolution (Carstensen, 1993).

Inorganic compounds usually crystallise in a specific crystal system, e.g. sodium and potassium chloride crystallise in to the cubic crystal system. However, organic compounds can crystallise in to different crystal systems, a phenomenon known as polymorphism (Carstensen, 1993). Different polymorphs of a crystalline material may be produced by manipulation of the conditions of crystallisation such as solvent of crystallisation, temperature, and rate of cooling. At a given temperature and pressure

only one of the polymorphs is stable; the others are called metastable polymorphs. The different polymorphs have different physical properties such as solubility, dissolution, and solid-state stability. They also differ in their processing behaviour such as powder flow and compression properties. Polymorphism is common among pharmaceuticals with 63% of barbiturates, 67% of steroids, and 40% of sulphonamides exhibiting polymorphism (Wells and Aulton, 1988).

During crystallisation, solvents may be entrapped in the crystal. Crystals that entrap the solvent of crystallisation are called solvates. The solvent may be either in a stoichiometric or nonstoichiometric amount. Crystallisation of a compound that results in no solvent of crystallisation within the crystal structure is called anhydrous. A stoichiometric amount of solvent involves a molecular complex that has incorporated the solvent molecules into specific sites within the crystal lattice. If the solvent of crystallisation is water then the solvate is called a hydrate. The terms hemihydrate, monohydrate, and dihydrate describe hydrated forms with molar ratios of water corresponding to half, one, and two respectively.

1.3 THE AMORPHOUS STATE

1.3.1 DEFINITION AND DESCRIPTION

The amorphous state does not have the long-range three-dimensional order that is present for the crystalline state. Instead, the positioning of molecules relative to each other is more random, rather more like in the liquid state. Figure 1.1 shows a model representing amorphous and crystalline regions. It shows parallel blocks that represent the crystalline regions within an amorphous matrix (Levine and Slade, 1988a).

1.3.2 THE AMORPHOUS STATE IN SOLIDS

Many pharmaceutical solids have a significant amount of amorphous character, either induced by high-energy processing or due to the large molecular size (e.g. polymers and proteins). The four most common ways that amorphous material is induced in to a solid are:

(1) condensation from the vapour state,

(2) supercooling of the melt,

(3) mechanical activation of a crystalline material (e.g. milling),

(4) rapid precipitation from solution (e.g. spray-drying, freeze-drying).

Active mechanical energy (e.g. from milling) that is partially transferred to the solid is stored in the form of lattice defects. The lattice defects due to mechanical processing only affect the surface layers of the solid, and involve an increase in the energy and entropy of the material (Huttenrauch et al, 1985).

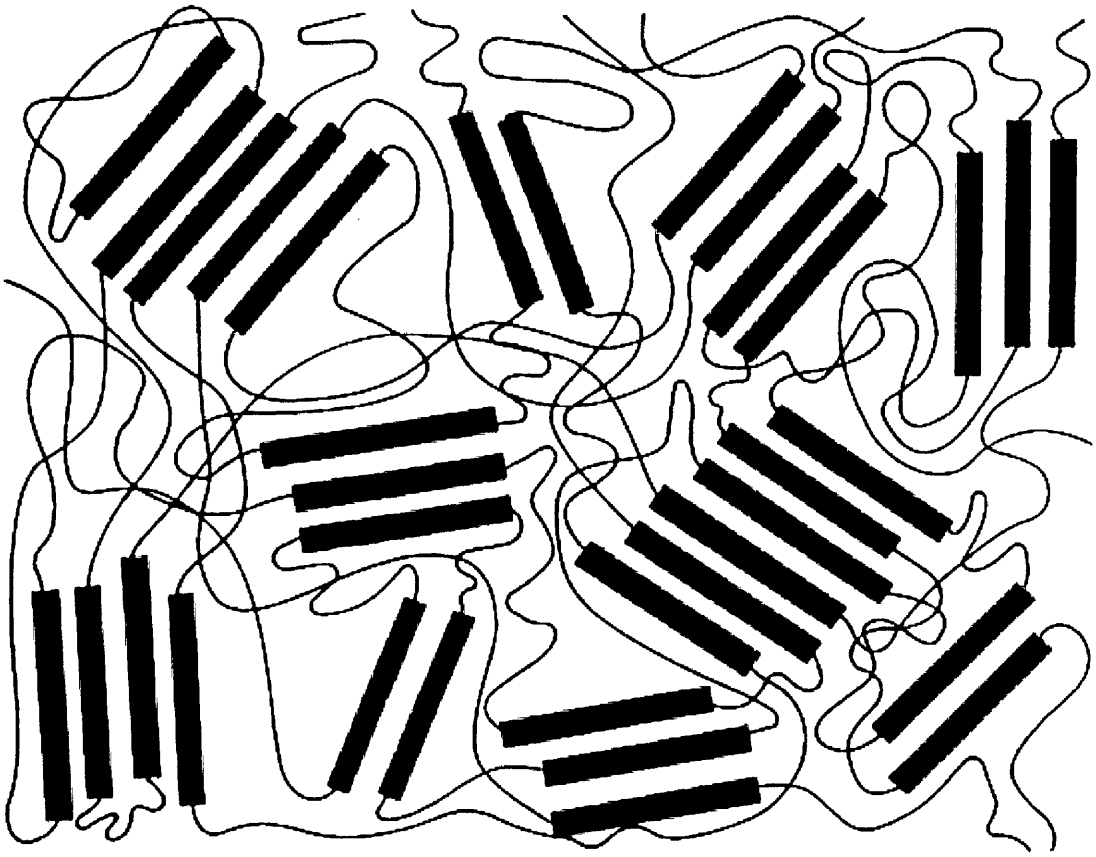

Figure 1.1 *Schematic model of a partially crystalline (PC) polymer showing the crystalline and amorphous regions (reproduced from Levine and Slade, 1998a)*

The high molecular weight (MW) polymers, such as starch, are commonly described as 'partially crystalline' (PC) polymers since they have small microcrystalline regions in an amorphous matrix, as shown in Figure 1.1. Native granular starch is composed of two different polysaccharides: linear amylose molecules that represent the amorphous part, and amylopectin, which is highly branched and represents the partially crystalline component (Zeleznak and Hoseney, 1987). The model in Figure 1.1 is particularly

applicable to amorphous polymers with relatively low amounts of crystallinity. A single, long polymer chain may have helical or other ordered segments within the microcrystalline regions and random-coil segments in the amorphous regions (Levine and Slade, 1988a).

1.3.3 CHARACTERISTICS OF THE AMORPHOUS STATE

Figure 1.2 shows a schematic of volume or enthalpy against temperature. For a crystalline material, starting from the liquid state, as the temperature is lowered there is a discontinuity at the melting temperature (Tm) that represents the phase transition of the crystalline material from the liquid to the solid state. If we begin again at the liquid state in Figure 1.2, but this time the liquid state undergoes rapid cooling, for example by transferring to liquid nitrogen, then the volume (or enthalpy) continues along the equilibrium liquid line beyond Tm into a supercooled region. There is no discontinuity present for the supercooled liquid below Tm, and this region is referred to as an equilibrium supercooled liquid. This region is also called the rubbery state due to its macroscopic properties. The movement of molecules (molecular motions) changes when the supercooled liquid is formed. The average time taken for molecular motions in the supercooled liquid is less than 100 seconds, compared to a few seconds just below Tm (Hancock et al, 1995). The viscosity in the supercooled liquid region is between 10^{-3} and 10^{12} Pa s (Hancock and Zografi, 1997). Salvetti et al (1996) investigated the differences in energy between crystalline and amorphous sucrose and glucose. They showed through heat of solution measurements that the differences between the amorphous and crystalline forms are due to differences in the van der Waals and hydrogen-bonding energy. Figure 1.2 shows that amorphous materials have greater enthalpy, and thereby a higher internal energy than the corresponding crystalline material. The higher energy of the amorphous state means that it has enhanced thermodynamic properties (e.g. solubility and dissolution) and greater molecular mobility relative to the crystalline state (Hancock and Zografi, 1997).

The irregular arrangement of molecules in the amorphous state causes the molecules to be spaced further apart than in the crystalline state; this leads to a higher volume and lower density for the amorphous state, and the amorphous material is considered to have a greater 'free volume' (Hancock and Zografi, 1997).

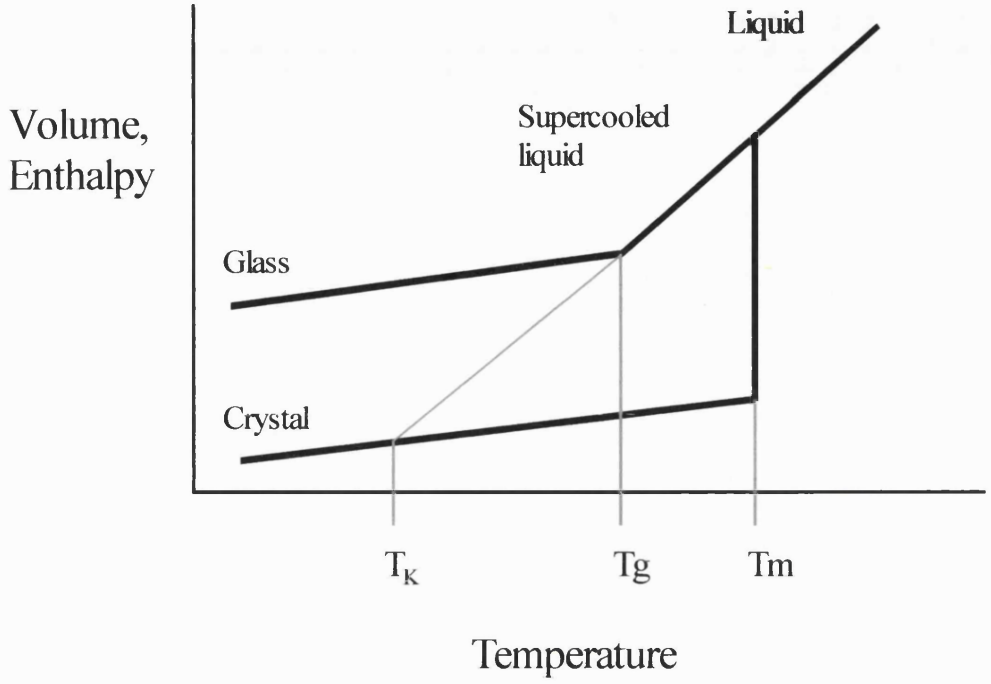

Figure 1.2 *Schematic diagram of enthalpy (or volume) against temperature (modified from Hancock and Zografi, 1997).*

For crystal forming materials, the main criteria that determines whether the solid is crystalline or amorphous is the extent to which the molecules are able to achieve equilibrium configurations. A high sample viscosity leading to low molecular mobility means that equilibrium configurations will not be achieved, resulting in formation of the amorphous state (Flink, 1983). The amorphous metastable state will tend to convert to the crystalline state if the molecular mobility is adequate. In thermodynamic terms, the presence of the metastable amorphous state indicates that there are free energy barriers that prevent the achievement of the stable crystalline state (Flink, 1983).

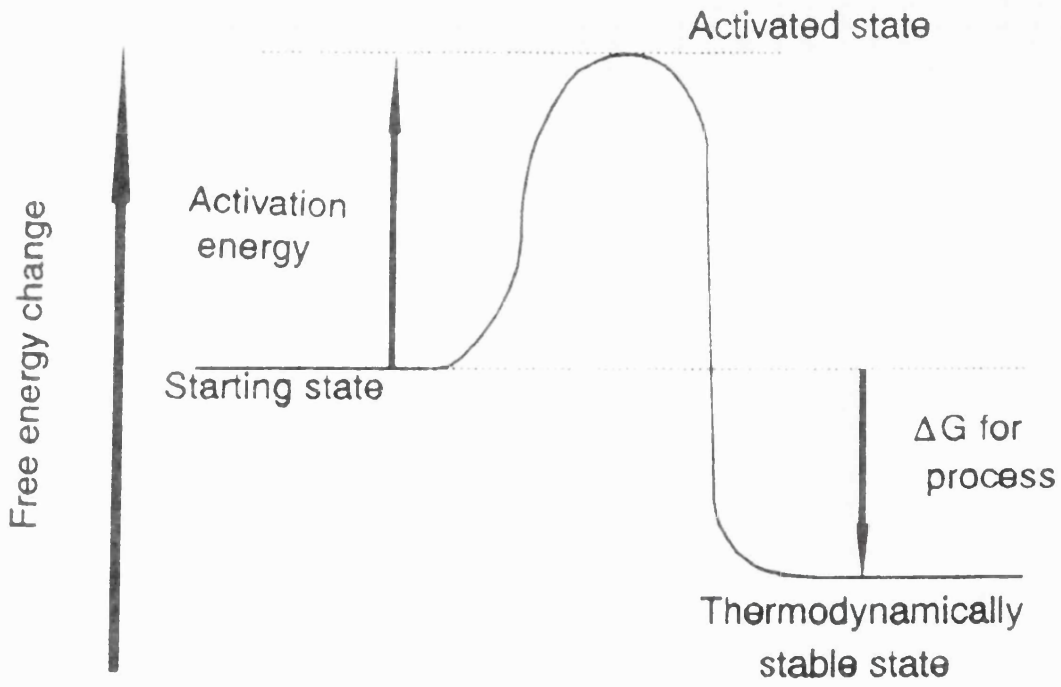

Figure 1.3 *Energy diagram showing the starting and thermodynamically stable state that is preceded by an activation energy barrier. Reproduced from Buckton (1995a).*

All systems will achieve equilibrium if they are left for a sufficient time and providing that a mechanism exists for the equilibrium to be achieved. The latter explains why in some cases, including supercooled liquids, the processes exist in non-equilibrium states despite appearing to be in an equilibrium state. Figure 1.3 shows the starting metastable amorphous state that is followed by an activation energy barrier, which must be overcome on the route to achieving the thermodynamically stable crystalline state. This activation energy barrier may be due an enthalpic or entropic barrier that must be overcome if the thermodynamically stable crystalline state is to be achieved. This means that if an entropic barrier exists then it may be necessary to impose a significant degree of order before the thermodynamically stable crystalline state can be reached. In some processes where the activation barrier cannot be overcome, such as in supercooled liquids, the materials remain in a non-equilibrium state (Buckton, 1995a).

1.4 THE GLASS TRANSITION IN AMORPHOUS MATERIALS

1.4.1 THE GLASS TRANSITION TEMPERATURE

The glass transition temperature (Tg) is a narrow temperature range when the material changes from a glassy state with low free volume to a rubbery state with greater free volume (Zografi and Hancock, 1993).

If the liquid above Tm in Figure 1.2 is supercooled to produce an amorphous material, at temperatures below but close to the melting temperature Tm, the mean speed of molecular motions over atomic distances is very rapid (Hancock et al, 1995). Cooling of the supercooled liquid further reduces the molecular mobility of the material to a point when the material is unable to achieve equilibrium as it loses its thermal energy. This results in a change in the temperature dependence of the enthalpy and volume at a characteristic temperature, the glass transition temperature (Tg). On passing through the glass transition, a number of changes in the material's physical properties are observed, including viscosity, density, and heat capacity. Slade and Levine (1991) describe the glass transition in amorphous systems as a material specific change from a glassy solid capable of supporting its own weight against flow to a rubbery viscous liquid that is capable of flow in real time. The Tg of an amorphous material determines its chemical and physical stability; the Tg usually becomes a critical parameter when the operating temperature is just below or above the Tg, as encountered during processing or storage of the amorphous material (Hancock and Zografi, 1994).

The glass transition event is usually considered to reflect the co-operative type translational molecular motions either by segments of a polymer molecule or smaller glass forming materials (Hancock et al, 1995). However, experimental studies of the glass transition temperature are complicated by the different types of molecular motions (such as rotational or translational), the effect of temperature on the type and extent of molecular motions, and the coupling or co-operativity of molecular motions (Hancock and Zografi, 1997). At the glass transition temperature, the average time taken for the predominant molecular motions to take place is 100 seconds, and the viscosity is 10^{11} - 10^{14} Pa s (Hancock and Zografi, 1997 and Slade and Levine, 1988a).

The experimental measurement of the glass transition temperature occurs when the time scale of molecular motions coincides with the time scale of the experimental technique being used to measure the Tg (Hancock et al, 1995). If we consider a newly formed amorphous supercooled liquid just below the melting temperature (Tm), the mean speed of molecular motions in this region is typically a few seconds, compared to the time

scale of experimental methods (minutes to hours). However, cooling of the material further leads to the glass transition temperature where the time scale of molecular motions of the amorphous material and that of the experimental technique coincide (Hancock et al, 1995). Experimental determination of the Tg is usually carried out by detecting the change in heat capacity at the glass transition temperature which is observed as a shift in the baseline.

The gradient of the enthalpy or volume line in Figure 1.2 changes at the characteristic glass transition temperature (Tg). The change in gradient means that the temperature dependence of the enthalpy and volume has changed. Below the glass transition temperature, if further cooling takes place the molecular motions are reduced even further. The amorphous material below Tg is referred to as glassy due to its macroscopic properties. Below Tg the molecular mobility is reduced sufficiently such that it is unable to reach equilibrium in the time scale of the measurement. Molecular mobility in the glassy amorphous state occurs over a period above 100 seconds, and the viscosity is typically above 10^{12} Pa s (Hancock and Zografi, 1997).

The temperature where the supercooled liquid line would then intersect the crystal line is called the Kauzmann temperature (T_K), as shown in Figure 1.2. It is thought to correspond to the lower limit of the experimental and theoretical glass transition temperature (Hancock and Zografi, 1997).

1.4.2 EFFECT OF MOLECULAR WEIGHT ON Tg

Increasing the molecular weight has the effect of increasing the glass transition temperature of the system. The effect of molecular weight on the glass transition temperature can be calculated using the Fox and Flory equation (1.5) (Fox and Flory, 1950).

$$Tg = Tg(\infty) - \frac{Kg}{M} \qquad (1.5)$$

Where M is the molecular weight, Kg is a constant, Tg (∞) is the limiting Tg at a high molecular weight, and Tg is the glass transition temperature.

The Tg increases with increase in the molecular weight up to a plateau level where further increases in the molecular weight show no further increase in the Tg (Levine and Slade, 1986). This linear relationship between the Tg and molecular weight is typical of polymers (Fox and Flory, 1950). The plateau level for the Tg corresponds to the molecular chain 'entanglement coupling' level at about 10^4 - 10^5 Daltons. This is where for high molecular weight polymers there is formation of a random network. These 'entanglements' behave as if they are cross-links but do not appear to involve chemical bonding (Levine and Slade, 1986).

The glass transition temperature of dry sucrose is 57°C, whereas that of the maltodextrins, which have large molecular weights, is between 140°C and 190°C depending on the maltodextrin considered (Roos and Karel, 1991a). The effect of binary mixtures of maltodextrins and sucrose were investigated by Roos and Karel (1991a). They found that maltodextrins have a significant effect on the Tg of the binary mixture but only at levels above 50%. However, only small amounts of sucrose resulted in large decreases in the Tg of the binary mixture. This information could be useful in the selection of binary mixtures during formulation depending on processing and storage requirements (Roos and Karel, 1991a).

1.5 EFFECT OF TEMPERATURE ON AMORPHOUS MATERIALS

Many of the physical properties of amorphous materials are determined by the temperature dependence of molecular motions, including the glass transition temperature itself and the ease of glass formation. Figure 1.4 shows that the temperature dependence of the viscosity (or molecular mobility) depends on whether the material is in a glassy, rubbery, or liquid state. In the glassy and liquid states the temperature dependence follows the Arrhenius equation, whereas in the rubbery state there is an exponential temperature dependence (Zografi, 1988). Equation (1.6) shows the Arrhenius equation.

$$\eta = \eta_0 \exp \frac{-Ea}{RT} \qquad (1.6)$$

Where η is the viscosity, η_0 is the pre-exponential factor, exp is the exponential (base for natural logs = 2.718), Ea is the activation energy, R is the gas constant (= 8.314 J mol^{-1} K^{-1}), and T is the temperature in K.

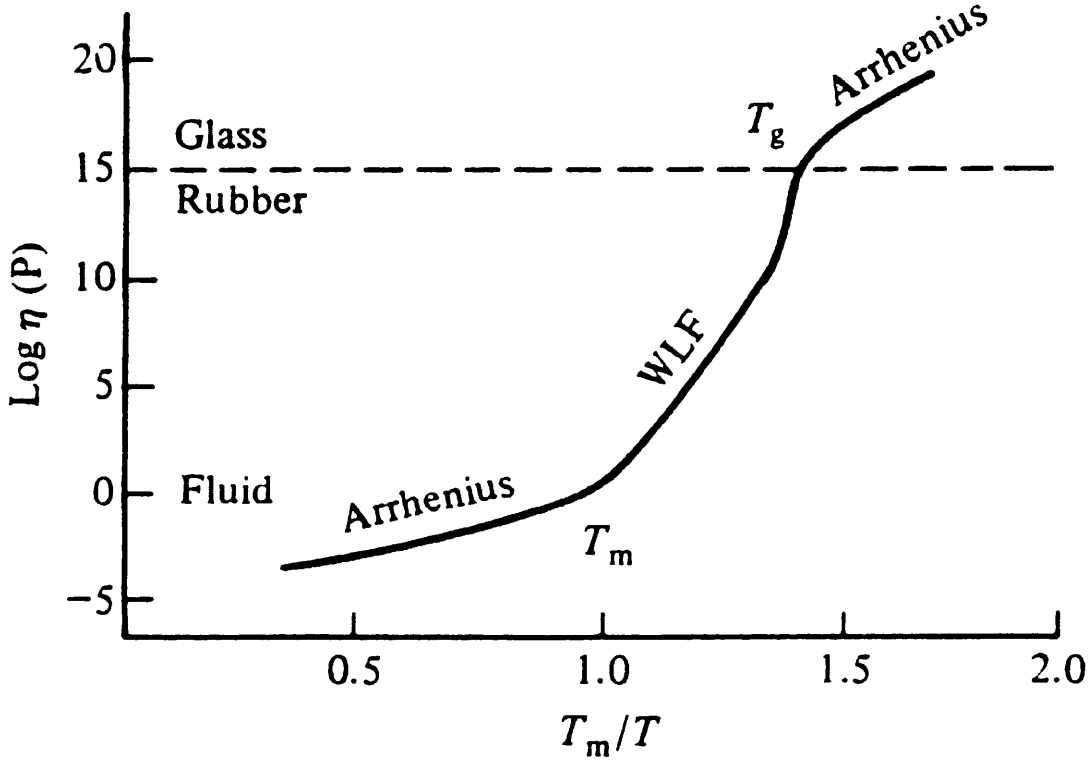

Figure 1.4 *Schematic representation of log viscosity as a function of reduced temperature (T_m/T). Reproduced from Levine and Slade (1988a).*

In the glassy amorphous state below Tg, the molecular mobility is generally considered to be much reduced (in normal experimental time scales) in relation to the molecular motions above Tg in the rubbery amorphous region (Hancock and Zografi, 1997 and Hancock et al, 1995). However, molecular motions (rotational and translational) do occur below Tg but these molecular motions occur over longer time scales (hours and days) that are slow in normal experimental terms (minutes to hours). They can however still have a significant effect over the lifetime of a pharmaceutical product, in the order of years (Hancock et al, 1995). The reason why such molecular mobility is present in

the glassy state is that on glass formation at Tg, excess enthalpy and entropy is 'kinetically trapped' as the system falls out of equilibrium and in to the non-equilibrium glassy state (Shamblin et al, 1999). Experimental methods with time scales of minutes to hours are usually unable to detect such reduced molecular mobility. Measurement of these reduced molecular motions requires the use of experimental methods that utilise extended time periods. These experiments are called 'ageing experiments'.

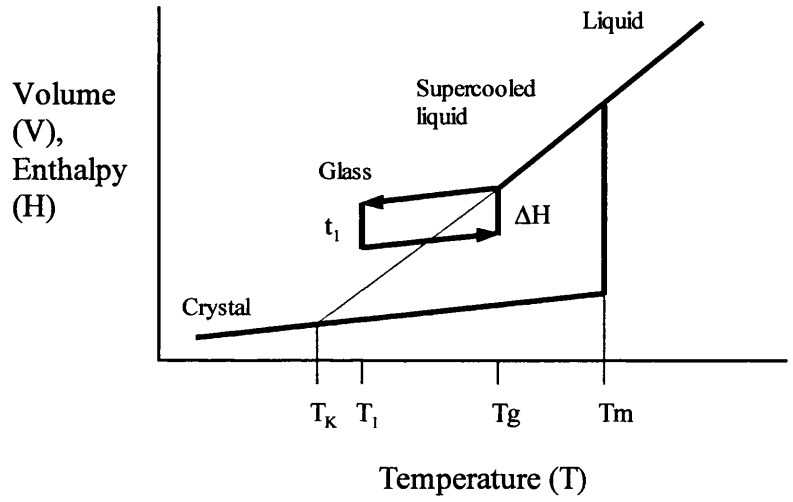

Figure 1.5 *Schematic representation of enthalpy (or volume) against temperature showing a relaxation enthalpy (ΔH). Modified from Hancock et al (1995)*

To measure the molecular motions below the glass transition temperature, Hancock et al (1995) employed DSC to measure the enthalpy relaxation that occurs with time. An explanation of relaxation phenomena is as follows. Figure 1.5 shows a schematic of enthalpy (H) or volume (V) against temperature (T). If an amorphous material in the glassy state below Tg is stored at a temperature (T_1) for a period of time (t_1), then it undergoes a gradual decrease in enthalpy (ΔH) or volume (ΔV). This decrease in enthalpy is due to the thermodynamic driving force for the glassy material towards the more stable crystalline state, with the resulting coupling of normal molecular motions. On reheating of the 'relaxed' glassy material, the enthalpy and volume losses are recovered in full at or near the Tg as shown in Figure 1.5. The enthalpy changes can be

measured using differential scanning calorimetry (DSC) in the form of an enthalpy relaxation endotherm at the glass transition temperature (Hancock et al, 1995). To obtain a meaningful value that could be used to compare molecular mobilities for different materials, they then calculated mean molecular relaxation times (τ) for the materials, which is the average time taken for a single molecular motion of a particular type to take place. The mean molecular relaxation times were calculated using experimental enthalpic relaxation data obtained from DSC (Hancock et al, 1995).

Hancock et al (1995) found using the 'ageing' experiments described above that for the materials studied (sucrose, PVP, and indomethacin) up to 50°C below Tg, significant translational molecular motions were occurring. This temperature 50°C below Tg appears to correspond to the Kauzmann (T_K) temperature, which is where the equilibrium supercooled line would cross the crystal line (see Figure 1.5). For a glassy material the T_K represents a temperature below which the time scale for molecular motions is in the order of years (Shamblin et al, 1999).

In Figure 1.4, as the temperature is increased above Tg, a very different, exponential temperature dependence takes effect. This exponential temperature dependence above Tg is defined by the Williams-Landel-Ferry (WLF) equation (1.7) (Williams et al, 1955). The WLF equation is universally applicable for any glass forming polymers, oligomers, or monomers (Slade and Levine, 1988a). The WLF equation defines the kinetics of molecular-level relaxation processes and is based on the temperature dependence of free volume (Ahlneck, 1993). The WLF equation defines the exponential temperature dependence of the rate of any diffusion-limited relaxation process (such as viscosity) that occurs at a temperature T compared to the rate at a reference temperature Tg (Slade and Levine, 1991, Levine and Slade, 1986).

$$\eta = \eta_g \exp \frac{17.4\,(T - Tg)}{51.6 + (T - Tg)} \qquad (1.7)$$

Where η is the viscosity, and η_g is the mean viscosity at Tg. This equation tells us that where we are relative to the Tg can have a significant effect on the viscosity of the

material, and therefore the molecular mobility of the amorphous material (Zografi, 1988).

The WLF equation (1.7) is based on the assumptions that polymer free volume increases in a linear manner with increasing temperature above Tg and that segmental (for polymers) or mobile unit viscosity decreases rapidly with the increasing free volume (Slade and Levine, 1991). The impact of WLF behaviour on the rates of relaxation phenomena in amorphous solid-water systems can be illustrated by the following example: if the rate at Tg is normalised to 1, then at a temperature 3, 7, 11, and 21°C above Tg, the corresponding rates are 10, 100, 1000, and 10^5 respectively (Levine and Slade, 1988b). Thus the greater the temperature above Tg, the further a system is able to move (due to increased free volume and decreased segmental or mobile unit viscosity) (Slade and Levine, 1991). These exponential increases in the rate are dramatically different from the familiar Arrhenius kinetics (Levine and Slade, 1988a). However, the WLF equation is only valid in the temperature range between Tg and Tg + 100°C, and is not applicable in the glassy or the very mobile liquid state where the Arrhenius equation applies (Slade and Levine, 1988a).

An example of the effect of WLF kinetics above Tg is the propagation (crystal growth) step in the overall mechanism of crystallisation for amorphous materials (see Figure 1.10). The propagation step increases exponentially (from a rate of zero at Tg) with increasing temperature above Tg (up to Tm) due to the much increased mobility in the rubbery state (Slade and Levine, 1988a).

Angell et al (1991, 1994) classified amorphous materials into strong or fragile glass formers. Strong glass formers typically exhibit small changes in heat capacity at their Tg, have a Tm/Tg ratio of greater than 1.5, and display Arrhenius-like changes in molecular mobility. Fragile glass formers have a relatively large change in heat capacity at Tg, have a Tm/Tg ratio between 1 and 1.5, and a stronger temperature dependence of molecular motions exists (more like WLF behaviour) (Hancock et al, 1995 and Shamblin et al, 1999).

1.6 EFFECT OF WATER ON AMORPHOUS MATERIALS

1.6.1 INTRODUCTION

Figure 1.6 shows that water in the disordered amorphous state is able to dissolve in the solid. Water uptake by an amorphous solid is determined by the total mass of amorphous solid (compared to the available surface area for crystalline solids). This means that water uptake by amorphous solids is far greater in the amorphous state compared to the crystalline state (Pikal et al, 1978). The uptake of water into amorphous solids is called 'absorption' or 'sorption'.

Deliquescence occurs for water-soluble materials when the relative humidity of the atmosphere is higher than a critical RH that is characteristic of the material. This critical RH is the relative humidity that is produced for a saturated solution of the material. Deliquescent materials are very water-soluble materials (such as salts and sugars) and have an ability to significantly reduce the vapour pressure (and thus the RH) of water in an aqueous solution of the material. At the point when the atmospheric RH exceeds the critical RH for the material, a liquid film consisting of a saturated solution of the solid is formed around the solid particle. The liquid film forms a concentration gradient of water vapour that results in atmospheric water vapour condensing onto the liquid film. This in turn dilutes the saturated solution leading to further solid dissolving in the liquid film. If the deliquescent material is stored at a RH below the critical value, then the solid will not dissolve (Zografi and Hancock, 1993, Buckton, 1995a).

Capillary condensation can occur in a material having a very porous structure with very small pore size. Liquid that condenses into the micropores develops a capillary pressure that allows water from the atmosphere to condense at a lower RH than normal (Zografi and Kontny, 1993).

1.6.2 PLASTICISATION OF AMORPHOUS MATERIALS

A plasticiser is defined as a substance that lowers the Tg of a solid (Zografi and Hancock, 1993). Water with its very low Tg value (-135°C), its small molecular size and hydrogen bonding ability can be a very effective plasticiser of amorphous solids (Zografi and Hancock, 1993). Figure 1.7 shows that for PVP, a highly water-soluble amorphous polymer with a high Tg in the dry state, water with its low Tg is able to continually decrease the Tg of the PVP/water mixture (Ahlneck, 1993).

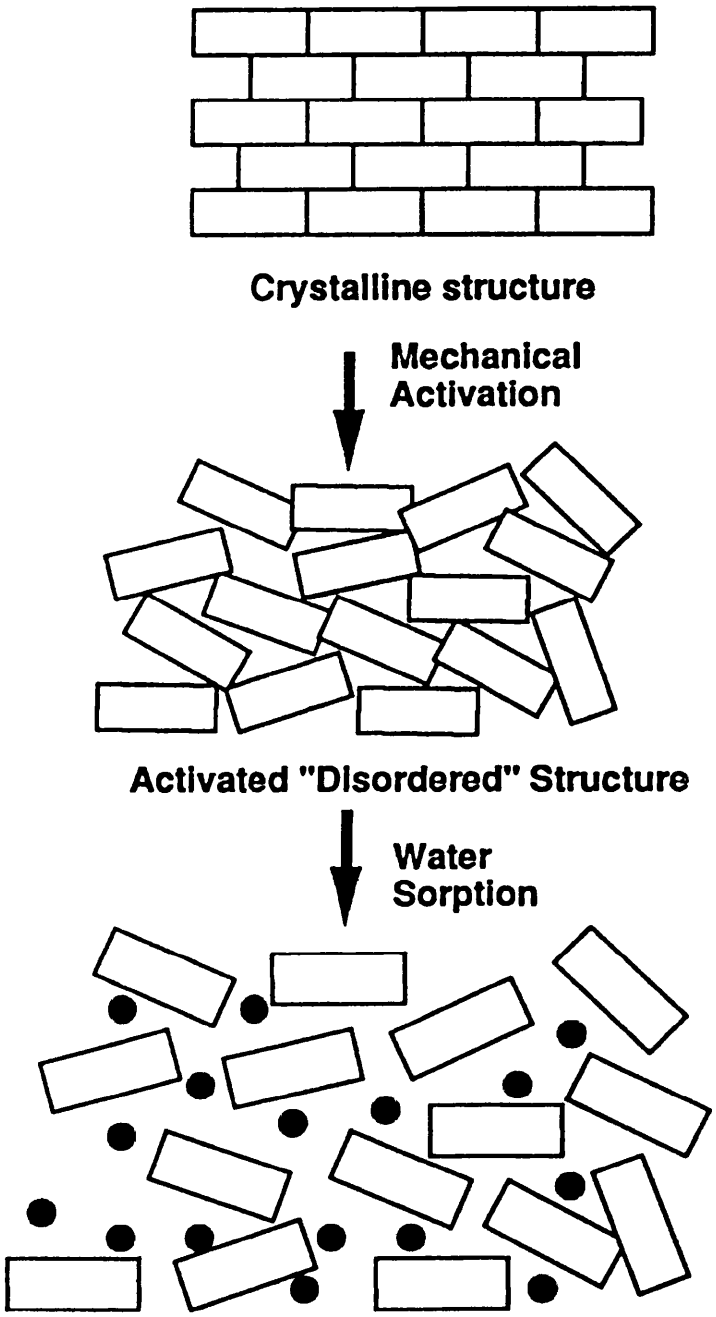

Figure 1.6 *Schematic representation of the effect of mechanical activation and water vapour sorption (reproduced from Ahlneck, 1993).*

The moisture sorption into the amorphous material leads to greater mobility of the polymer chains, which then goes on to produce a structural relaxation transition at the glass transition temperature, Tg (Levine and Slade, 1988a). The effect of water plasticisation of amorphous materials on the Tg is most dramatic at low moisture levels. In the case of PVP, for the first 10% moisture added to the dry state, the Tg decreases at 6°C / % water. A range of about 5-10°C / % water appears to apply widely to amorphous and partially crystalline water-soluble materials, including monomeric and oligomeric carbohydrates (Levine and Slade, 1988a).

The important effect of water plasticisation is the change in the viscoelastic properties of the material as the Tg is decreased below T (the operating temperature), which is equivalent to the effect of increasing the temperature T above Tg. As the Tg is plasticised below T, so the domain of WLF kinetics takes effect with the associated significant increases in molecular mobility, as described earlier. In Figure 1.7, if the PVP sample is stored at 25°C and 80% RH then its Tg would be depressed to about 10°C, and would be converted from the glassy to the rubbery state. If the temperature were increased to 40°C, then a humidity level of about 65% RH would be required to have the same effect (Ahlneck and Zografi, 1990).

The effect of plasticisation of an amorphous material on the Tg by water can be predicted using the Gordon-Taylor equation (1.8) (Gordon and Taylor, 1952).

$$Tg = \frac{w_1 Tg_1 + k w_2 Tg_2}{w_1 + k w_2} \qquad (1.8)$$

Where Tg is the Tg of the mixture, Tg_1 and Tg_2 are the glass transition temperatures of component 1 (solid) and component 2 (water), w_1 and w_2 are the weight fractions of the solid and water respectively, and k is a constant. The constant k can be obtained from the densities (ρ) and glass transition temperatures (Tg) of the components, according to equation (1.9).

$$k = \frac{\rho_1 Tg_1}{\rho_2 Tg_2} \qquad (1.9)$$

The constant k is a measure of the relative free volume contribution to the mixture by each of the components (Zografi and Hancock, 1993).

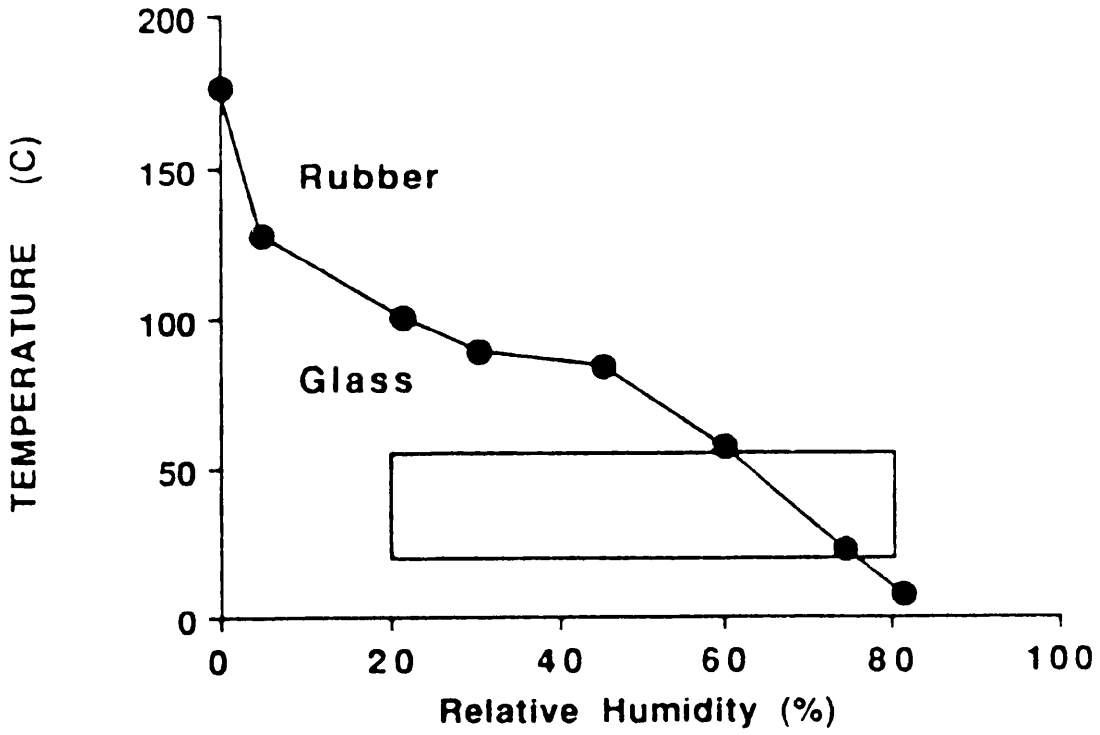

Figure 1.7 *Schematic diagram of the effect of water plasticisation on the glass transition temperature for PVP (Reproduced from Ahlneck and Zografi, 1990).*

1.6.3 SORPTION ISOTHERMS FOR AMORPHOUS POLYMERS

Water vapour sorption in to amorphous polymers is a diffusion-controlled process that involves the changing structural state of the polymers, relative to the glass transition temperature, due to plasticisation of the polymer by water (Levine and Slade, 1988a). The absorption of water by an amorphous solid is typically presented by a sorption isotherm, which is a plot of the equilibrium moisture content against the RH for a material. Figure 1.8 shows a typical absorption isotherm for an amorphous non-

crystallisable polymer, with its characteristic sigmoidal shape. Figure 1.8 shows that there is an upward inflection in the sorption curve at higher RHs. This has been found to occur in the region where the Tg is plasticised to T by the absorption of water (Oksanen and Zografi, 1990).

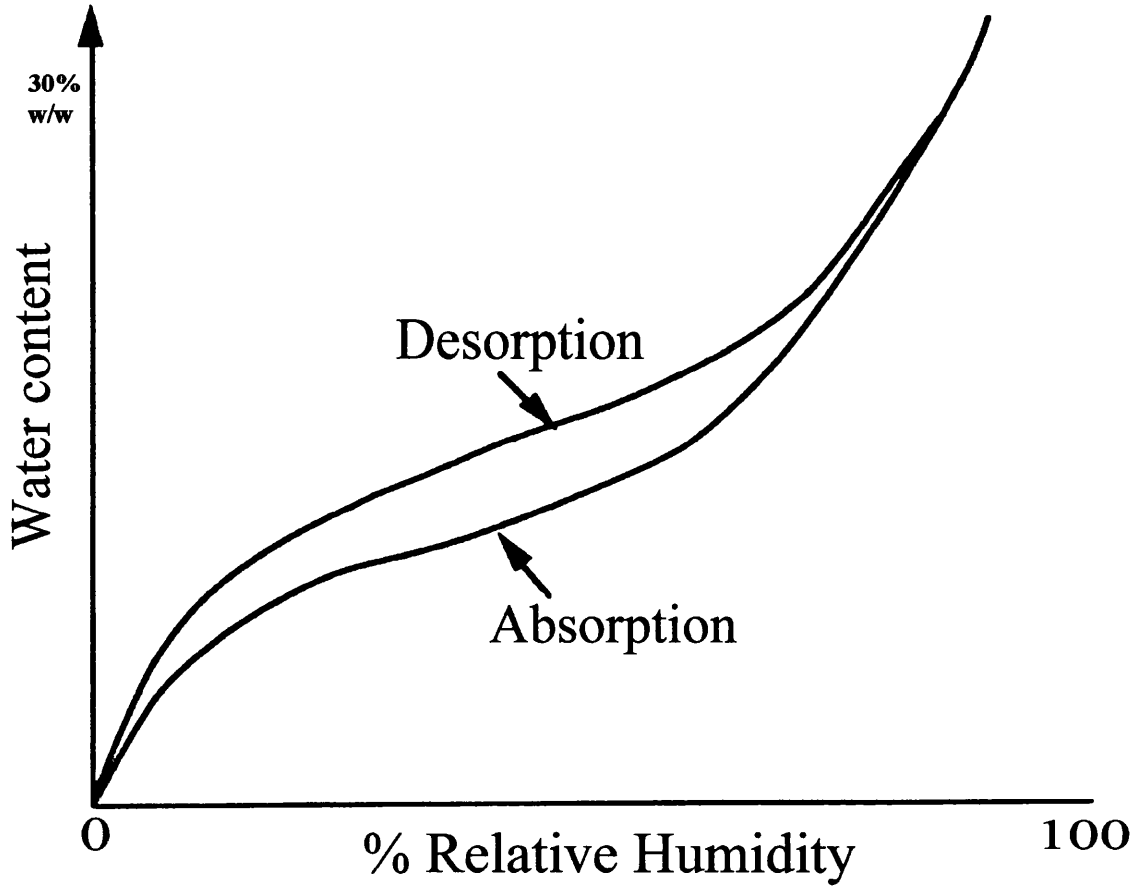

Figure 1.8 *Schematic representation of a typical absorption isotherm for an amorphous polymer (Modified from Roos, 1995).*

Water sorption produces a morphological change from a glassy to a rubbery material that allows a larger amount of water to be absorbed by the amorphous polymer. For water sorption below the glass transition temperature, the absorption of water in to amorphous polymers involves the diffusion of water in to the polymer. This occurs relatively slowly and shows an Arrhenius-like temperature dependence. In the region

just below and above Tg, there is an increased uptake of water vapour due to increasing polymer segmental mobility as the Tg approaches the operating temperature T. In the rubbery state above Tg, WLF temperature dependence takes over with a corresponding increase in free volume causing a dramatic increase in the uptake of water vapour (Levine and Slade, 1988a).

Figure 1.8 shows that there is hysteresis present, that is the amount of water associated with the desorption isotherm is greater than that for the absorption isotherm under a given RH. This is thought to be due to a change in the polymeric chain conformation caused by the water absorption into the amorphous structure (Zografi and Kontny, 1986) and has also been related to polymer chain unfolding (Karel, 1985). Hysteresis occurs in amorphous polymers that swell irreversibly during the absorption of water. However, not all amorphous polymers swell, and those that do not swell or swell reversibly show little or no hysteresis (Levine and Slade, 1988a).

1.6.4 MECHANISM OF PLASTICISATION IN AMORPHOUS POLYMERS

The mechanism behind the plasticisation of polymers by water will now be considered. The overall mechanism for the plasticisation of polymers by water derives from free volume theory in that low molecular weight molecules, such as water, have a large free volume. Molecular interactions between water and a non-plasticised polymer glass lead to an increased free volume in the newly formed aqueous polymer rubber (Levine and Slade 1988a) by reducing hydrogen bonding between adjoining molecules of the amorphous solid (Ahlneck and Zografi, 1990).

The increase in the free volume of the polymer leads to an increase in the mobility of segments of the polymer backbone, and this in turn leads to a decrease in the glass transition temperature (Tg) of the polymer. This forms the major part of the plasticisation mechanism for amorphous polymers. However, it has been suggested that for polymers that have the ability to hydrogen bond with water, a second mechanism may act in addition to the free volume mechanism explained above. The second part of the overall mechanism relates to the hydrogen-bonding (H-bonding) capacity of the polymer with water molecules. H-bonding may take place between water and polar groups present in the polymer. This effect will be greater for more hydrophilic polymers

due to a greater number of possible binding sites between water and the polymer. The impact of the H-bonding effect on the decrease of Tg is even more apparent where polymer chains are cross-linked by H-bonds as well as covalent cross-linking. In this case, water would then replace the H-bond cross-links between polymer chains and thus increase molecular mobility (Levine and Slade, 1988a).

1.7 COLLAPSE PHENOMENA

1.7.1 COLLAPSE

Processing and storage of amorphous materials often results in changes in their structures. The same basic phenomenon is responsible for these changes, however the terms used to describe them varies from process to process. During processing, such as freeze-drying, this loss of structure is called 'collapse', whereas for storage phenomena occurring for dried powders it is referred to as 'stickiness' (Tsourouflis et al, 1976). Levine and Slade (1988a) describe the collapse phenomena in amorphous materials as time-dependent structural relaxation processes which occur above the glass transition temperature. They considered the collapse phenomena to include stickiness, agglomeration, lumping, caking, flow of amorphous powders, and structural collapse in amorphous powders. The collapse phenomena represent the microscopic and macroscopic manifestations of the transition from amorphous glass to rubber that occurs at the glass transition temperature (Levine and Slade, 1986).

Collapse as a physicochemical phenomenon can be described as viscous flow resulting from decreasing viscosity above the glass transition temperature (Roos, 1995). These structure transformations that occur from the dried material to the viscous state are due to added moisture and/or increased temperature (Tsourouflis et al, 1976). This viscous flow is time-dependent and it can be observed from reduction of the macroscopic volume of the material (Roos, 1995). The 'structural collapse' aspect of the collapse phenomena is noticeable as a shrinkage of the material and is the result of a reduction in the viscosity of the material when it becomes too low to support its own weight, resulting in flow of the amorphous material (To and Flink, 1978b). The temperature at which the structural change takes place is called the 'collapse temperature' (Tc).

The amorphous state is able to encapsulate small molecules due to the existence of free volume in the system. The crystalline state has limited free volume and is thus unable to accommodate such 'impurities' in the structure. Repeated recrystallisation of a

substance is well known as a method of purifying a substance. The amorphous state obtained from freeze-drying is known to have exploitable properties such as flavour retention and protection of emulsified fats against oxidation. However, retention of these properties depends on the maintenance of the amorphous, non-collapsed state (To and Flink, 1978b,c). Collapse occurs in freeze-dried samples when the frozen sample temperature is higher than the collapse temperature. Collapse of the sample results in a loss of structure and the resulting formation of a highly viscous liquid. When collapse occurs during the freeze-drying process there is loss of entrapped materials such as flavour volatiles or fats by amorphous freeze-dried carbohydrates (To and Flink, 1978c and Flink and Karel, 1972) and the ice crystals which normally sublime (during the freeze-drying process) instead dissolve, resulting in the blockage of capillaries and inefficient drying of the sample (Tsourouflis et al, 1976).

To and Flink (1978b) found significant similarities between the collapse temperature and the glass transition temperature of polymers. They found that the molecular weight and composition dependence of the glass transition temperature also applied to the collapse temperature. They concluded that collapse and glass transition are phenomenologically similar events but distinguished between the two by stating that glass transitions for polymeric materials were reversible, whereas the collapse phenomena was irreversible.

Levine and Slade (1988a) point out that collapse may be irreversible but that this statement is misleading. They suggest that at the molecular level, the glass-to-rubber transition for an amorphous thermoplastic material is reversible. Further they suggest that the reason that collapse is said to be irreversible is due to a loss of porosity, which is a macroscopic, morphological consequence of viscous flow of the amorphous material in the rubbery state at $T > Tg$, whereby the porous glass relaxes to a fluid, incapable of supporting its own weight, which then becomes non-porous and more dense. Subsequent recooling to $T < Tg$ results in a non-porous glass of the original composition. The only irreversible aspect of Tg- governed collapse is loss of porosity (Levine and Slade, 1988a).

1.7.2 MECHANISM OF COLLAPSE

All of the collapse phenomena mentioned above are translational diffusion-controlled processes with a mechanism involving viscous flow above Tg. Levine and Slade (1988b) proposed a general mechanism for collapse, based on Williams-Landel-Ferry (WLF) theory described earlier for amorphous materials. The mechanism is as follows: As the Tg falls below the ambient temperature due to plasticisation by water, polymer free volume increases. This leads to an increase in the segmental mobility of the polymer chains. As a result, the viscosity (η) of the dynamically constrained solid falls below a characteristic value η_g at the glass transition temperature, Tg, allowing the glass-to-rubber transition and viscous liquid flow to occur. In this liquid state, diffusion-controlled relaxations (including structural collapse) are free to proceed at rates determined by the WLF equation, where rates increase exponentially with increasing ΔT above Tg.

1.7.3 STICKINESS, AGGLOMERATION, AND CAKING

Stickiness refers to the tendency for adhesion between particles of similar or different type. This may be temporary and does not necessarily mean that caking will occur. The 'sticky point' temperature marks the transition from a stable dry powder to a viscous state and is related to the collapse phenomena (Tsourouflis et al, 1976). The cause of the stickiness is the plasticisation of particle surfaces, allowing a sufficient decrease in surface viscosity for adhesion between particles. Figure 1.9 shows the surface of two free-flowing particles being plasticised to form cohesive, sticky particles (Roos, 1995). Downton et al (1982) found that lowering of the surface viscosity to between 10^6 and 10^8 Pa s by water plasticisation was sufficient to allow stickiness to occur in the mixture of fructose and sucrose studied. The same viscosity range was also found to apply to a mixture of maltodextrin, sucrose, and fructose (Wallack and King, 1988).

An example of where stickiness can cause a problem is during the spray-drying of hygroscopic, amorphous materials. Stickiness occurs between particles which are insufficiently dry and they collide with one another or with the walls of the spray dryer, leading to lower product yields and powder-handling problems (Downton et al, 1982).

The process of agglomeration, where dry powders are carefully re-wetted to allow them to stick together into clumps which are then re-dried is related to this collapse phenomena (To and Flink, 1978b). Downton et al (1982) describes this as an attribute of

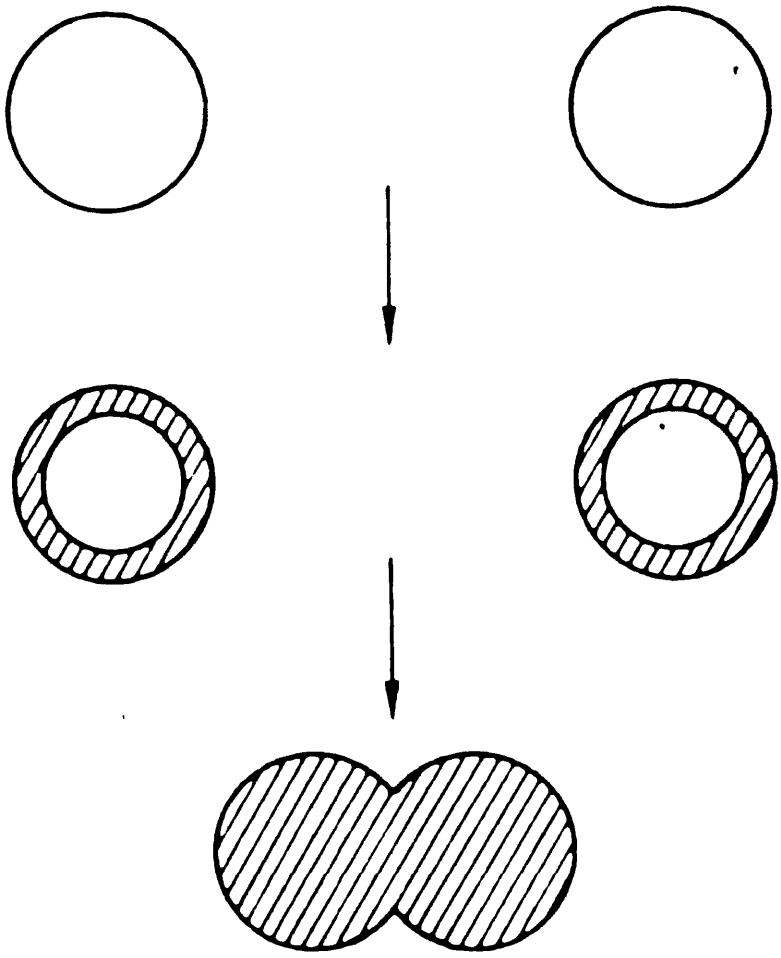

Figure 1.9 *Schematic representation of the process of stickiness and caking in amorphous powders (reproduced from Downton et al, 1982). The shaded areas represent moisture sorption. The free-flowing particles (top) change to cohesive, sticky particles on water sorption on the particle surface (middle). Formation of liquid bridges results in caking of the particles (bottom).*

the stickiness in that it can be used in the process of agglomeration. This is a process of controlled stickiness where particles are deliberately exposed to moisture and repeated contact between particles, so that particle surfaces become sticky and clusters form through adhesion between particles (Masters and Stoltze, 1973).

If the contact between sticky particles is allowed for sufficient time, caking results which involves the formation of permanent aggregates that form a hardened mass due to adhesion between particles, resulting in the loss of free-flowing properties of the powder (Roos, 1995). An example of this is the storage of milk powder at high humidities allowing the lactose glass to sorb moisture, allowing the milk particles to become sticky and adhere to each other. On crystallisation of the lactose, the presence of undesirable solid lumps is found (White and Cakebread, 1966).

Both the onset and rate of caking do not necessarily require liquefaction of the whole particle; only part of the surface of the particle needs to be wetted (Peleg, 1983). Caking of amorphous powders results from the change of the material from a glassy state to the less viscous liquid-like rubbery state, which then allows viscous flow and formation of liquid bridges between particles (Roos, 1995 and Wallack and King, 1988). The formation of liquid bridges between particles is an important phenomenon, and may be caused by the following reasons (Peleg, 1977):

(1) Moisture absorption
(2) Melting of component compounds (e.g. lipids)
(3) Excessive liquid ingredient
(4) Water released during crystallisation of amorphous sugars
(5) Accidental wetting of the powder or equipment.

Downton et al (1982) suggested that if two particles come in to contact, depending on whether or not sufficient liquid can flow between the particles to build a bridge that is sufficiently strong to withstand subsequent mechanical processing, then the particles may or may not stick together. Figure 1.9 shows the formation of a liquid bridge between the particles and plasticisation of the whole particle, resulting in a caked, plasticised material.

1.8 THE AMORPHOUS TO CRYSTALLINE TRANSITION

The process of crystallisation is one of ordering, where randomly organised molecules in a solution or a melt take up regular positions in the crystalline solid (Byrn, 1982). The crystallisation of amorphous materials from the solid-state is dependent on sufficient translational and rotational molecular mobility to allow the molecular rearrangements to take place (Ahlneck, 1993). Crystallisation of amorphous materials is triggered by an increase in temperature and/or the addition of a plasticiser such as water; the effect of this is to increase the molecular mobility of the amorphous material (Yonemochi et al, 1999).

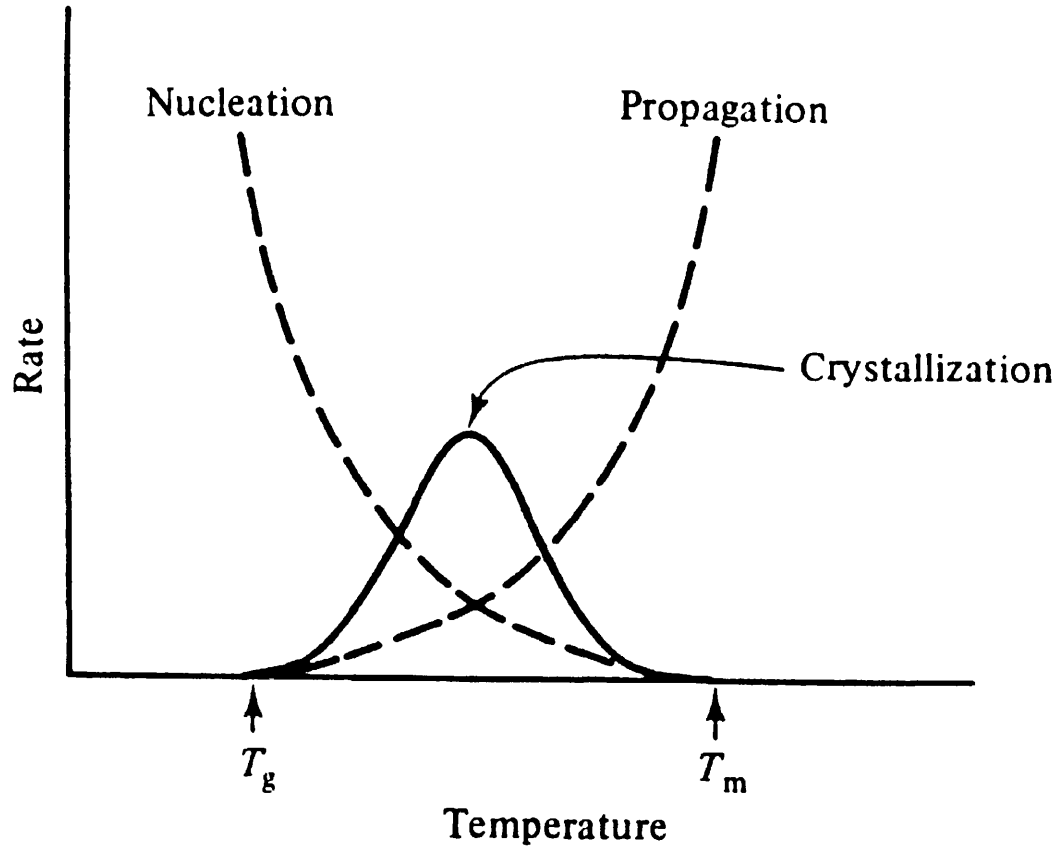

Figure 1.10 *Schematic of the rates of nucleation and propagation (crystal growth) associated with crystallisation from the amorphous state between Tg and Tm, with the overall rate of crystallisation occurring between Tg and Tm. Reproduced from Slade and Levine (1988a).*

The two main stages of crystallisation are nucleation and propagation (or crystal growth). Upon crystallisation, an amorphous material must go through intermediate states that can be considered as free energy barriers that can reduce or prevent the transformation from the metastable amorphous state to the stable crystalline state (Van Scoik and Carstensen, 1990).

Nucleation involves the formation of a critical nucleus, whereas propagation (crystal growth) involves the deposition of molecules on to crystal faces (Byrn, 1982). There are two main paths for nucleation: homogeneous and heterogeneous. Homogeneous nucleation occurs spontaneously and is where the molecules of the material come together and form the critical nuclei. Heterogeneous nucleation involves the presence of impurities or foreign bodies that can act as nucleating sites (Roos, 1995). In heterogeneous nucleation, the free energy needed for formation of the critical nucleus is reduced (Van Scoik and Carstensen, 1990).

Figure 1.10 shows the rates of nucleation and propagation processes that make up the crystallisation process. The rate of nucleation increases with the degree of supercooling (with a decrease in temperature). However, this is offset against the increase in viscosity as the temperature is decreased (Yoshioka et al, 1994) since nucleation is a liquid-state phenomenon that requires molecular mobility, and such mobility is much reduced below Tg (Levine and Slade, 1988a). However, this does not exclude crystallisation from occurring below Tg since Yoshioka et al (1994) found that crystallisation of indomethacin took place down to 30°C below its Tg when investigated using extended time scales of the order of days (rather than normal experimental time scales in the order of minutes to hours). They suggested that sufficient rotational molecular mobility exists below Tg for crystallisation of indomethacin to occur during the time period used (days), and that such rotational molecular motions would be enough to allow the very nearest neighbours to successfully form a critical nucleus followed by crystal growth. It was found that a temperature 50°C below Tg was required to reduce the rotational molecular mobility sufficiently to prevent crystallisation over a time period of several months (Yoshioka et al, 1994). Hancock et al (1995) also found that a temperature at least 50°C below the Tg of indomethacin was required to slow down the molecular motions to a level where they are insignificant on a time scale typical of pharmaceutical products (in the order of years).

1.9 PROCESSING OF SOLIDS

1.9.1 INTRODUCTION

Formulation of a pharmaceutical material in the solid state involves subjecting the material to a variety of processes. Processing of pharmaceutical solids can lead to significant transformations from the crystalline form to a disordered form (activation). The extent of activation depends on the energy input during processing (Ahlneck, 1993). Activation can occur throughout the entire crystal (thereby forming an amorphous material) or may be localised to the particle surface of crystalline materials to form so-called 'frictional hot spots' (Elamin et al, 1995). Such local regions of molecular disorder exhibit greater chemical reactivity (Huttenrauch et al, 1985) and solubility (Waltersson and Lundgren, 1985, Elamin et al, 1994). Elamin et al (1994) found that milling of griseofulvin (an insoluble drug) leads to an increase in its solubility due to the introduction of disorder at the particle surface. Activation arises from a combination of greater molecular mobility and exposure of more reactive chemical groups (Ahlneck and Zografi, 1990).

1.9.2 COMMINUTION AND MIXING

Comminution is used for the particle size reduction of materials leading to a greater surface area, and a greater bioavailability through effects on the dissolution rate (Otsuka and Kaneniwa, 1990). However, comminution is a high-energy process that can lead to activation of the material. The effect of such 'mechanical activation' is shown in Figure 1.6 where the crystalline structure at the top undergoes mechanical activation (e.g. comminution) to form the disordered structure in the centre. During the comminution process, particles that undergo size reduction are subjected to stress and thereby become deformed. When the deformation occurs, cracks in the particles can be formed. As the cracks/fracture of the particles occur, energy will be released that may in turn generate new cracks and fractures. After the comminution process is completed, the cracks and defects produced during the size reduction process will remain. This means that local regions of particles or 'hot spots' storing energy are created at the surface of the particles (Ahlneck, 1993). Various comminution techniques such as milling (Krycer and Hersey, 1981), grinding (Lerk et al, 1984b, Otsuka and Kaneniwa, 1990), and micronization (Ward and Schultz, 1995) have been found to induce disordered regions. Comminution of materials for inhalation delivery is particularly important since particle sizes of less than 5μm are required for successful lung deposition (Buckton et al,

1995a). Otsuka and Kaneniwa (1990) found that grinding of cephalothin sodium for up to 10 hours reached an equilibrium value of 50% crystallinity. Otsuka et al (1991) also found that solid-state isomerisation of lactose takes place on grinding. They found that after 10 hours grinding, 10% of α-lactose was transformed to β-lactose. In the case of anhydrous β-lactose, it was found that 20% of the β-lactose was transformed into α-lactose (Otsuka et al, 1991). Chloramphenicol palmitate occurs in three polymorphic forms, designated A, B, and C. Kaneniwa and Otsuka (1985) found that grinding of chloramphenicol palmitate lead to the transformation of the therapeutically active forms B and C to the less effective form A.

The process of mixing can involve large amounts of material being transported and rearranged in the mixer, leading to friction between particles (Ahlneck, 1993). Konno et al (1986) found that mixing can also produce amorphous material. They found that two crystalline materials, aspirin and phenacetin, when mixed with an adsorbent at 25°C lead to the production of amorphous material.

1.9.3 DRYING PROCESSES LEADING TO DISORDER

Huttenrauch and Keiner (1979) found that heat drying of crystalline α-lactose monohydrate under vacuum at 125-126°C led to the crystallinity of lactose decreasing to nearly 50%. Spray-drying is a process where dissolved material is transformed into a dried particulate form by spraying the material into a drying air stream (Chidavaenzi et al, 1997). It is well known that spray-drying can lead to the production of amorphous material. Elamin et al (1995) showed using x-ray diffraction that spray-drying of sucrose and lactose leads to the amorphous forms of these materials. Buckton et al (1995a) used microcalorimetry to detect the amorphous material that resulted from spray-drying of salbutamol sulphate. Lyophilisation (freeze-drying) is a process where the material to be dried is first frozen then heated under high vacuum, so that the frozen liquid undergoes sublimation to leave the solid, dried components (Rankell et al, 1986). Freeze-drying of materials can lead to the production of the amorphous form. Pikal et al (1978) freeze-dried a 20% aqueous solution of cephalothin sodium to produce the amorphous form. Freeze-drying of an aqueous solution of lactose also produces the amorphous form (Berlin et al, 1971).

1.9.4 EFFECT OF WATER ON LOCALLY DISORDERED MATERIALS

As described above, processing of pharmaceutical solids can lead to the production of local regions of molecular disorder. These local regions of disorder would exhibit a greater uptake of water than would be expected on the crystalline portions of the solid (Ahlneck and Zografi, 1990) in a similar manner to the uptake of water in to totally amorphous materials described in section 1.6. The sorption of small amounts of water may not be significant when considered in terms of the particle as a whole, however, since the amorphous regions act as targets for water sorption the effects may be more significant due to the plasticising ability of water.

Amount of moisture (%)	Amount of amorphous material (%)	Moisture content in amorphous material (mg water/100mg solid)	Glass transition temperature (^{o}C)
0.1	0.5	20	9
	1	10	27
	2.5	4	45
	5	2	49
0.5	0.5	100	-73
	1	50	-36
	2.5	20	9
	5	10	27

Table 1.1 *Moisture content and glass transition temperature of the amorphous portion of sucrose if a total of 0.1% and 0.5% moisture is taken up (reproduced from Ahlneck and Zografi, 1990).*

This can be explained using sucrose as an example. Table 1.1 shows the effect of 0.1% and 0.5% total moisture uptake by the sucrose for various percentages of amorphous structure between 0.5 and 5% of the total solid, assuming that all of the water is taken up by the amorphous regions (Ahlneck and Zografi, 1990). The effect of the moisture

on the Tg of sucrose is also shown in Table 1.1. Table 1.1 shows that a total moisture content of only 0.1%, if concentrated in to 1% of the total mass of the solid that is amorphous, can lower the Tg of sucrose to a temperature close to room temperature. Table 1.1 also shows that a total moisture content of 0.5% (commonly encountered in pharmaceutical solids) when concentrated in to the amorphous regions can lower the Tg of sucrose even further (Ahlneck and Zografi, 1990). This 'amplification' effect increases for a given total moisture content (e.g. 0.5%) as the amount of amorphous material decreases, with a corresponding decrease in the Tg (Ahlneck and Zografi, 1990). The higher molecular mobility of the amorphous regions of the solid can be enhanced by plasticisation of the solid due to water absorption. This can have the effect of recrystallisation of the amorphous material (Ahlneck and Zografi, 1990).

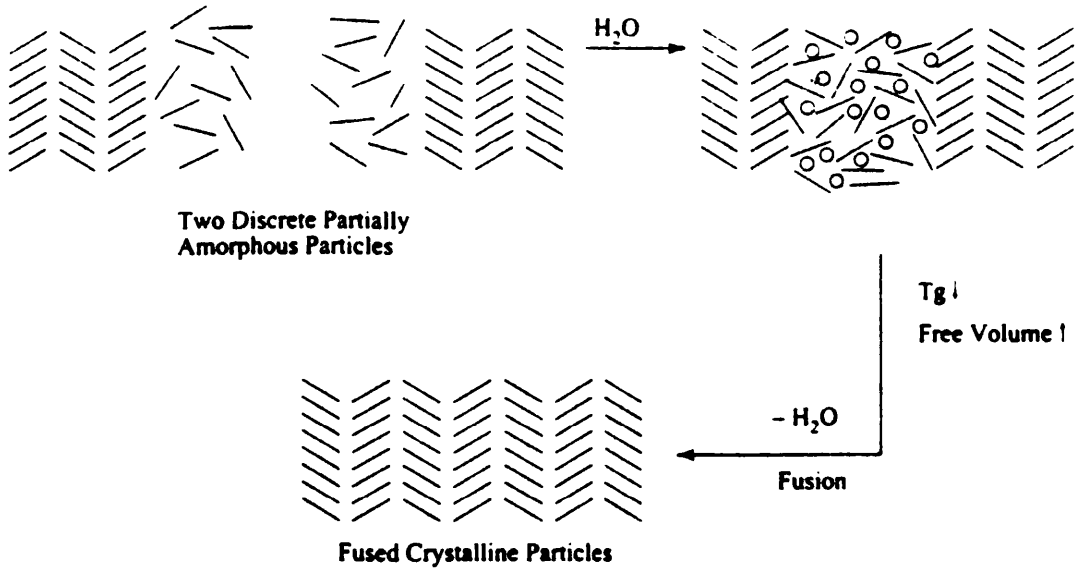

Figure 1.11 *Schematic representation of the crystalline surfaces of two discrete particles after milling, and the effects of water absorption (circles) in to the amorphous regions (reproduced from Ward and Schultz, 1995)*

Figure 1.11 shows the surface of two discrete particles that have been rendered amorphous by processing (e.g. milling). This results in a partially amorphous material that when exposed to water vapour and/or heat can lead to significant changes in the

state of the powder. Figure 1.11 shows that if the particles are in contact, on exposure to water (represented by circles) the amorphous regions of the particles absorb a sufficient amount of water to decrease the Tg, allowing crystallisation to take place. As the molecular mobility at the surface of the particles increases, the material then rearranges in to the stable crystalline form, with expulsion of water upon crystallisation (Ward and Schultz, 1995). This fusion between the original milled particles may cancel out the beneficial particle size reduction effect of milling that is particularly important for inhalation products (Ward and Schultz, 1995).

1.10 MICROWAVE DRYING

Electromagnetic waves are waves of electric and magnetic forces, where a wave motion is defined as propagation of disturbances in a physical system (Stuchly and Stuchly, 1967). Microwaves derive from the electromagnetic spectrum and have high frequencies above 500 MHz (Metaxes and Meredith, 1983). The microwave frequencies that have been allocated to industrial, scientific, medical, and domestic uses are 915MHz and 2.45GHz (Doyle and Cliff, 1987).

A non-conducting material (or an insulating material) in which polarisation takes place in an electric field is called a dielectric (Metaxes and Meredith, 1983). All matter is made up of positively and negatively charged particles, and in the normal undisturbed position there are an equal number of positively and negatively charged particles, resulting in an overall neutral material (Goldblith, 1967). The microwave heating effect is due to the ability of the electric field to polarise charges in the material and the inability of this polarisation to follow the very fast reversals of the electric field (Metaxes and Meredith, 1983). If the non-conducting (dielectric) material is placed in an electromagnetic field, the charged molecules of the material are driven first one way and then another way in an attempt to follow the fast reversals of the alternating electric field, as shown in Figure 1.12. In an attempt to go to the proper positive and negative poles, intermolecular friction is created between the molecules and this results in the heating effect of microwave energy. The very fast reversals of the electric field is demonstrated by considering one of the microwave frequencies used, 915MHz, where the molecules oscillate back and forth 915 million times per second (Goldblith, 1967).

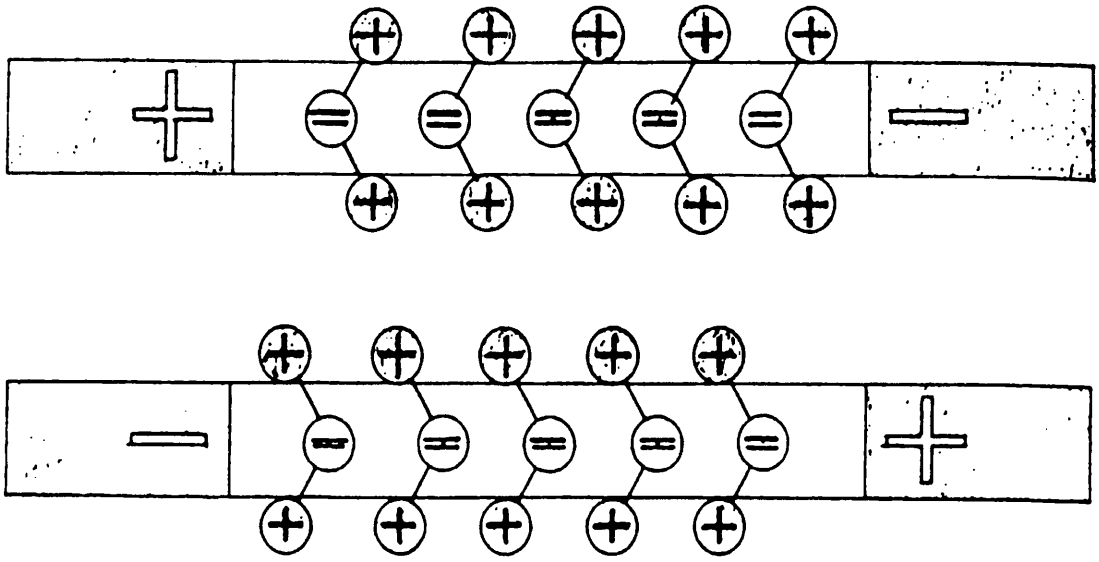

Figure 1.12 *Schematic representation showing oscillation of the charged particles of a dielectric in an alternating electric field. Reproduced from Goldblith (1967).*

When charged particles are displaced from their equilibrium positions, this leads to induced dipoles that respond to the applied field. This type of induced polarisation mainly involves electron displacement around the nuclei, and is referred to as electronic polarisation. If the atomic nuclei within a molecule are displaced, due to unequal charge distribution, then this is referred to as atomic polarisation. Some dielectrics have permanent polarisation (dipoles) which is due to the asymmetric charge distribution of the unlike charge partners within a molecule. These charges tend to reorientate under a changing electric field, referred to as orientation polarisation (Metaxes and Meredith, 1983).

Microwave drying uses a selective effect where only materials of a suitable structure are heated. An example is that water is heated 100 times quicker than some pharmaceutical excipients such as lactose (Doyle and Cliff, 1987). This selective effect means that water can be efficiently removed with little or no effect on the dry areas of the material. The properties of the material are also important. The dielectric constant represents the material's ability to store electrical energy (Stuchly and Stuchly, 1983) and is related to

the polarisability of the material (Doyle and Cliff, 1987). The material's 'loss factor' is a relative measure of how easily a material will be heated by microwave energy (Doyle and Cliff, 1987). Water has a high loss factor relative to lactose and is thus more easily heated by microwave energy. Microwave drying is thus most effective for removing a solvent that absorbs microwave energy, such as water, from a solid that only slightly absorbs microwave energy, such as lactose.

The pairing of microwave and vacuum drying allows more efficient drying with the vacuum removing the moisture that is removed from the material due to microwave drying (Lucisano and Poska, 1990). The presence of the vacuum allows drying of materials at a lower temperature. At the surface of a liquid, some molecules have sufficient energy to overcome the attractive forces that are present between molecules in the liquid state. These higher energy molecules escape from the liquid to form a vapour phase. If a constant temperature is maintained, then equilibrium is reached between the vapour and liquid states; the pressure exerted by the vapour at equilibrium is then called the 'vapour pressure' of the material. The boiling point of a liquid occurs at a temperature at which the vapour pressure of the liquid is equal to the surrounding pressure. The normal boiling point is quoted at a vapour pressure of 1 atmosphere (atmospheric pressure). If the surrounding pressure is reduced, such as in a vacuum, the temperature at which the liquid achieves the same lower vapour pressure as the surroundings is lower, and hence the boiling point at reduced surrounding pressure is lower (Chambers et al, 1989). This lowering of the boiling point of the liquid when drying under vacuum then allows drying at lower temperatures.

1.11 LACTOSE

1.11.1 INTRODUCTION

Lactose is extensively used as a diluent in tablets and capsules for pharmaceutical formulations. It is a disaccharide composed of galactose and glucose, and consists of two isomeric forms α- and β-lactose, shown in Figure 1.13. Lactose has been identified with three crystalline forms: α-lactose monohydrate, α-anhydrate and β-anhydrate, and also an amorphous form (Otsuka et al 1991, 1993). The production of α- and β-lactose isomers is dependent on the temperature. If lactose is dissolved in water at a temperature below 93.5°C, then crystallisation of the α-lactose isomer takes place. However, if the temperature is above 93.5°C, then the β-lactose isomer crystallises from

the aqueous solution (Olano et al, 1983). There is also a difference in the way α- and β-lactose crystallise. When β-lactose is crystallised, no water is incorporated into its crystal lattice, and therefore β-lactose exists in an anhydrous form only. This is different from α-lactose, which can exist as a monohydrate and anhydrous crystalline forms (Lerk et al, 1984).

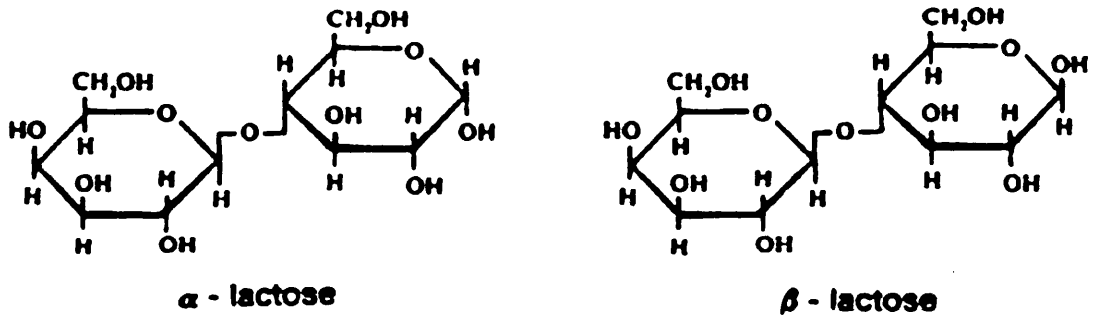

Figure 1.13 Structural formula of α- and β-lactose (Reproduced from Handbook of Pharmaceutical Excipients, 1986)

1.11.2 PHARMACEUTICAL APPLICATIONS OF LACTOSE POWDERS

α-lactose monohydrate is the most common of the lactose powders and is mainly used for granulation formulations (Angberg, 1995). Anhydrous lactose powders, with different proportions of anhydrous α- and β-lactose, are mainly used as direct compression excipients (Angberg et al, 1991). Bolhuis et al (1995) found that anhydrous lactose is a suitable direct compression excipient for use in tabletting. Amorphous lactose can be formed by rapid drying of dissolved lactose from solution (as in spray-drying) or by mechanical activation (as in milling). Commercial spray-dried lactose is used as a direct compression excipient and consists of a mixture of α-lactose monohydrate and amorphous lactose. The amorphous lactose comes from the rapid drying of dissolved lactose during spray-drying (Sebhatu et al, 1994b). The amorphous portion of the commercial spray-dried lactose is responsible for the good qualities as a direct compression excipient, such as good binding and flow properties (Sebhatu et al, 1994b).

1.11.3 THERMAL ANALYSIS OF LACTOSE

Thermal analysis of α-lactose monohydrate shows a water loss (dehydration) peak at ca. 145°C and a melting peak at ca. 220°C. A 5% weight loss is detected, usually between 100°C and 150°C, representing the loss of the crystal water and corresponding to the dehydration peak at ca. 145°C (Otsuka et al, 1991).

It is well known that various processes such as spray-drying (Elamin et al, 1995), freeze-drying (Berlin et al, 1971), and milling (Krycer and Hersey, 1981) lead to the production of amorphous lactose. The detection of amorphous lactose has been studied using microcalorimetry, which accurately measures the heat flow accompanying the amorphous to crystalline transition on exposure to water vapour. The measurements are carried out at conditions that favour crystallisation e.g. suitable RH and temperature (Sebhatu et al, 1994a). DSC (differential scanning calorimetry) and XRPD (X-ray powder diffraction) can also be used to detect amorphous material; however, the minimum amount of amorphous material that can be accurately detected is 10% (Angberg, 1995 and Saleki-Gerhardt et al, 1994). Bulk analytical techniques such as DSC and XRPD are unable to accurately detect the small amounts of amorphous material (< 10%) that is produced at the surface of the particle as a result of processing. However, since the amorphous regions of the solid preferentially absorb water over the crystalline regions, microcalorimetry is able to detect even small amounts of amorphous material through its use of water vapour sorption to induce crystallisation of the amorphous regions (Elamin et al, 1995 and Angberg et al, 1995). Crystallisation of amorphous spray-dried lactose can lead to a mixture of α- and β-lactose (Sebhatu et al, 1994a and Briggner et al, 1994). β-lactose exists as a stable anhydrate and thermal analysis of β-lactose shows that a melting peak at about 230°C occurs, with no other thermal transitions occurring below this temperature (Berlin et al, 1971).

1.11.4 MUTAROTATION OF LACTOSE

Berlin et al (1971) found that there was no measurable water sorption by β-lactose below 97% RH. It was then concluded that β-lactose is completely non-hygroscopic below 97% RH. However, it was also found that above 97% RH, β-lactose sorbs sufficient moisture to form a concentrated solution and undergo mutarotation to α-lactose (Berlin et al, 1971). Angberg et al (1991) investigated the effect of water uptake on anhydrous lactose consisting of 31% α- and 69% β-lactose. It was found that the

incorporation of water in to the anhydrous α-lactose could be followed using microcalorimetry at 58% RH. When the anhydrous lactose was studied using microcalorimetry at 94% RH, it was found that as well as the incorporation of water, the anhydrous β-lactose mutarotates to anhydrous α-lactose with subsequent incorporation of hydrate water to form α-lactose monohydrate. Mutarotation was also found to occur at lower humidities up to 75% RH. At 75% RH, it was found using gas chromatography (GC) that mutarotation of β-lactose occurs to a more limited extent when compared to mutarotation at 94% RH. However, it was also found that the mutarotation occurs in parallel with the incorporation of water in to the original 31% anhydrous α-lactose. An explanation for this may be that certain regions in the powder have a higher water content despite the overall humidity being relatively low, thus allowing mutarotation to occur (Angberg, 1991). As described earlier, this could be due to the 'amplification' effect of water sorption by a material that is activated by processing to produce local regions of disorder.

Mutarotation of lactose may also occur during the heating of lactose. Olano et al (1983) found that mutarotation of α-lactose monohydrate proceeds below the melting point, and that unstable anhydrous α-lactose may be an intermediate in the transformation. Lerk et al (1984a) showed that unstable anhydrous α-lactose, formed when α-lactose monohydrate is heated under vacuum at 100-130°C, displayed an increase in the β-lactose content when heated to 180°C in the DSC. A significant increase in the β-lactose content was also noted for α-lactose monohydrate and stable anhydrous α-lactose, formed by desiccation over methanol, at a temperature of ca. 220°C (Lerk et al, 1984a). The relative humidity has been found to affect the mutarotation of lactose during heating (Olano et al, 1983). Olano et al (1983) found that in the absence of water vapour, lactose can be heated up to 170°C at 4°C/min without alteration of the initial isomeric composition of lactose. The maximum transformation occurred when the humidity used was 100% RH, leading to the presence of up to 95% β-lactose. The rate of mutarotation increased with temperature, and also depended on the crystalline form of lactose. Stable anhydrous α-lactose mutarotated at the slowest rate, and unstable anhydrous α-lactose and α-lactose monohydrate at the fastest rates.

1.11.5 SELECTION OF LACTOSE FOR DRYING INVESTIGATIONS

Lactose has been selected as a model substance for microwave-vacuum drying investigations since, as described above, during processes such as spray-drying, freeze-drying, and milling, crystalline lactose can be transformed in to the amorphous form. The detection of amorphous lactose, particularly small amounts due to processing, has been well established so that the effect of microwave-vacuum drying investigations can be easily detected.

1.12 MALTODEXTRINS

1.12.1 INTRODUCTION

Maltodextrins are starch-derived materials prepared by controlled hydrolysis of corn starch with acid and/or enzyme (Li and Peck, 1990). They can be used as direct compression excipients. This has the advantages of lower handling and processing costs, relative to the wet granulation method. The hydrolyisis of starch down to glucose polymers can be controlled by using either enzymic (α-amylase) or acidic (hydrochloric acid) means. However, acid hydrolysis results in the production of too much free dextrose. Therefore, commercially available maltodextrins are produced by controlled enzymic hydrolysis (Kennedy et al, 1995). Maltodextrins consist of α-D-glucose units linked together to form glucose polymers. Li and Peck (1990) studied maltodextrins using x-ray diffraction, and found that the maltodextrins had diffused diffraction patterns demonstrating their amorphous nature.

1.12.2 PRODUCTION

Starch slurry is first liquefied by heating to 70-90°C at neutral pH. Acid- and enzyme-catalysed hydrolysis then takes place. Acid-catalysed hydrolysis to a dextrose equivalent (explained below) of 5-15 is followed by neutralisation, then further hydrolysis with bacterial α-amylase to the desired dextrose equivalent. After hydrolysis, the pH of the solution is adjusted to 4.5 and filtration carried out to remove any residual fibre, lipid or protein. The solution is then carbon refined, followed by spray-drying to a white powder with 3-5% moisture. The material is then packaged or agglomerated then packaged.

1.12.3 DEFINITION

The maltodextrins are defined as having a dextrose equivalent (DE) of less than twenty (Mollan and Celik, 1993). DE value is measured as the amount of reducing sugars present and is expressed as percentage of dextrose on a dry weight basis. Figure 1.12 shows a schematic of the DE values. By definition, dextrose itself has a DE value of 100. On the opposite end of the scale is starch with a DE value of zero. Maltodextrins are defined as having a DE value of less than twenty, and so occupy the region of the scale in Figure 1.12 highlighted in blue. Starch hydrolysis products having a DE value greater than twenty are called corn syrup solids. Figure 1.13 shows the components that constitute a maltodextrin mixture. It shows that the maltodextrin mixture is composed of amylose (a linear glucose polymer), amylopectin (a branched glucose polymer), and smaller saccharides up to the monomer glucose. The composition for each maltodextrin varies depending on the DE value, with a high DE maltodextrin having a greater proportion of glucose (dextrose) than a low DE maltodextrin.

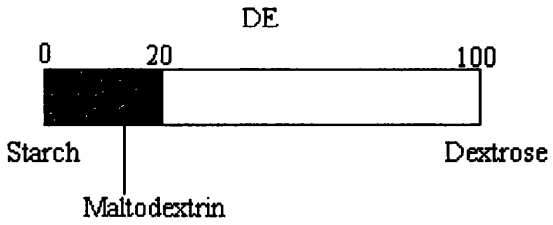

Figure 1.14 *Schematic diagram showing the Dextrose Equivalent (DE) value for the maltodextrins*

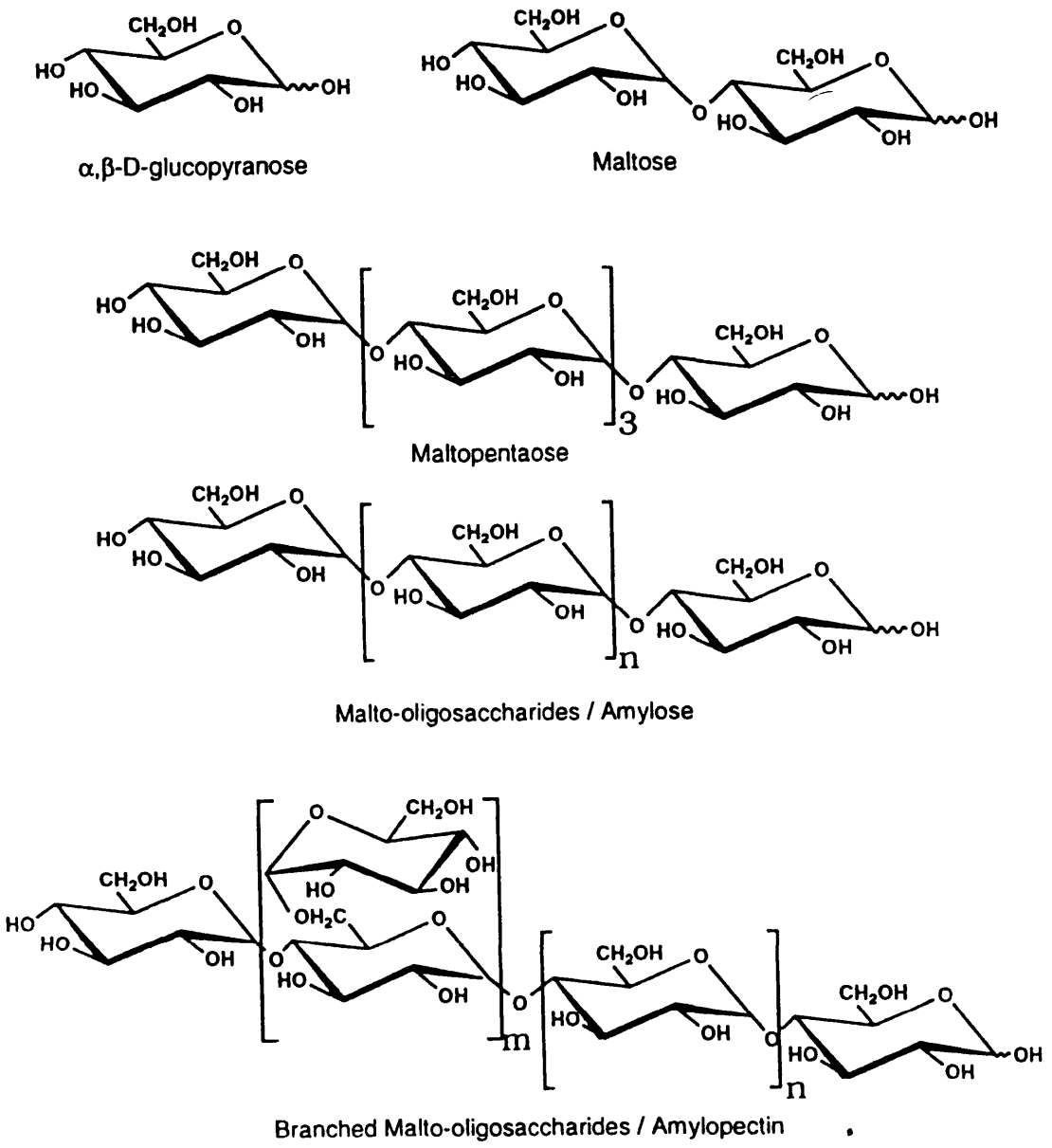

Figure 1.15 *The components of a maltodextrin mixture (reproduced from Kennedy et al, 1995).*

1.12.4 GLASS TRANSITION AND MOLECULAR WEIGHT

The maltodextrins were found to have high Tg values between 140°C and 190°C when measured by DSC. It was found that the Tg values decreased as the moisture content increased, as a result of the plasticisation by water (Roos and Karel, 1991a). This was in agreement with the plasticisation effects of water on maltose, maltotriose, and maltohexaose (Orford et al, 1989). The effect of this plasticisation was to produce a structural change in the maltodextrins from a powder to a clear paste (Roos and Karel, 1991a). Mollan and Celik (1995) noted that maltodextrin powders appeared to 'gel' by visual observation after storage for 2 weeks at above 75% RH.

It was found that the Tg values of the maltodextrins were lower than that based on their average molecular weights. A DE = 5 maltodextrin (average MW 3600) was found to have a similar Tg value to maltohexaose (MW 991), and a DE = 20 maltodextrin (average MW 900) a similar Tg value to maltotriose (MW 504) (Roos and Karel 1991c and Orford et al, 1989). This was thought to be due to the presence of low molecular weight substances in maltodextrin mixtures (see Figure 1.15). Low molecular weight compounds in carbohydrate mixtures, such as maltodextrins, may significantly decrease the effective Tg of the high molecular weight compounds in the mixture (Roos and Karel, 1991c).

1.12.5 FLOW PROPERTIES

Maltodextrins can be used as direct compression excipients and thus the flow property of the material is an important factor to consider. Mollan and Celik (1995) investigated the effect of humidity on the flow properties of the maltodextrins and compared them to other commonly used direct compression pharmaceutical excipients. They found that at high humidities, the flow rate for the maltodextrins decreases. An example is for Maltrin M500 maltodextrin where the flow rate changes from 162g/min at 11.3% RH to 140g/min at 70.9% RH. In comparison Fast-Flo lactose changes from 548g/min at 11.3% RH to 554g/min at 70.9% RH. Mollan and Celik (1995) recommended that when the maltodextrins are used as direct compression excipients, they must be used in humidity-controlled environments to avoid the absorption of water and the resulting detrimental effects on powder flow properties.

1.12.6 COMPRESSION PROPERTIES

Li and Peck (1990a) investigated the relative density of maltodextrin compacts to assess the effect of humidity up to 52% RH. The relative density was calculated using the ratio of the apparent density of the compact to the particle density of the powdered maltodextrin. They found that an increase in moisture content facilitated powder consolidation. Mollan and Celik (1995) also investigated the effect of pre-compaction humidity storage of the powders on the compression properties of maltodextrin compacts. They found that a high pre-compaction humidity resulted in compacts with higher tablet strength compared to samples that were stored at a low humidity. This effect is thought to be due to the moisture acting as an internal lubricant leading to powder consolidation being facilitated (Li and Peck, 1990a). The tensile strength for compacts after pre-compaction storage up to 52% RH was investigated (Li and Peck, 1990a). It was found that the tensile strength of the maltodextrins increased markedly with increase in humidity up to 52% RH. This was thought to be due to the lubrication effect of water improving the force transmission from the upper to lower punch resulting in greater consolidation.

The effect of degree of polymerisation (DP) was also investigated (Li and Peck, 1990a). It was found that at a given compression pressure, the maltodextrins with a lower degree of polymerisation (a higher DE value) formed tablets with a higher relative density. It was hypothesised that the maltodextrins with a lower degree of polymerisation (a higher DE value) are able to deform more easily to fill inter-particle spaces in a compact; this ability is thought to be due to the greater proportion of low molecular weight saccharides in the low degree of polymerisation (high DE) maltodextrins (Li and Peck, 1990a).

1.12.7 SELECTION OF MALTODEXTRINS FOR INVESTIGATION

When the maltodextrins are used as diluents/fillers in pharmaceutical formulations, they can form a large proportion of the formulation. It is therefore important to have knowledge of the effects that humidity can have on the maltodextrins. As described above, the humidity level can affect the flow properties, density, and compression properties of the maltodextrins. It is known that maltodextrins undergo changes in physical form on increasing humidity (Roos and Karel, 1991a), but these have not been investigated further in the literature. The maltodextrins were therefore selected for investigation of the effect of water interaction with the maltodextrins.

1.13 AIMS OF THE THESIS

The aim of this thesis is to study the transitions occurring as a result of water interaction with carbohydrates, and the resulting changes in physical form. The effect of drying processes on the introduction of the amorphous form in to a model pharmaceutical material (lactose) will be investigated. The interaction of water with the maltodextrin series will be studied. This will include the water sorption behaviour, and the effect of water uptake on the glass transition and collapse phenomena for the maltodextrins. The effect of water uptake on the physical form of the maltodextrins will be studied. The nature of the water interaction with maltodextrins will be studied using the thermodynamics of absorption.

Chapter 2

Materials and methods

2.1 MATERIALS

2.1.1 Lactose monohydrate

α-lactose monohydrate (Lactochem lactose, Borculo whey products, Saltny, UK) was used as received in drying investigations.

2.1.2 Spray-dried lactose

Spray-dried lactose (Fast-flo lactose-316, ex Univar Plc, Croydon, UK) was used as received in drying investigations.

2.1.3 Maltodextrins

Maltodextrins (Maltrin, Grain Processing Corporation, Iowa, USA) were used as received. Maltodextrins used during investigations were between Dextrose Equivalent (DE) values 5 and 20.

2.2 METHODS

2.2.1 THERMOGRAVIMETRIC ANALYSIS (TGA)

2.2.1.1 Introduction

Thermogravimetric analysis uses a thermobalance to monitor the sample weight as a function of temperature. This can be carried out using a constant heating or cooling program or maintaining a fixed temperature. Thermogravimetric analysis has been used by Otsuka et al (1991) to quantify the proportions of adsorbed and crystal water in crystalline monohydrate and anhydrous lactose during grinding.

2.2.1.2 Instrumentation

A TGA 2950 Thermogravimetric Analyser (TA Instruments, New Castle, DE 109720, USA) was used to investigate changes in the sample weight as a function of temperature. The TGA is made up three components: the controller (the computer), the module (TGA instrument), and the heat exchanger (water bath). The module consists of two main components: the balance chamber and the furnace. Figure 2.1 shows a schematic representation of the TGA 2950.

2.2.1.3 Balance

The sample hang down wire connects the sample pan to the balance arm in the balance chamber, via a kapton loop. A reference arm is also connected to the opposite side, with reference hang down wire and tare pan. The TGA uses the null-balance principle. The balance arm is kept in the horizontal position using a flag on top of the balance arm which blocks light from a LED from reaching two photodiodes. If there is any weight change in the sample pan, the position of the balance arm and flag will move to cause an unequal amount of light to reach the two photodiodes. The control circuitry applies a restoring force to bring the balance arm back to the horizontal (null) position. The current required for the restoring force is directly proportional to the change in sample mass, and is recorded by the software as a weight signal. The null-balance principle ensures that the sample pan remains at a constant position within the furnace. Keeping the sample in the same position ensures that temperature differences in the furnace are avoided thus providing accurate temperature control. The balance is capable of detecting a weight change of 0.1μg, and has an accuracy of 0.1%. It is thermally isolated from the furnace to reduce any interference.

2.2.1.4 Furnace

The furnace uses a low mass alumina resistance wound that can be heated up to 1000°C. Heating and cooling rates can be programmed from 0.1 to 200°C/minute in 0.1°C increments. A purge gas must always be used to prevent contamination of the furnace and balance chamber. The purge gas used was nitrogen and the flow was divided into two, with flow rates of 60ml/min for the purge flow through the furnace, and 40ml/min for the balance inlet. The furnace purge is sent across the furnace to remove any contaminants through the outlet tube. The balance purge is required to prevent contaminants entering the delicate balance chamber. The smaller balance flow is sent through the balance chamber and then down into the furnace. A thermocouple positioned above the sample pan was used to measure the environmental temperature.

2.2.1.5 Heat exchanger

A water reservoir is used to send a continuous supply of water around the furnace. During a heating experiment, the cooling effect of the water gives the heater something to work against, thus ensuring accurate temperature control.

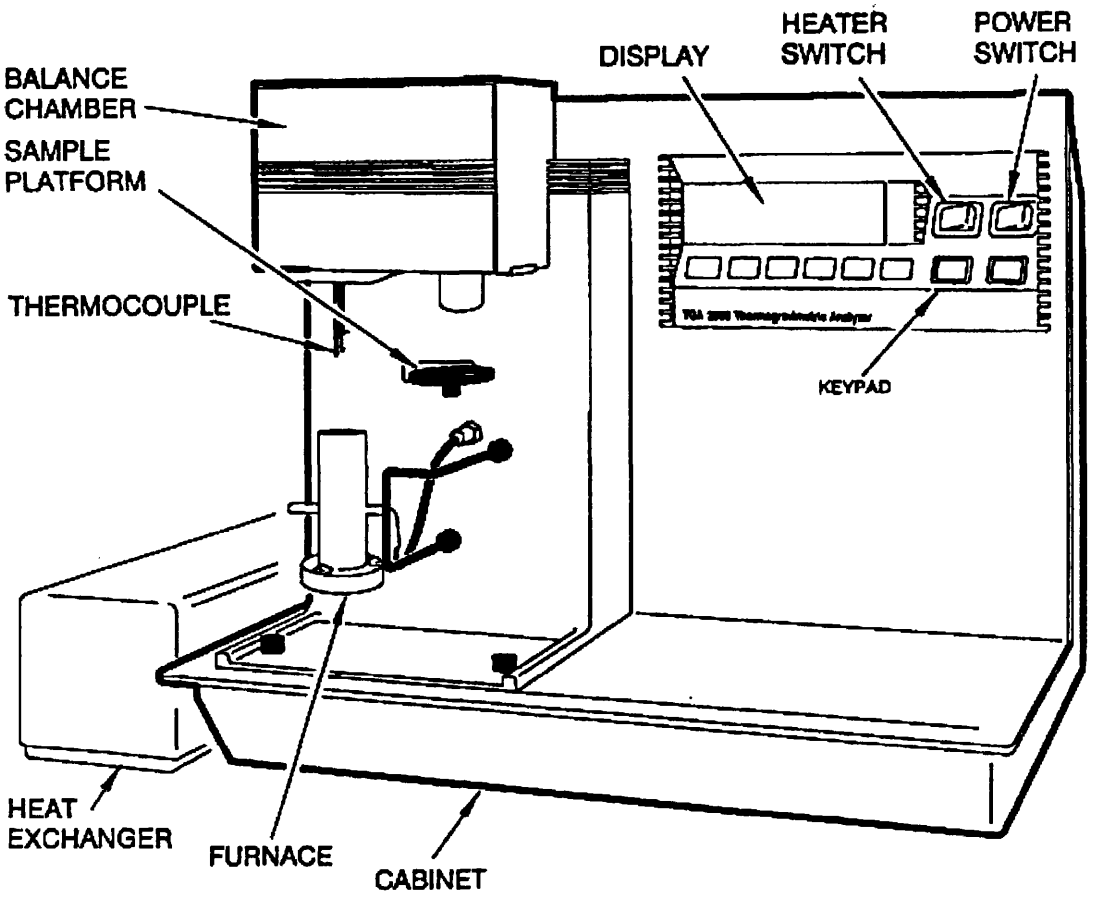

Figure 2.1 *Schematic representation of the Thermogravimetric Analyser (TGA) 2950 (Reproduced from TGA 2950 operating manual).*

2.2.1.6 Compressed air

A supply of compressed air was connected to the TGA, which serves to cool the furnace between experimental runs. The compressed air was activated after the end of an experiment for a set amount of time.

2.2.1.7 Controller

The controller used for the TGA instrument was a computer, which was used to program the heating cycle. It was also used for data analysis, where the derivative weight curve could be plotted.

2.2.1.8 Experimental

Perkin Elmer aluminium sample pans were used to load the samples. These pans were tared prior to weighing the sample into the pan. A sample weight of 5mg +/- 0.5 mg was used.

2.2.2 DIFFERENTIAL SCANNING CALORIMETRY (DSC)

2.2.2.1 Introduction

Differential scanning calorimetry (DSC) is a thermal method of analysing samples that involves the use of temperature to produce a change in a measured parameter, from which information concerning the physical and chemical events via changes in either enthalpy or heat capacity of a sample can be derived (Coleman and Craig, 1996). There are two recognised forms of DSC: power compensation and heat flux DSC. The instrument used for DSC analysis of samples was the Perkin-Elmer DSC 7 Power compensation design. The power compensation form of DSC will therefore be discussed further.

2.2.2.2 Power compensation DSC

For the power compensation DSC system, the sample and reference pans are positioned in separate micro-furnaces (see Figure 2.2). The sample and reference furnaces are mounted in an aluminium block, which acts as a heat sink. This aluminium heat sink is kept at a constant temperature that is well below the temperature of the experiment, so that heat is quickly dissipated from the micro-furnace to the heat sink. The system operates a 'thermal-null' whereby the differential temperature between the sample and reference pans is maintained at zero.

This thermal-null principle operates using two separate control loops. The Average Temperature Control (ATC) loop provides power to the sample and reference furnaces according to the temperature program selected. The ATC loop provides heat at the rate selected and ensures that the sample and reference furnaces are at the same temperature (Coleman and Craig, 1996).

The Differential Temperature Control (DTC) loop is the circuit that detects any temperature differences and provides the power to maintain a thermal-null. The DTC loop detects any temperature differences between the sample and reference pans by the use of platinum resistance thermometers at the base of the furnace (see Figure 2.2). The DTC loop then provides power to bring the sample and reference pans to the same

temperature, thus always maintaining a thermal-null. For an endothermic change in the sample, the DTC loop will provide power to the sample; for an exothermic change, the DTC loop will provide power to the reference to maintain a thermal-null.

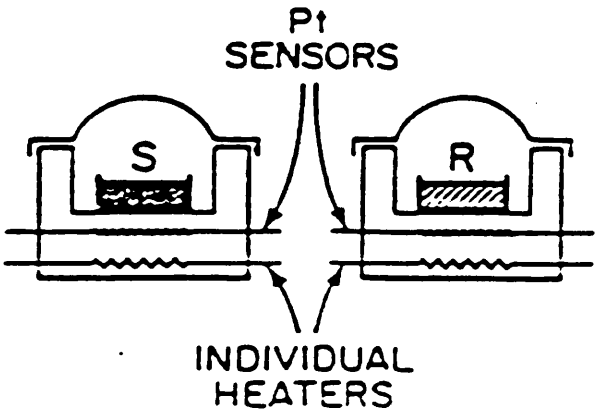

Figure 2.2 *Schematic representation of the power compensation DSC system (Reproduced from DSC 7 users manual).*

The power supplied to maintain the same temperature in the sample and reference pans is measured and is directly proportional to the energy change of the system, given by equation (2.1) (Coleman and Craig, 1996).

$$P = dQ/dt = I^2R \qquad (2.1)$$

Where P (W) = Power, I (A) = current supplied to the heater, R (Ohms) = resistance of the heater.

2.2.2.3 Calibration

The DSC 7 was calibrated using a high purity standard with transitions within the temperature range of the experiments to be carried out. Indium was used to measure the melting temperature and enthalpy using a scanning rate of 10°C/minute, the same as for the experiments to be carried out. Indium has an expected onset melting temperature of

156.6°C and peak area of 28.45 J/g. If the values obtained for the Indium standard did not correspond to the literature values, then the measured values were used in the DSC calibration program. The indium standard would then be repeated to ensure that the literature values were obtained. Calibrations were generally carried out on a daily basis prior to any experimental measurements.

2.2.2.4 Factors affecting the DSC response

The factors affecting DSC scans can be considered to derive from instrument conditions or sample conditions. These will now be considered.

2.2.2.5 Instrument conditions: heating rate

The heating rate can be selected as part of the heating program for a DSC experiment. Selection of a low or high heating rate can affect the result and will therefore be considered. A low heating rate results in a high resolution but low sensitivity. A high heating rate results in a low resolution and high sensitivity. If two thermal events of similar temperature are considered, at a low heating rate the first event will have been completed before the second event starts; thereby at a low heating rate, the two thermal events have been resolved. However, at a higher heating rate, due to the faster progression of the reference side, the first thermal event may not have been completed before the second event starts, and thereby the two events are not resolved. The low sensitivity at low heating rates means that smaller events may not be detected.

2.2.2.6 Sample conditions: sample size and encapsulation

Small sample weights, in the order of a few mg are recommended since large sample weights lead to poor heat transfer rates, leading to poor resolution. Aluminium pans are normally used for DSC investigations. The type of pan is selected depending on the nature of the sample. Non-hermetically sealed aluminium pans are suitable for most solid samples, at temperature programs up to 600°C. The lids for the pans should be crimped onto the pans to obtain good thermal contact between the sample and the detection system and to reduce any thermal gradients within the sample. Crimping may also have the effect of flattening the sample, which will further improve the thermal conductivity.

Open pans can be used where contact between the sample and the purge gas is required, such as in desolvation studies. Hermetically sealed pans, which are airtight, are used for

volatile samples, aqueous solutions, and samples that undergo sublimation. This ensures that the transitions of interest are measured rather than for instance the latent heat of volatilisation (Ford and Timmins, 1989). Careful placement of the sample pans in the micro-furnaces and replacement of cell covers is important to ensure that the sample does not move out of position.

2.2.2.7 Particle size

In general, large particle sizes lead to melting peaks that have a lower onset temperature, a higher peak temperature, and a lower peak area. This is thought to be due to the heat transfer problems relating to large particles. The heat transfer between large particles is lower than for small particles. This may result in a thermal lag between different parts of the sample due to the relative poor heat transfer between large particles. The hot side of the sample would melt first and then release its energy to the cold side. This would lead to a lower onset temperature and increase the total transition interval. Also due to the thermal lags between large particles, the peak may become wider perhaps resulting in a higher peak temperature (Ford and Timmins, 1989).

2.2.2.8 Experimental

Perkin Elmer aluminium non-hermetically sealed pans were used for the DSC investigations carried out. The sample weight used was 5mg +/- 0.5mg, weighed using an AD Perkin Elmer autobalance. For the reference furnace, an empty non-hermetically sealed pan was used. Nitrogen was used as the purge gas at a pressure of 30psi.

2.2.3 MICROWAVE-VACUUM DRYING

2.2.3.1 Introduction

Microwave-vacuum drying uses low temperature drying due to the presence of the vacuum making it suitable for temperature-sensitive products. The oxygen free atmosphere also makes microwave-vacuum drying suitable for oxygen-sensitive products. Microwave-vacuum drying also has the advantages of shorter processing times, worker safety due to dust control, and automation of the granulating and drying process.

2.2.3.2 Instrumentation

A GP1-MG microwave-vacuum drier (Aeromatic-Fielder Ltd, Eastleigh, UK) was used at Aeromatic-Fielder Ltd. The GP1-MG combines a high-shear granulator with microwave-vacuum drying.

2.2.3.3 High-shear granulator

Figure 2.3 shows a schematic representation of the GP1-MG used at Aeromatic-Fielder. A heated jacket surrounds the mixing bowl to ensure that condensation on the inner wall does not take place. Granulating fluid is introduced from a pressure pot assembly (Niro-Fielder, UK) mounted on top of the GP1-MG and is supplied through a 2.65 V jet at 0.5 Bar pressure.

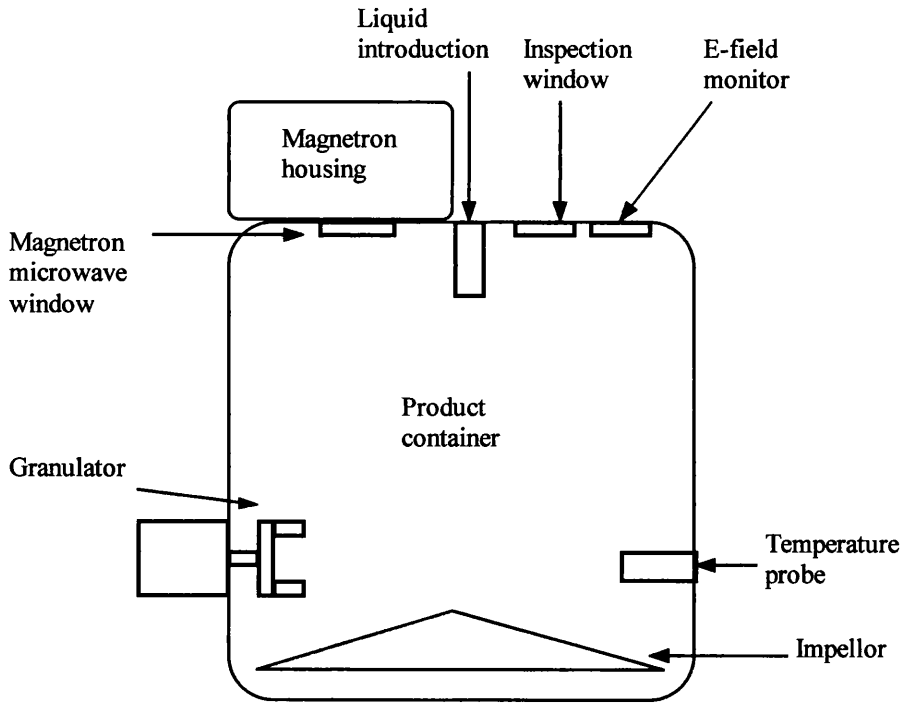

Figure 2.3 *Schematic representation of the GP1-MG used for granulating and microwave-vacuum drying*

2.2.3.4 Microwave-vacuum drying

Microwaves are generated by the magnetrons that are housed in the lid of the GP1-MG. The magnetrons are protected by a window that allows the microwaves to pass through but prevents the magnetrons from being exposed to the product or the vacuum. The water vapour that is produced during drying is removed by the vacuum system.

2.2.3.5 End-point determination

Determination of the end-point of the drying process was determined using a combination of the % E-field and product temperature. The % E-field is the percentage of free or reflected electric field from the product expressed as a percentage of the supplied electric field. A product temperature exceeding 45°C was used as an end-point. The % E-field was also taken into consideration. However, it was found that the product temperature began increasing more rapidly and reached 45°C before the % E-field reached values above 50%. Chatrath and Staniforth (1990) found that the % E-field tended to fluctuate in a random manner, whereas the product temperature increased in a more regular manner. Visual observation of the product through the inspection window also showed the change in appearance to a dry powder.

2.2.3.6 Experimental

Batch sizes of 1 kg were loaded into the mixing bowl of the GP1-MG, which is a typical loading for experimental studies for the GP1-MG used at Aeromatic-Fielder.

2.2.4 FLUID-BED DRYING

2.2.4.1 Introduction

Fluidised-bed drying results in efficient heat and mass transfer rates leading to shorter dying times, typically 20-30 minutes for a batch of tablet granules compared to several hours for static bed driers. The fluidised state means that drying from individual particles takes place rather than from the entire bed, thus giving efficient heat transfer to the particles and moisture transfer through and away from the particles.

2.2.4.2 Principle

In fluid-bed drying, a sample bed is contained in a vessel, the base of which is perforated, thus enabling air to pass through the bed. If air is allowed to flow through the sample bed at a velocity greater than the settling velocity of the particles, then the

particles are buoyed up and become suspended in the air stream. The resulting mixture of solid and air behaves like a liquid, and the solid particles are said to be 'fluidised' (Rankell et al, 1986). The fluidisation technique provides conditions of great turbulence that results in good mixing between the solid and air, and is an efficient method of drying for tablet granulations. The only requirements are that the granules are not so wet that they stick together on drying, and that the dried product does not produce excessive amounts of fine particles due to the turbulent conditions encountered. If hot air is used, then the turbulent conditions provide high heat and mass (moisture) transfer rates, allowing the fluid-bed technique to offer rapid drying of granules.

2.2.4.3 Instrumentation

A laboratory fluid-bed drier (model FBD/L70, PRL Engineering Ltd, Mostyn, Flintshire, UK) was used for fluid-bed drying investigations. The exit was sealed by a dust bag filter.

2.2.5 DYNAMIC VAPOUR SORPTION (DVS)

2.2.5.1 Introduction

Dynamic vapour sorption (DVS) is a humidity-controlled microbalance housed in an incubator where the sample is exposed to a continuous flow of air with a pre-programmed relative humidity.

2.2.5.2 Instrumentation

Gravimetric studies were carried out in a humidity-controlled microbalance system, Dynamic Vapour Sorption (DVS-1, Surface Measurement Systems, UK). The humidity is controlled by the flow of nitrogen through switching valves, which determine the total flow of nitrogen through a humidification stage. The humidified air passes over both the sample and reference sides of the balance, where the reference contains an empty pan. The mass change of a sample due to water sorption / desorption between 0% RH and 98% RH across a temperature range of 25°C to 80°C can be measured.

Figure 2.4 shows a schematic representation of the DVS apparatus used. It shows a Cahn microbalance with sample and reference holders attached. The Cahn microbalance has its own balance purge of dry nitrogen gas to ensure that the sensitive microbalance

is not exposed to atmospheric humidity. Beneath the sample and reference holders are temperature and humidity probes.

The DVS is computer controlled allowing the sorption / desorption program to be pre-set. The change in RH for the step method is controlled by a time limit for holding at each RH or when equilibrium has been reached at the RH being used. The equilibrium uptake could be determined by programming a desired rate of change of mass with time, dm/dt (%/min).

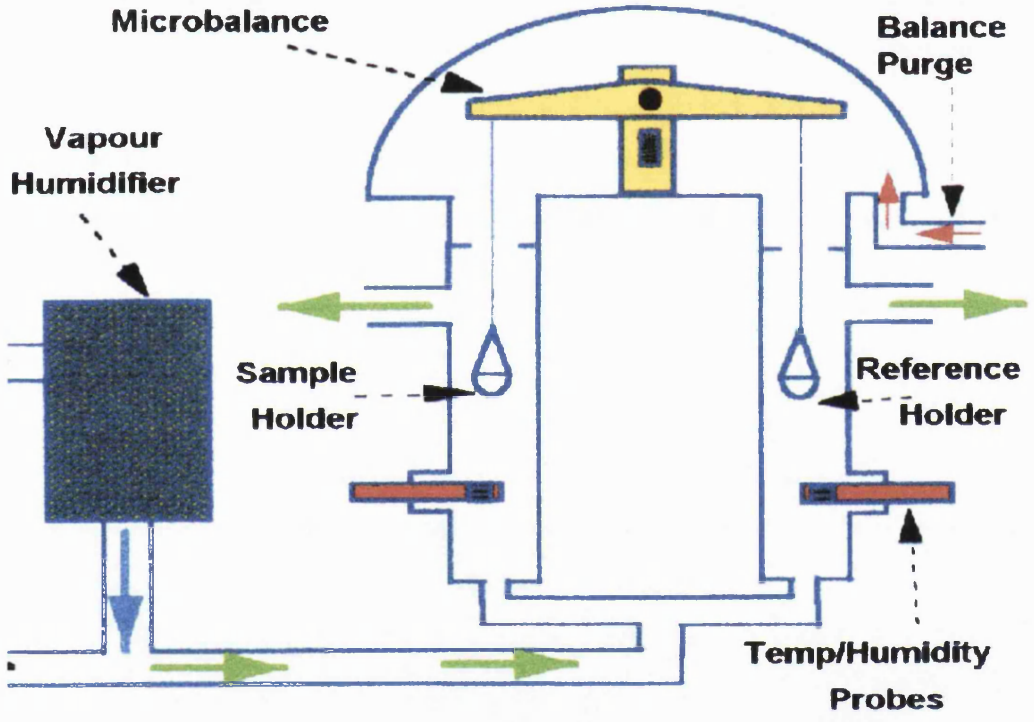

Figure 2.4 *Schematic representation of the Dynamic Vapour Sorption (DVS) technique (Reproduced from DVS-1 operating manual).*

2.2.5.3 Preparation and handling

The removal of the delicate quartz sample pan from the hang-down wire requires great care and should only be handled using tweezers. Gloves should not be worn during this procedure as they may introduce static to the pan leading to disruption of the sensitive microbalance. It is important that the sample pan is cleaned thoroughly between DVS runs. Sample pans were therefore washed with distilled water, then with ethanol or IMS to remove any remaining water on the pan. The pan was then placed directly onto the hang-down wire using tweezers, and the DVS set up to dry the sample pan at 0% RH for 5 minutes. The RH was then changed to 90% RH and held for 5 minutes to remove any static that had built-up. The moisture introduced by changing the RH to 90% RH provides a route for the removal of static. Following this, the RH was changed back to 0% RH to dry the sample pan. Once the weight had stabilised the balance could be tared in readiness for sample loading.

2.2.5.4 Sample loading

The sample is loaded directly into the sample pan whilst attached to the hang-down wire. To prevent any contamination of the instrument a piece of card is placed underneath the sample pan. A sample weight in the range 20 to 100mg is typically used. Lower weights are used for hygroscopic materials and higher weights for more hydrophobic materials. After sample loading is completed, 2-3 minutes is allowed for the sample pan to stabilise before starting the experiment.

2.2.5.5 Programming a method

The step or ramp method can be programmed using the DVS software. The step method consists of separate stages that consist of the different RH steps of the experiment. For example, the program could start at 0% RH and then increase in steps of 10% RH up to 90% RH. The conditions for changing between steps can be either a time limit or a set dm/dt (%/min) value. For the dm/dt value method, the program will not move to the next step until the dm/dt is below the chosen value for a set amount of time, called the minimum stage time. The maximum stage time is the upper time limit for the dm/dt control method. The minimum and maximum stage times used were 15 minutes and 360 minutes respectively. The ramp method is where the RH is constantly changing and there are no separate stages as for the step method.

2.2.5.6 Weight calibration

Weight calibrations were carried out on a monthly basis, and involved placing a 100mg calibration weight on the sample pan. A mass of 100mg +/- 0.002mg would be expected. However, if the mass was outside this range then the weight was adjusted to the expected value.

2.2.5.7 Relative Humidity (RH) validation

The RH validation method relies on the principle that the vapour pressure of water above a given saturated salt solution in equilibrium with its surroundings is constant at a particular temperature. The method involves placing a known mass of a particular salt (e.g. sodium chloride) on the sample pan. The pure dry salt or a saturated salt solution may be used. An experiment is set up that uses a RH ramp of 1 or 2% / hour over a range around the literature value for the critical relative humidity of the salt being used (Nyqvist, 1985). By plotting the change in mass and target RH against time, the critical RH of the salt can be obtained, thus allowing the RH of the system to be validated.

2.2.5.8 Experimental

Samples were weighed directly onto the sample pan, with the exact weight being recorded by the DVS software. The step method was used for all investigations; the details will be considered in the relevant chapters.

2.2.6 AMPOULE MICROCALORIMETRY

2.2.6.1 Introduction

Isothermal microcalorimetry is a technique that continuously measures the rate of heat change in a sample (Angberg et al, 1992). It has been used to assess the amount of amorphous material present in a sample by measuring the crystallisation response in the presence of water vapour (Briggner et al, 1994 and Sebhatu et al, 1994). Amorphous material as low as 0.5% can be detected using isothermal microcalorimetry, as demonstrated by Buckton et al (1995b) in detection of small degrees of amorphous lactose.

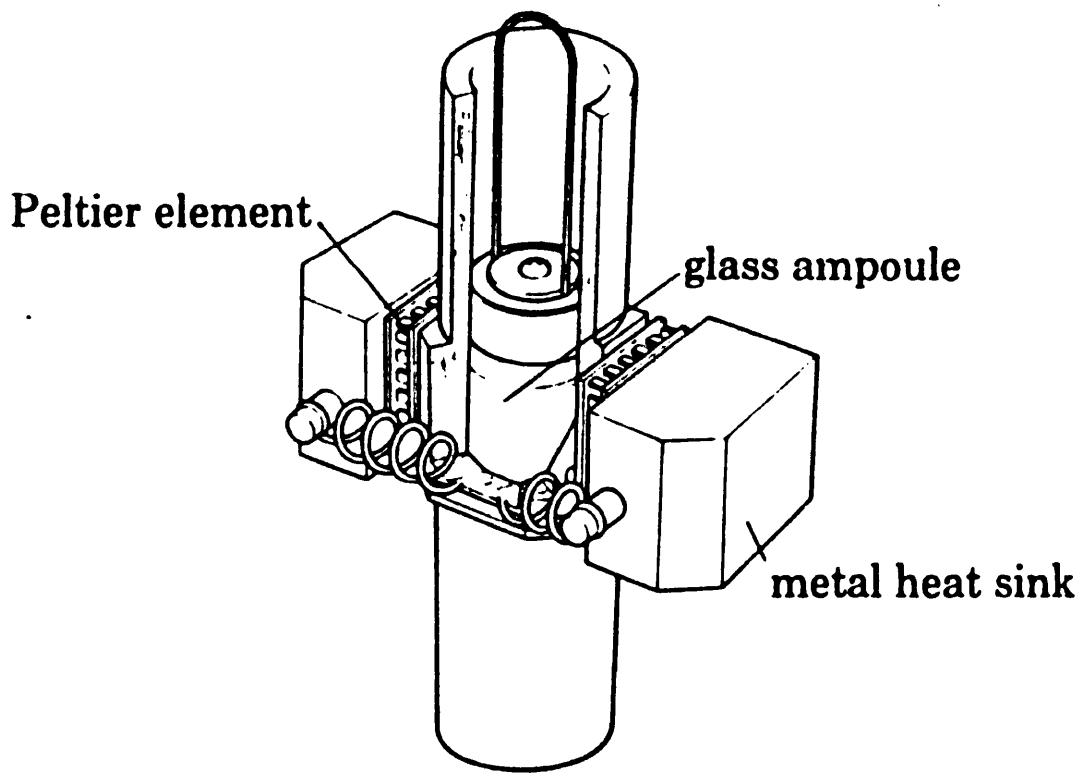

Figure 2.5 *Glass ampoule in the measurement position of the Thermal Activity Monitor (TAM). Reproduced from TAM instruction manual.*

2.2.6.2 Instrumentation

The isothermal microcalorimeter used was the 2277 Thermal Activity Monitor (TAM), Thermometric AB, Sweden. The system consists of up to four independent measurement channels, positioned in a 25-litre thermostated water bath. The water bath can be used to maintain isothermal conditions in the range 5 to 80°C. The water bath temperature is maintained to within +/- 2 x 10^{-4} °C. The precision of the TAM is largely due to the thermal stability maintained by the water bath surrounding the measuring channels.

2.2.6.3 Principle

The microcalorimeter uses the heat flow principle to detect heat changes. Figure 2.5 shows a glass ampoule in the measurement position of the channel. In this position, the glass ampoule is sandwiched between a pair of Peltier heat sensors. The Peltier heat sensors in turn are in contact with a metal heat sink. This set up means that heat energy to or from the glass ampoule is channelled through the Peltier heat sensors. The Peltier heat sensors are able to respond to temperature gradients of up to 10^{-6} °C. The Peltier heat sensors act as thermoelectric generators that convert the heat energy detected into a proportional voltage signal. The results are then quantified using electrical calibration where known power values are passed through built-in precision resistors that are wound around the measuring cup. The glass ampoule shown in Figure 2.5 is positioned inside a measuring cup, part of which can be seen in Figure 2.5. This assembly is positioned alongside another identical measurement assembly containing the measuring cup, glass ampoule, and detection system. This whole assembly is then positioned in the lower part of a steel canister that forms the lower part of the measuring cylinder for a channel. The two measuring cup assemblies are electrically oppositely connected, so that the overall output is the difference in the heat flows between the two assemblies. This allows one of the measuring assemblies to be used as a reference side and the other as a sample measurement side.

2.2.6.4 Calibration

Calibration is carried using a precision heater resistor built into the measuring cup assembly. When a known current is passed through the heater resistor, the thermal power that is produced is measured by the detection system in the normal manner. The measured power level can then be adjusted to the correct level to calibrate the channel. Calibration was carried out using two freshly sealed glass ampoules with small glass tubes containing the saturated salt solution to be used for the subsequent experiments. Before starting the electrical calibration, the heat flow output is adjusted to zero using the zero control on the TAM. The Digitam software is then used to commence electrical calibration. When the signal has stabilised, the fine control on the TAM is adjusted to a stated value. The electrical calibration is then switched off using the Digitam software, and the zero level re-adjusted if necessary.

2.2.6.5 Experimental

The sample is sealed in a 3ml glass ampoule with a small tube containing a saturated salt solution. The saturated salt solution produces a certain relative humidity (RH) at a given temperature (Nyqvist, 1983). The reference ampoule used was a freshly sealed ampoule with a small tube containing the saturated salt solution being used for the experiment.

2.2.7 PERFUSION MICROCALORIMETRY

2.2.7.1 Introduction

Microcalorimetry has been widely used for samples that are placed in a sealed ampoule with a small tube containing a saturated salt solution, and the heat flow measured. However, in this closed system, the relative humidity cannot be changed during the experiment. Perfusion microcalorimetry enables the sample to be exposed to a programmed RH increase or decrease between 0% and 100% RH throughout the operating temperature of the TAM (Bakri, 1993). Bakri (1993) originally designed the controlled RH perfusion system used in conjunction with the 2277 TAM. Briggner (1993) used the perfusion technique to investigate the crystallisation of micronized samples. It was found that not only could it be determined if a sample is affected by changes in RH, but in addition the specific RH at which the crystallisation takes place could be determined, and the precise values of the heat evolved or absorbed during the process could be calculated (Briggner, 1993). Sheridan et al (1995) engineered a flow cell unit to study adsorption isotherms for three different supplies of α-lactose monohydrate. They found that the resulting adsorption isotherm data were able to distinguish between the different lactose samples due to surface variations between the samples. Pudipeddi et al (1996) used the perfusion technique to test a modified version of the BET equation that allows calculation of monolayer capacity and surface area, with water being used as the adsorbate.

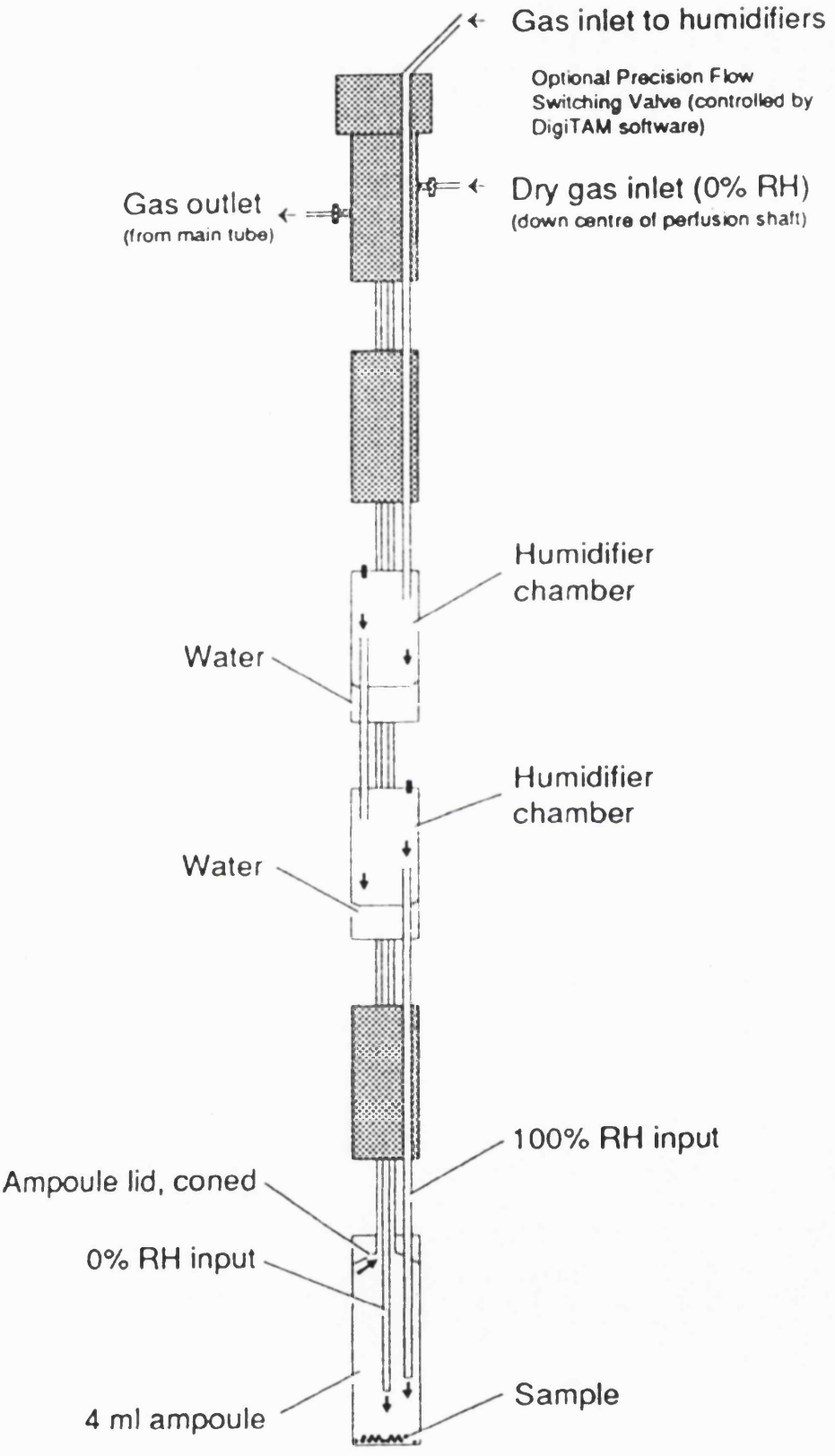

Figure 2.6 *Schematic representation of the perfusion microcalorimetry unit (Reproduced from Thermometric micro reaction systems manual).*

2.2.7.2 Instrumentation

The experiments were performed in the TAM (Thermometric 2277) described above, with Thermometric's 2250 perfusion accessory as shown in Figure 2.6. The perfusion unit has a saturated line (100% RH) and a dry nitrogen line (0% RH). The wet line is passed through two humidity chambers that are in thermal contact with the TAM water bath, to produce the 100% RH wet line. The sample ampoule is constructed of stainless steel and is of 4 ml capacity. The sample ampoule is positioned in the measuring site of the TAM. The RH in the ampoule is regulated by a 2281 flow switch that is positioned at the top of the perfusion column in Figure 2.6. Dry nitrogen gas enters the flow switch via a mass flow controller. The gas that exits the flow switch goes either directly to the ampoule (0% RH) or through the humidifiers and onwards to the ampoule (100% RH), as shown in Figure 2.6. The flow switch is controlled by the Digitam software program, and produces the desired RH in the ampoule by switching between the two lines to produce the required ratio of dry (0% RH) to saturated (100% RH) gas. As well as the switching function, the flow switch also contains a heater that is used to prevent condensation forming in the outlet tube from the perfusion unit.

2.2.7.3 Programming a method

The perfusion unit can be programmed through the Digitam software to produce either a series of discrete steps or an upward or downward ramp (Bakri, 1993). The step method consists of separate stages that consist of the different RH steps of the experiment. For example, the program could start at 0% RH and then increase in steps of 10% RH up to 90% RH. The ramp method allows a continuous increase in the RH after a ramp start and end RH, and a ramp time is entered. This allows a linear increase in the RH between the start and end value during the time specified.

2.2.7.4 Sample loading and calibration

Calibration of the perfusion microcalorimetry unit is carried out before each experiment at 0% RH (or the starting RH of the subsequent experiment). The sample is first loaded in to the steel ampoule, and the perfusion column attached. The perfusion column is then lowered to the measurement position in three stages of 5, 10, and 20 minutes to allow temperature equilibration to occur and minimize the disturbance caused by contact of the column with the measuring channel. Electrical calibration is then carried out in the same way as described for ampoule microcalorimetry above. The reference

side consists of an equivalent steel ampoule containing the same mass of sample as in the sample ampoule. A flow rate 2ml/min was used for all investigations and calibration was performed at 300μW.

2.2.7.5 Relative humidity (RH) validation

The RH validation method uses saturated salt solutions to test that the perfusion unit is generating the correct RH. The saturated salt solution is loaded in to the steel ampoule and the ampoule attached to the perfusion column in the normal manner. The RH is set to the literature value for the RH generated by the salt being used. Once the ampoule is in the measurement position, the nitrogen is reattached. When the nitrogen is first introduced, this will produce an exothermic peak that will then stabilize. The RH is then manually changed in 1% RH increments or decrements depending on the position of the baseline. The % RH when the curve crosses the heat flow (y-axis) at zero is the RH setting on the perfusion unit that produces the same RH as that above the saturated salt solution being used, thus allowing the RH of the system to be validated.

2.2.8 GAS CHROMATOGRAPHY (GC)

2.2.8.1 Introduction

The excipient lactose exists in two isomeric forms, α- and β-lactose. β-lactose is present in an anhydrous form only, whereas α-lactose can exist as a monohydrate or anhydrous forms. A solution of lactose results in an equilibrium ratio of α- and β-lactose, which is temperature dependent. The isomeric composition of a lactose sample depends on the production process and the temperature used. Processes such as spray drying result in lactose samples with different amounts of α- and β-lactose depending on the temperature used.

2.2.8.2 Principles

Gas chromatography is a method of separation of sample components where the partition or adsorption of sample components to the stationary phase results in physical separation of the components. The stationary phase lies in the separating column that can be either a capillary with a liquid coating on the inside, or alternatively a small diameter tubing containing the stationary phase. The mobile phase is the carrier gas that is used to move the sample through the column. Sample components with a higher

affinity for the stationary phase in the column will take the longest time to pass through the column and will therefore be retained for longer. Components with a lower affinity for the stationary phase will be retained for the least time and would be the first to be detected at the outlet of the column. After the components have passed through the column they enter the detector. Detection of a component results in a peak, with each component ideally having separate peaks. The individual components are identified by the time lapse between injecting the sample in the column and the time when the component registers as a peak. The area under the individual peaks, corresponding to the sample components, gives a quantitative output of the proportions of each component in the sample.

2.2.8.3 Instrument components: Injection system

The purpose of the sample injection system is to vaporise the sample and introduce the sample to the column. This is required to be carried out in a reproducible manner. The injection system contains a heated metal flash evaporator that vaporises the liquid sample. The liquid sample is inserted into the injection device by using a hypodermic needle. The technique for injecting the liquid sample into the injection device is important for obtaining reliable and reproducible results. The needle needs to be inserted fully into the injection system, before injecting the sample followed by removal. Following vaporisation, the sample is transferred to the column by the carrier gas.

2.2.8.4 Separating column

Two different types of column are available for gas chromatographic analysis. The first is a capillary column, which is liquid coated on the inside to form the stationary phase. They typically have an internal diameter of 0.25 to 50mm and a length of up to 300m. The second type of column available is a packed column, where the stationary phase is packed into the column. Internal diameters are typically 4mm and lengths up to 150m. The capillary columns have higher separating efficiency relative to the packed column, allowing separations to take place over a shorter time scale. The capillary type column was used during GC investigations.

2.2.8.5 Thermal compartment

The thermal compartment of the gas chromatograph is present to control the column temperature. The control system for the column temperature maintains temperature control to +/- 0.1°C and is able to detect temperature changes of 0.01°C. Separate temperature control systems are used for the injection port and detector. The maintenance of close temperature control of the column is aided by an air bath surrounding the column, where a blower inside the thermal compartment circulates the air.

2.2.8.6 Detector

The choice of detector used depends on the type of column used in the investigation. For the capillary column used in this investigation, a flame ionisation detector is used and this will therefore be discussed further. The flame ionisation detector consists of a burner assembly, an electrometer system, and a collector electrode. The basis of the flame ionisation detector is that the motion of charged molecules or free electrons present in a gas in the direction of an electric field enables a gas to conduct electricity, which would otherwise be non-conducting. The column effluent enters the detector through the base of the burner and is mixed with hydrogen gas. The collector electrode is positioned near the tip of the burning flame. A current is produced that is proportional to the number of ions or electrons in the flame gas. The collector electrode then detects this.

2.2.8.7 Experimental

The gas chromatograph that was used was the Carlo Erba, model HRGC 5300, Milan, Italy. A CP-sil 43CB capillary column with 0.32 mm internal diameter and 25 m length was used. A flame ionisation detector (FID) was used. The column was set to 200°C, the injection port to 250°C, and the flame ionisation detector to 250°C. The column was conditioned at the temperature of the experiment before starting any measurements in order to remove any unwanted material present in the column. 2µl aliquots of the solutions were injected directly into the gas chromatography column.

The procedure for determining the isomeric composition of the lactose samples first involved preparing the derivatisation mixture, using the method of Dwivedi and Mitchell (1989). It consisted of 19.5% dimethylsulphoxide (DMSO), 22% trimethylsilylimidazole (TSIM), and 58.5% pyridine. 1mg of the dry lactose samples

were dissolved in 2.25ml of the derivatisation mixture. The samples were then vortexed for 2 minutes, then kept at room temperature for 20 minutes for the derivatisation reaction to be completed. Reference samples were used first to ensure accurate determination of the isomeric composition of lactose. The reference α-lactose used was α-lactose monohydrate. A β-lactose reference was tested and found to correspond to the manufacturers specifications.

2.2.9 SCANNING ELECTRON MICROSCOPY (SEM)

2.2.9.1 Introduction

Scanning electron microscopy (SEM) allows surface examination of a sample. Elamin et al (1995) used SEM in studying spray-dried lactose before and after crystallisation. Also studied was spray-dried lactose in the rubbery state after plasticisation by water.

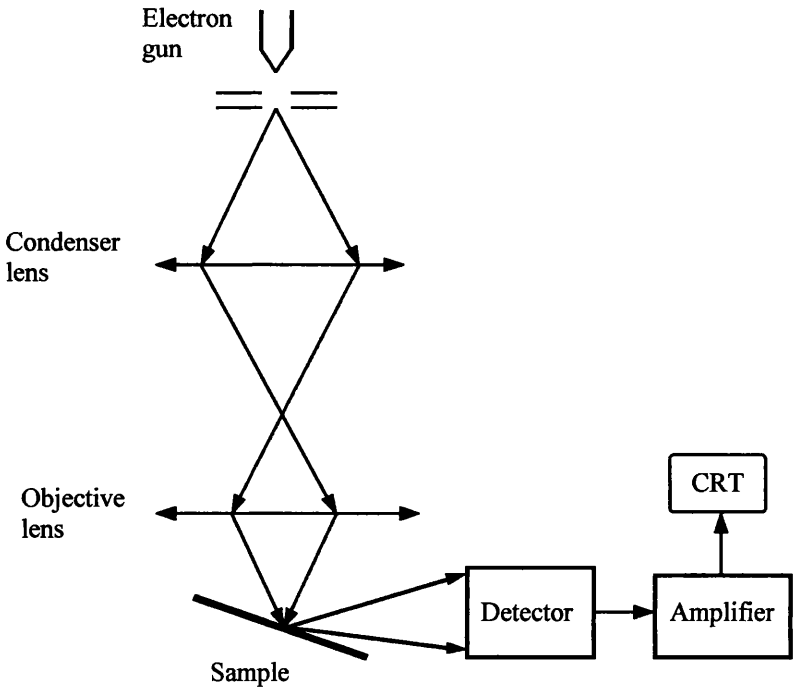

Figure 2.7 *Schematic representation of Scanning Electron Microscopy (SEM). Modified from Slayter and Slayter (1992).*

2.2.9.2 Operating principles

In scanning microscopes, radiation from a source is focused to form a fine probe. The probe is then moved rapidly across the sample of interest, and the radiation leaving individual sample positions are collected by an input transducer. The input transducer signal is then sent to an amplifier, causing proportional levels of intensity to appear on a screen, or sent directly to a computer (Slayter and Slayter, 1992).

In scanning electron microscopy (SEM), the sample is positioned at an angle, as shown in Figure 2.7. A focused electron beam scans the surface of the sample, and the detector monitors secondary electrons. After electronic amplification, the signal can be used to produce an image of the sample. A point on the sample produces a point on the image as it is irradiated with electrons. The main advantage of SEM relates to image contrast. The electron source is typically a tungsten filament. The electron probe is focused by an objective lens above the sample.

2.2.9.3 Experimental

A Phillips XL20 Scanning Electron Microscope was used. Accelerating voltages used were 8-12 kV. Prior to each sample run, the samples were attached to a SEM stub using double-sided carbon discs. The samples were then transferred to an Emitech K550 sputter coater, set at 40mA for 4 minutes, where the samples were coated with gold.

2.2.10 LIGHT MICROSCOPY

2.2.10.1 Introduction

Compound light microscope systems consist of illumination systems (source and condenser lens), the microscope itself (the objective lens, eyepiece lens, microscope column, sample stage, and the microscope stage), and the viewing or photographic equipment.

2.2.10.2 Function of elements of the light microscope

The illumination system consists of the source and the condenser lens. Microscopes used for research purposes normally use a high-intensity lamp for illumination. The light source used during investigations was a halogen bulb. The main function of the condenser lens is simply to provide intense and evenly distributed illumination of the specimen. The objective lens determines the quality of the image. The function of the

eyepiece lens is to remagnify the intermediate image (see Figure 2.8) that is formed by the objective lens. Focusing is achieved by adjusting the distance between the specimen and the objective lens.

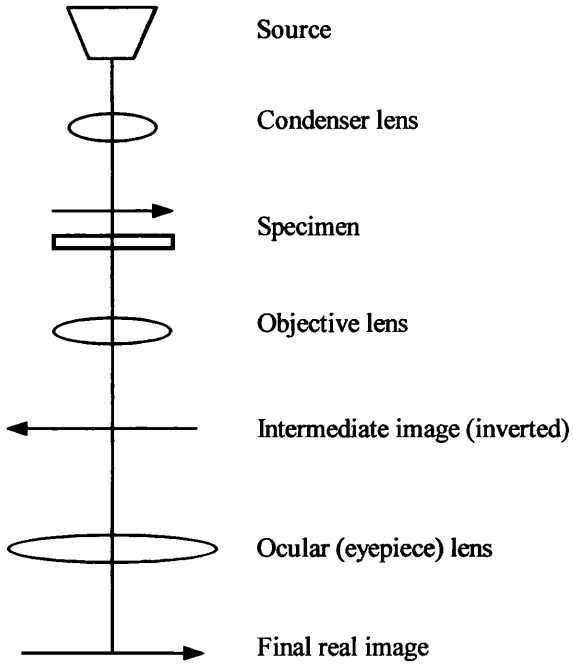

Figure 2.8 *Schematic representation of the light microscope. Modified from Slayter and Slayter (1992).*

2.2.10.3 Experimental

A Nikon Microphot FXA light microscope was used for investigations. This assembly includes a camera enabling images to be viewed on a screen and prints to be obtained.

Chapter 3

Microwave-vacuum drying of lactose monohydrate

3.1 INTRODUCTION

Lactose monohydrate is a commonly used pharmaceutical excipient used as a filler or diluent. Lactose exists in four crystallographic forms: α-monohydrate, α-anhydrate, β-anhydrate, and amorphous lactose (Morita et al, 1984). Various pharmaceutical processes such as spray-drying, milling, and lyophilization are known to lead to activation of the crystal structure leading to the production of amorphous material. Huttenrauch and Keiner (1979) used lactose as a model substance to investigate the effect of heat drying on the crystallinity of lactose. It was found that progressive drying lead to an increase in lattice defects, with crystallinity decreasing to nearly 50%. Morita et al (1984) found that dehydration of α-lactose monohydrate to α-anhydrate by heating in air resulted in a disordered crystal lattice. Vacuum drying has been combined with conductive drying for many years. The pairing of microwave with vacuum drying means that the additional thermal energy provided by the microwaves allows more efficient drying. Microwave-vacuum drying allows low-temperature drying, an oxygen-free atmosphere, and solvent recovery.

The main aims of this investigation were:

- To investigate the effect of microwave-vacuum drying on the introduction of amorphous material into the lactose

- To investigate the effect of variations in the microwave-vacuum drying parameters on the introduction of amorphous material and thermal properties of lactose

3.2 MATERIALS AND METHODS

3.2.1 Materials

Regular lactose monohydrate (Lactochem) was used for the investigations.

3.2.2 Methods

3.2.2.1 Microwave-vacuum drying

A GP1-MG high-shear granulator with microwave-vacuum drying was used during the investigations. The general method used was as described in Chapter 2. Initial batches were used to establish a standard protocol, which ensured good mixing of the product. Once the standard protocol was established, subsequent batches were carried out using a change in one of the drying parameters.

The standard protocol consisted of a dry mixing, liquid addition, and wet massing phases followed by the microwave-vacuum drying phase. 1kg of lactose was dry mixed for 3 minutes at an impeller speed of 700 rpm and a chopper speed of 1000rpm. After 3 minutes, 50ml water was added from a Niro-Fielder pressure pot assembly mounted on top of the GP1-MG at 0.5 Bar pressure. Wet massing was then carried out for 3 minutes. Before starting the drying phase the jacket temperature was set to 30°C, the impeller speed to 10rpm, and the chopper switched off. The microwave power was set to 150W and the vacuum pressure to 45mBar. The drying phase was then started. After 20 and 30 minutes of the drying phase, the jacket temperature was increased to 40°C and 50°C respectively.

Subsequent batches were carried out with one of the drying parameters changed. The dry mixing, liquid addition, and wet massing stages were the same as the standard protocol in each case. The drying parameters changed were:

- Jacket temperature 50°C
- Microwave power 250W
- Vacuum drying at 10mBar (microwave power switched off)
- Impeller speed 200rpm

3.2.2.2 Thermogravimetric Analysis (TGA)

TGA was used for the microwave-vacuum dried samples to analyse the weight loss associated with heating of the samples of lactose up to 230°C. A sample weight of 5mg +/- 0.5 mg was used for all measurements.

3.2.2.3 Differential Scanning Calorimetry (DSC)

DSC was used to investigate the thermal properties of lactose and changes occurring as a result of microwave-vacuum drying. A sample weight of 5mg +/- 0.5 mg was used for all measurements. The samples were scanned between 30°C and 240°C, at a scanning rate of 10°C/minute. Non-hermetically sealed aluminium pans were used for DSC investigations.

3.2.2.4 Ampoule microcalorimetry

Ampoule microcalorimetry was used to analyse the microwave-vacuum dried samples and detect amorphous material in the sample. The general method used was as described in Chapter 2. A sample weight of 300 mg was weighed into the 3ml glass ampoule. A small tube containing sodium chloride saturated salt solution (75% RH) was placed inside the ampoule. The ampoule was then sealed and placed in the equilibration position for 30 minutes before lowering into the measuring site of the microcalorimeter.

3.3 CHARACTERISATION OF LACTOSE MONOHYDRATE

Figure 3.1 shows a typical TGA trace for the as received lactose monohydrate. TGA analysis shows that 5.0 % +/- 0.1 (n = 3) weight loss for hydrate water between 95°C and 187°C. The 5% hydrate weight loss is the same as the theoretical weight loss for a 100% α-lactose monohydrate sample. The temperature limits used for TGA analysis were kept constant for all subsequent samples in this investigation.

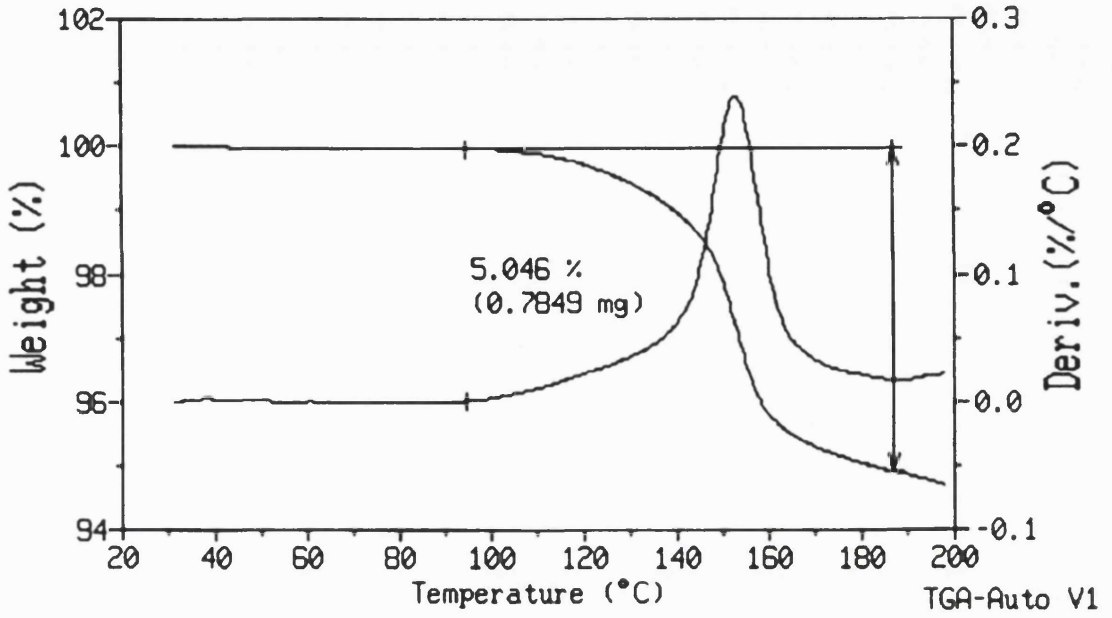

Figure 3.1 *Typical TGA trace for as received lactose monohydrate. Weight loss measured between temperature limits of 95°C and 187°C*

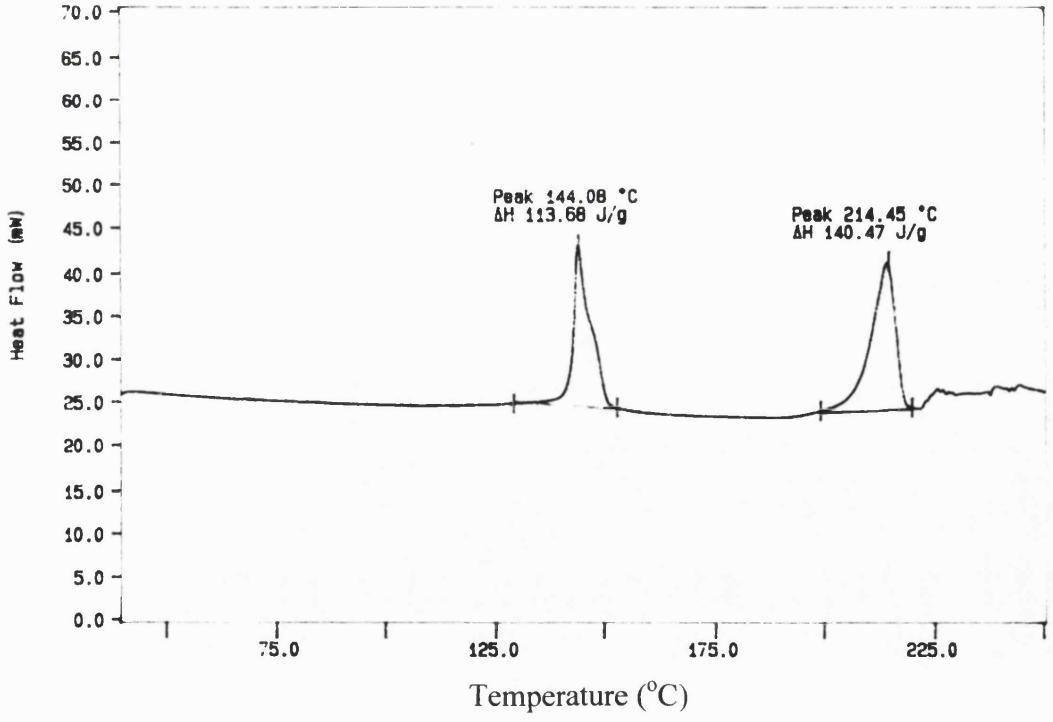

Figure 3.2 *Typical differential scanning calorimetry (DSC) trace for as received lactose monohydrate*

Figure 3.2 shows a typical DSC trace for the as received lactose monohydrate. It shows peaks at 142.7°C +/- 1.2 (n = 3) and 214.6°C +/- 1.1 (n = 3). The peak at 142°C is due to the loss of hydrate water, and the peak at 214°C can be attributed to the melting of α-lactose monohydrate.

3.4 MICROWAVE-VACUUM DRYING OF LACTOSE MONOHYDRATE

3.4.1 Investigation of microwave-vacuum dried lactose using a jacket temperature of 50°C

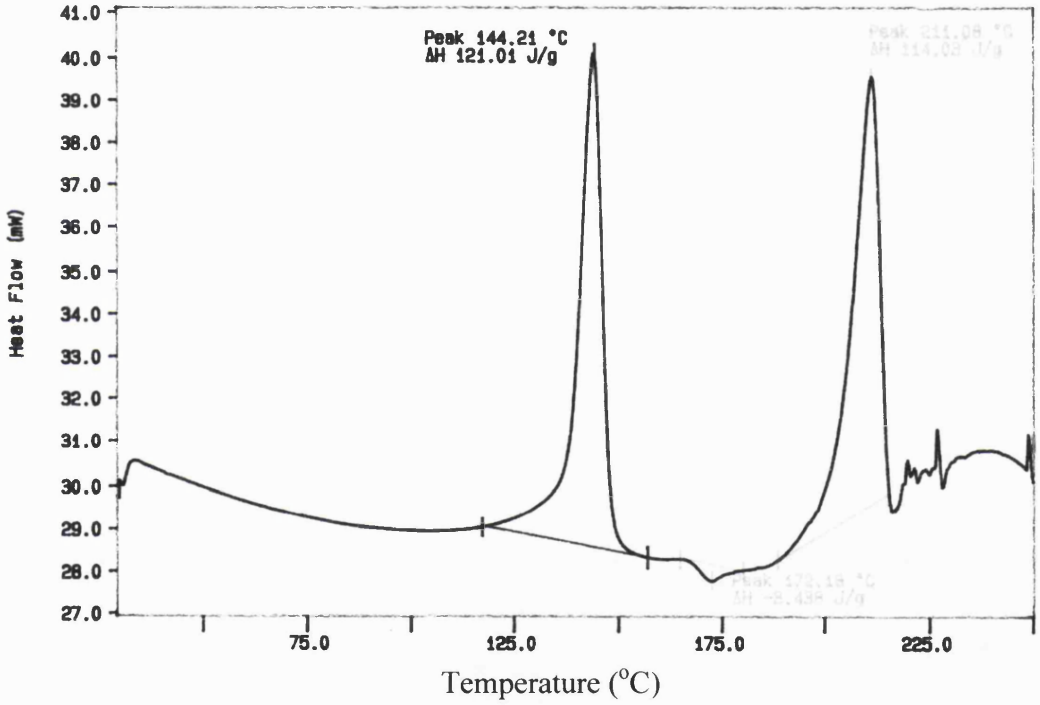

Figure 3.3 *Differential scanning calorimetry (DSC) trace for lactose after wetting and microwave-vacuum drying using a jacket temperature of 50°C*

Figure 3.3 shows a typical DSC trace for microwave-vacuum dried lactose using a jacket temperature of 50°C. It shows a dehydration peak at 145.0°C +/- 2.4 (n = 3) and a melting peak at 213.3°C +/- 1.9 (n = 3). TGA data shows a water loss of 5.0 % +/- 0.1 (n = 3). Figure 3.3 also shows that there are endothermic and exothermic peaks between 160°C and 180°C present. These additional peaks are present for two out of three DSC

runs for this sample. The exothermic peak at 174.0 +/- 2.5 (n = 2) suggests that it may be due to crystallisation of amorphous material. This is in the region of the high temperature crystallisation exotherm described by Darcy and Buckton (1997) for the crystallisation of non-collapsed lactose. Ampoule microcalorimetry data showed that there was no crystallisation peak present indicating the absence of detectable amounts of amorphous material. Furthermore, the TGA results show that the sample has a water loss of 5.0 % +/- 0.1 (n = 3). This equates to a sample consisting of 100% crystalline α-lactose monohydrate. The presence of amorphous lactose in the sample would decrease the hydrate weight loss to below 5.0% (Chidavaenzi et al, 1997). For the microwave-vacuum dried lactose sample using a jacket temperature of 50°C it can be concluded from the evidence presented above that no detectable amorphous material is present in the sample.

Itoh et al (1977) studied the thermal properties of α-lactose monohydrate and observed an exothermic peak at 181°C using differential thermal analysis (DTA). They used dry methanol to dehydrate the α-lactose monohydrate into α-anhydrous lactose. It is known that dehydration using dry methanol leads to the production of stable anhydrous α-lactose (Itoh et al, 1977). The DTA traces for the stable anhydrous α-lactose showed, as expected, the hydrate peak had disappeared. However, the exothermic peak at 181°C observed for the starting material also disappeared, suggesting that the stable anhydrous α-lactose was not responsible for the exothermic peak at 181°C. DSC analysis of stable anhydrous α-lactose showed only a melting peak at 220°C (Lerk et al, 1984a).

Heat drying of α-lactose monohydrate in the absence of moisture leads to the production of a hygroscopic product called unstable anhydrous α-lactose (Itoh et al, 1977). Thermal analysis of unstable anhydrous α-lactose produces an endothermic and exothermic peak between 160°C and 180°C (Lerk et al, 1984a) in addition to the α-lactose melting peak. Lerk et al (1984a) described the solid-state changes occurring in α-lactoses when analysed using DSC. Lerk et al (1984a) described that on heating of α-lactose monohydrate in the DSC, that after dehydration of the lactose, stable and unstable anhydrous α-lactose are formed.

The endothermic and exothermic peaks for the microwave-vacuum dried lactose using a jacket temperature of 50°C suggests that they may be due to the DSC-induced

transformation of unstable anhydrous α-lactose following dehydration of the sample in the DSC.

Therefore, it appears that in the jacket temperature 50°C sample, the α-lactose monohydrate after losing its hydrate water, transforms into both stable and unstable anhydrous α-lactose. However, the stable anhydrous α-lactose does not show any peaks in the 160°C to 180°C temperature range. The endothermic and exothermic peaks in this temperature range may be due to the unstable anhydrous α-lactose.

3.4.2 Investigation of microwave-vacuum dried lactose using other drying parameters

Sample	TGA	DSC Dehydration peak	DSC Melting peak
	Weight loss (%)	Temp (°C)	Temp (°C)
Lactose as received	5.0 +/- 0.1	142.7 +/- 1.2	214.6 +/- 1.1
Standard protocol	5.1 +/- 0.1	144.4 +/- 1.5	215.4 +/- 0.9
Vacuum dried	5.0 +/- 0.1	143.4 +/- 0.5	215.1 +/- 1.2
Microwave power 250W	5.0 +/- 0.1	144.3 +/- 2.5	215.8 +/- 0.2
Jacket temperature 50°C	5.0 +/- 0.1	145.0 +/- 2.4	213.3 +/- 1.9
Impeller speed 200rpm	5.1 +/- 0.2	144.2 +/- 2.6	215.7 +/- 0.2

Table 3.1 *Summary of TGA and DSC data for microwave-vacuum dried lactose with variations in drying parameters (n = 3)*

The DSC and TGA data for the other microwave-vacuum dried samples did not show differences compared to the as received lactose. Ampoule microcalorimetry data for these samples did not show any crystallisation peaks. Table 3.1 is a summary of the TGA and DSC results for all the microwave-vacuum dried samples using variations in one of the drying parameters subsequent to the standard drying protocol, as explained in the methods section above. Table 3.1 shows that all the samples have a TGA weight loss between 95°C and 187°C of 5%, which equates to a sample containing 100% α-lactose monohydrate. The DSC hydrate and melting peaks also show similar temperatures to the as received material. This data indicates that microwave-vacuum drying does not introduce detectable amounts of amorphous material, and also does not affect the thermal properties of lactose, as measured by DSC and TGA.

This lack of changes in the thermal properties of lactose may be due to the specific nature of microwave drying. Microwaves are absorbed by water 300 times more quickly than lactose. In addition, the boiling point of water at 45 mBar pressure is reduced to ca. 30°C (Chambers et al, 1989). This means that the water is efficiently removed in conjunction with the vacuum leaving the final dry product (Doyle and Cliff, 1987). In the process of spray drying, the dissolved material is transformed in to a dried particulate form by spraying the material in to a drying air stream. This can lead to the dissolved material solidifying in to the amorphous form, as a result of the rapid drying conditions encountered during spray drying giving no opportunity for the dissolved material to crystallise (Chidavaenzi et al, 1997). For the microwave-vacuum dried lactose, the absence of a microcalorimetry crystallisation peak and the TGA detecting the presence of 100% α-lactose monohydrate in all of the dried samples (Table 3.1), indicates that the dissolved lactose solidifies as crystalline α-lactose monohydrate. This may be due to water removal in the microwave-vacuum drying process not being sufficiently rapid for amorphous material to form.

3.5 CONCLUSIONS

- Microwave-vacuum drying of lactose monohydrate does not appear to introduce amorphous material into the sample.

- TGA and DSC data show that microwave-vacuum drying of lactose monohydrate does not appear to alter the thermal properties of lactose.

- The endothermic and exothermic peaks between 160°C and 180°C, detected by DSC for the lactose microwave-vacuum dried using a jacket temperature of 50°C appears to be due to DSC-induced transformation of lactose monohydrate into unstable anhydrous α-lactose.

Chapter 4

Fluid-bed drying of spray-dried lactose

4.1 INTRODUCTION

Spray-dried lactose is a well-established direct compression excipient. Its properties include good flow and binding properties. Spray-dried lactose has an advantage over crystalline lactose in that it results in the production of stronger tablets, which is due to the presence of amorphous lactose acting as a binder (Sebhatu et al, 1994b). The spray-dried lactose used in this investigation consists of a mixture of crystalline and amorphous lactose. Moisture uptake is known to take place preferentially in the amorphous regions over the crystalline regions (Hancock and Zografi, 1994 and Sebhatu et al, 1994b). Thus the amorphous regions act as a target for moisture sorption. If the amorphous regions of the sample absorb sufficient moisture then crystallisation of the amorphous lactose may take place. This will result in the sharp loss of water as crystallisation takes place. In the previous chapter, the effect of microwave-vacuum drying on the physical properties of lactose monohydrate was investigated. This study found that microwave-vacuum drying did not introduce detectable amounts of crystal defects into the crystalline lactose investigated, as was proposed by Huttenrauch and Keiner (1979). This chapter follows on with this theme by investigating commercial spray-dried lactose, which contains a proportion of amorphous lactose in the starting material, and finding out what effect drying has on the level of amorphous material in the sample.

The main aims of this investigation were:

- To characterise the level of amorphous material and thermal properties of as received spray-dried lactose

- To investigate the effect of fluid-bed drying on the level of amorphous material and thermal properties of spray-dried lactose

- To investigate the effect of wetting and fluid-bed drying on the level of amorphous material and thermal properties of spray-dried lactose

4.2 MATERIALS AND METHODS

4.2.1 Materials

Commercial spray-dried lactose (Fast-flo lactose) was used for the investigations.

4.2.2 Methods

4.2.2.1 Ampoule microcalorimetry

Ampoule microcalorimetry was used to analyse the lactose samples and detect amorphous material in the sample. The general method used was as described in Chapter 2. A sample weight of 300 mg was weighed into the 3ml glass ampoule. A small tube containing sodium chloride saturated salt solution (75% RH) was placed inside the ampoule. The ampoule was then sealed and placed in the equilibration position for 30 minutes before lowering into the measuring site of the microcalorimeter.

4.2.2.2 Thermogravimetric Analysis (TGA)

TGA was used to analyse the weight loss associated with heating of the spray-dried lactose samples up to 230°C, at a scanning rate of 10°C/minute. A sample weight of 5mg +/- 0.5mg was used for all measurements.

4.2.2.3 Differential Scanning Calorimetry (DSC)

DSC was used to investigate the thermal properties of the spray-dried lactose and changes occurring as a result of wetting and drying. A sample weight of 5mg +/- 0.5mg was used for all measurements. The samples were scanned between 30°C and 240°C, at a scanning rate of 10°C/minute.

4.2.2.4 Gas Chromatography (GC)

Gas chromatography was used to determine the isomeric composition of lactose. The method used was as described in Chapter 2.

4.3 CHARACTERIZATION OF AS RECEIVED SPRAY-DRIED LACTOSE

4.3.1 Ampoule microcalorimetry investigation

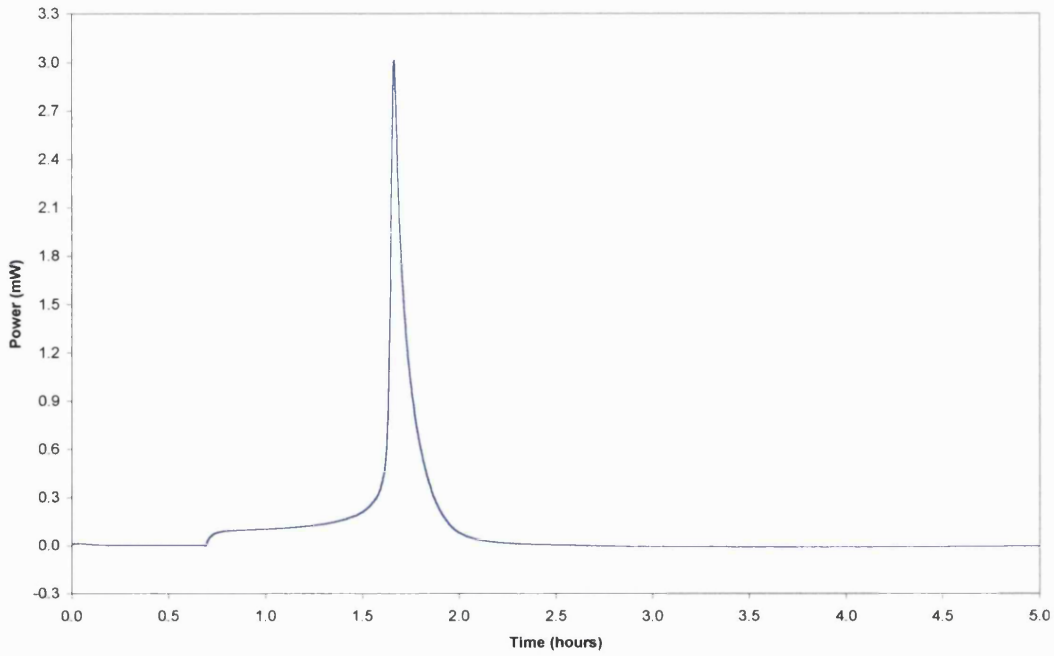

Figure 4.1 *Ampoule microcalorimetry response for the as received spray-dried lactose at 75 % RH*

Figure 4.1 shows a typical microcalorimetry response for the as received spray-dried lactose. The analysis of 100% amorphous spray-dried lactose has been covered in the literature (Briggner et al, 1994, Buckton and Darcy, 1995, and Chidavaenzi et al, 1997). The amorphous lactose recrystallises in a cooperative manner, whereby the entire powder bed becomes saturated with water vapour before crystallisation commences. This could also apply to the spray-dried lactose studied here since despite the sample containing only a small amount of amorphous lactose, the same sharp peak is seen in Figure 4.1 followed by a rapid decline to the baseline, as for the 100% amorphous lactose in the literature.

The area under the curve (AUC) for a plot of power (dQ/dt) against time (t) gives the heat associated with the process being measured. In the case of recrystallisation of 100% amorphous spray-dried lactose, a value of 48 mJ/mg has been found to correspond to recrystallisation of all of the amorphous lactose in the sample (Darcy,

1998). The magnitude of the recrystallisation has been shown by Briggner et al (1994) to be directly proportional to the degree of crystalline material in the sample. The amount of amorphous material in a sample can then be calculated by the ratio of the area under the crystallisation peak for the test sample to that of a 100% amorphous sample. Briggner et al (1994) state that for this to apply the powder loading must be identical, or is normalised. For the experiments carried out for spray-dried lactose, the areas under the curve are expressed in mJ/mg of the total weight of the sample.

For the spray-dried lactose used in this investigation, the area under the curve was 5.2 mJ/mg +/- 0.4 (n = 3). The area under the curve for 100% amorphous spray-dried lactose is 48 mJ/mg (Darcy, 1998). The percentage amorphous content of the spray-dried lactose was then calculated as 10.8 %.

Figure 4.1 shows a broad response prior to the recrystallisation event. This initial response has been observed in studies of 100% amorphous spray-dried lactose. It was previously thought that this peak was due to water sorption (Sebhatu et al, 1994, and Briggner et al, 1994). However, recent studies have shown that the initial peak is also due to collapse of the amorphous lactose (Buckton and Darcy, 1996). The studies of 100% amorphous lactose have shown that the initial collapse peak has been a separate peak to the main recrystallisation peak (Buckton et al, 1995, and Sebhatu et al, 1994a) with the curve returning to the baseline prior to the main recrystallisation peak. Figure 4.1 shows that the initial peak does not return to the baseline prior to the recrystallisation peak, and instead has a small quasi-plateau region before developing into the main recrystallisation peak. This has previously been observed by Briggner et al (1994) when lactose samples that were fluid energy milled were analysed using isothermal microcalorimetry. The microcalorimetry outputs consisted of a quasi-plateau region prior to the main recrystallisation peak. The percentage of amorphous material induced in the samples as a result of the fluid energy milling was in the range of 7.3 to 14.5% depending on the pressures used.

The quasi-plateau peak observed for the spray-dried lactose sample and the fluid energy milled samples both consist of small amounts of amorphous material (typically 10-12%) suggesting that the absence of the collapse peak returning to the baseline prior to the main recrystallisation peak may be due to this. It may be that since the amount of amorphous material is small, saturation of the amorphous portion of the sample with water vapour will take place faster than for a sample with 100% amorphous lactose

material. This would allow recrystallisation to take place faster, perhaps then resulting in the collapse and recrystallisation peaks joining together.

4.3.2 Thermogravimetric Analysis (TGA) investigation

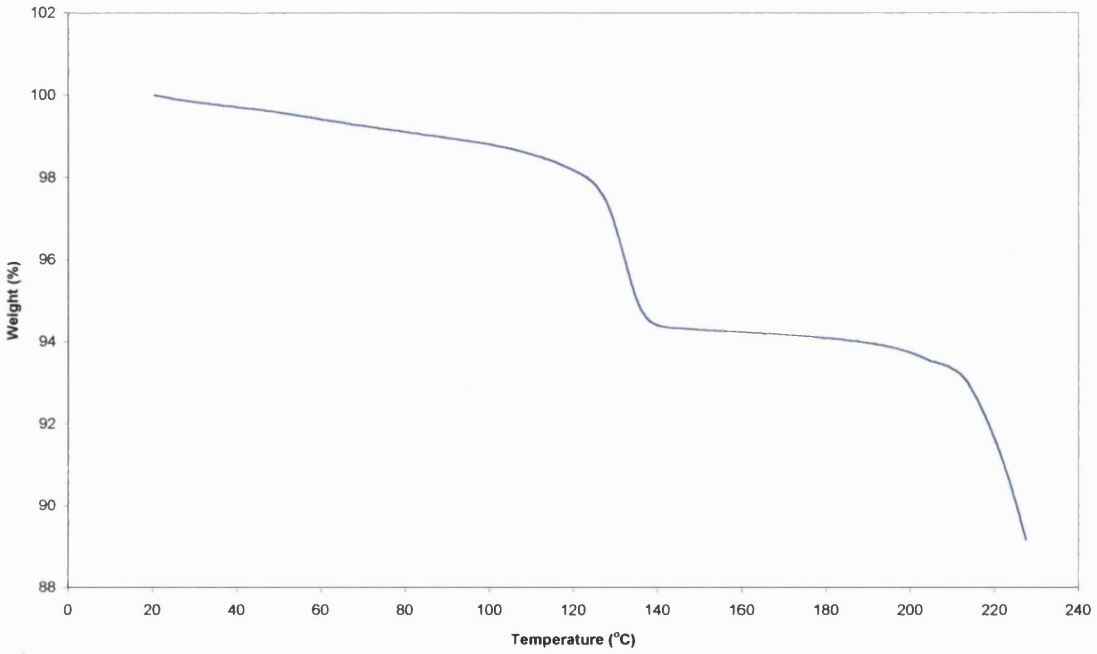

Figure 4.2 *Typical TGA curve for as received spray-dried lactose up to 230°C at 10°C/minute*

Figure 4.2 shows a typical TGA trace for as received spray-dried lactose. It shows the lactose, which has been shown to consist of 10.8% amorphous lactose, loses 1.2% +/- 0.01 (n = 3) water below 100°C and 4.5% +/- 0.01 (n = 3) crystal water between 100°C and 150°C. The percentage α-lactose monohydrate in the sample can be quantitatively obtained from the TGA data knowing that the theoretical weight loss of hydrate water for 100% α-lactose monohydrate is 5%. The percentage of α-lactose monohydrate in the spray-dried sample amounts to 90.0% +/- 0.2 (n = 3). This corresponds with the 10.8% amorphous lactose present, determined using isothermal microcalorimetry. The TGA results indicate that the remaining ca. 90% consists of α-lactose monohydrate.

4.3.3 Differential Scanning Calorimetry (DSC) investigation

Figure 4.3 shows three DSC scans for as received spray-dried lactose. It shows a dehydration peak at 142.0°C +/- 0.4 (n = 3) and a melting peak at 220.2°C +/- 0.5 (n = 3). The endothermic peak at 142°C can be attributed to the loss of hydrate water. The melting endotherm at 220°C can be attributed to the melting of α-lactose. The DSC trace does not show any recrystallisation exotherms as would have been expected given that the sample has been shown to consist of 10.8% amorphous lactose by isothermal microcalorimtery. However, this may be due to the lower sensitivity of the DSC towards small amounts of amorphous material (Angberg, 1995). In contrast, isothermal microcalorimetry has already been shown to be able to detect small amounts of amorphous lactose (Buckton et al, 1995).

The DSC trace for spray-dried lactose shows the absence of a β-lactose melting peak at around 230°C, suggesting that no crystalline β-lactose is present. The absence of a β-lactose melting response does not prove complete absence of crystalline β-lactose since it may be below the detection limits of the instrument.

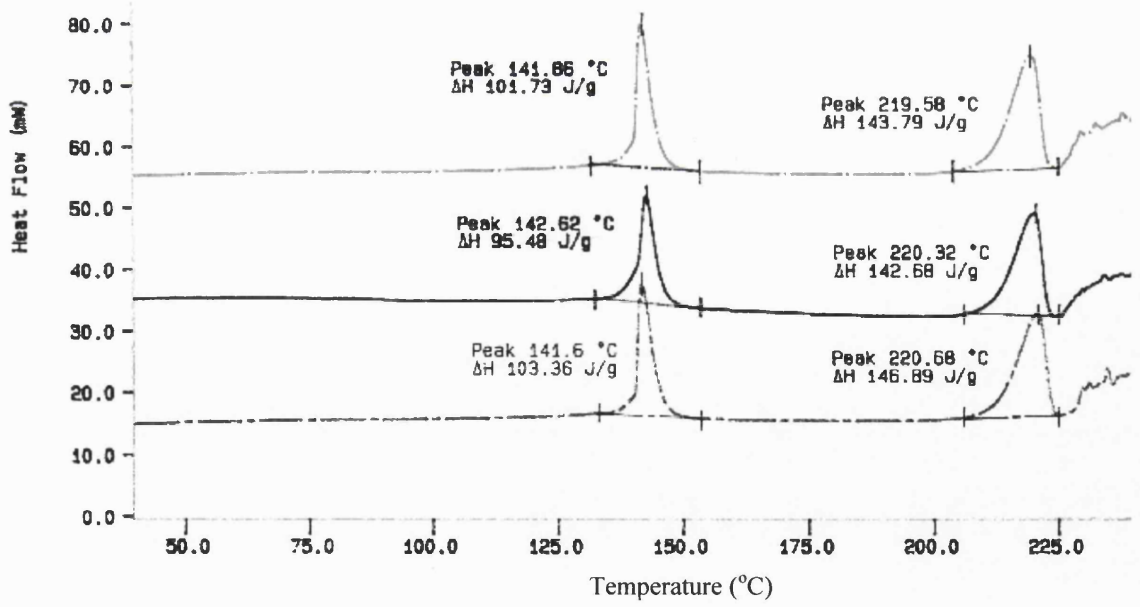

Figure 4.3 *DSC traces for as received spray-dried lactose showing a dehydration peak at 142°C and a melting peak at 220°C*

4.3.4 Conclusion

The above analysis of the as received spray-dried lactose shows that it consists of ca. 90% α-lactose monohydrate and ca. 10% amorphous lactose.

4.4 INVESTIGATION OF FLUID-BED DRYING OF SPRAY-DRIED LACTOSE

4.4.1 Introduction

This investigation involved the fluid-bed drying of spray-dried lactose without the addition of water. The main aim is to find out what effect fluid-bed drying has on the amorphous material in the spray-dried lactose.

4.4.2 Methods

The as received spray-dried lactose was weighed and transferred to a laboratory fluid-bed drier (model FBD/L70, PRL Engineering Ltd, Mostyn, Flintshire, UK). The drying conditions used were a temperature of 50°C for 30 minutes. The exit was sealed by a dust bag filter. Any material that was trapped on the dust bag filter at the end of the drying experiment was carefully guided back into the drying chamber.

4.4.3 Ampoule microcalorimtery investigation

Figure 4.4 shows a typical microcalorimetry response for spray-dried lactose that has been fluid-bed dried at 50°C for 30 minutes without the addition of water, and the ampoule response for the as received material for comparison. The dried sample shows a response that appears to be typical of the recrystallisation of amorphous lactose samples. The area under the curve was calculated as 6.20 mJ/mg +/- 0.02 (n = 3) using the same method as for the as received sample. This equates to a calculated amorphous content of 12.9%. Figure 4.4 shows that the fluid-bed dried sample peak occurs very close to that of the as received material. The percentage amorphous content appears to have increased. However, it should be noted that the initial broad peak, attributed to collapse and moisture sorption is larger than the corresponding peak for the as received material.

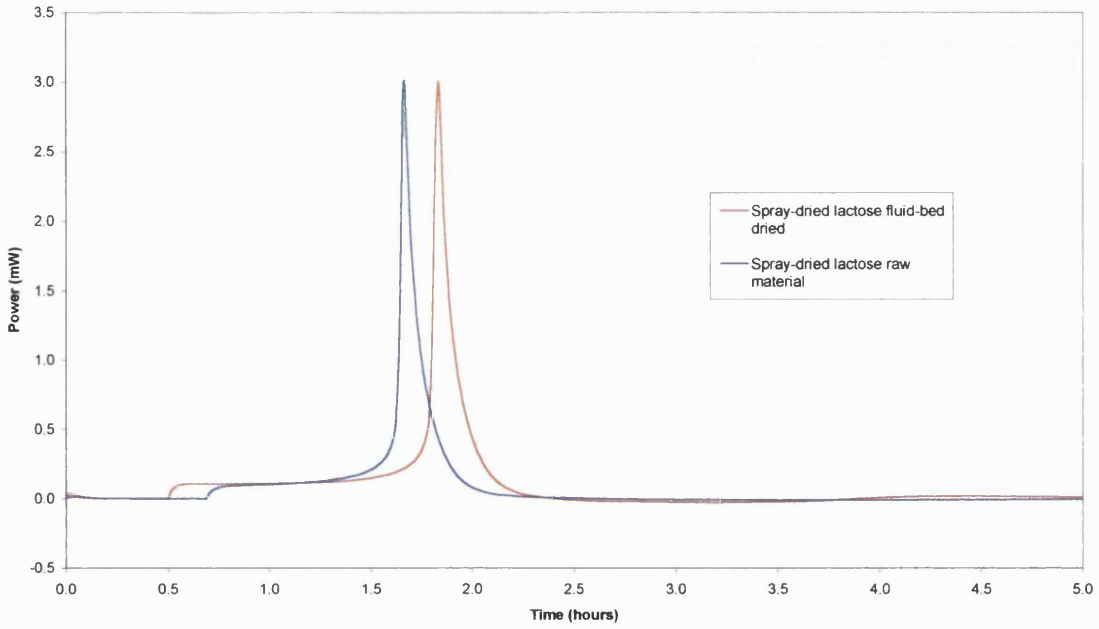

Figure 4.4 *Typical microcalorimetry response for spray-dried lactose after fluid-bed drying at 50°C for 30 minutes (without the addition of water)*

This may provide the additional area that makes it appear that the percentage amorphous material has increased. Figure 4.4 shows that the fluid-bed dried sample has a plateau region at the beginning of the collapse / moisture sorption peak, whereas for the as received material this collapse peak is continually rising towards the crystallisation peak. If this plateau region of the fluid-bed dried samples is removed from the area under the curve, then it is calculated as 5.5 mJ/mg +/- 0.1 (n = 3). This is similar to the as received material, taking into account the standard deviations. Thus it appears that there may be no increase in the amorphous content but that the collapse / moisture sorption peak is more protracted for the fluid-bed dried sample in relation to the as received spray-dried lactose, making it appear that the overall area under the curve is greater.

4.4.4 Thermogravimetric Analysis (TGA) investigation

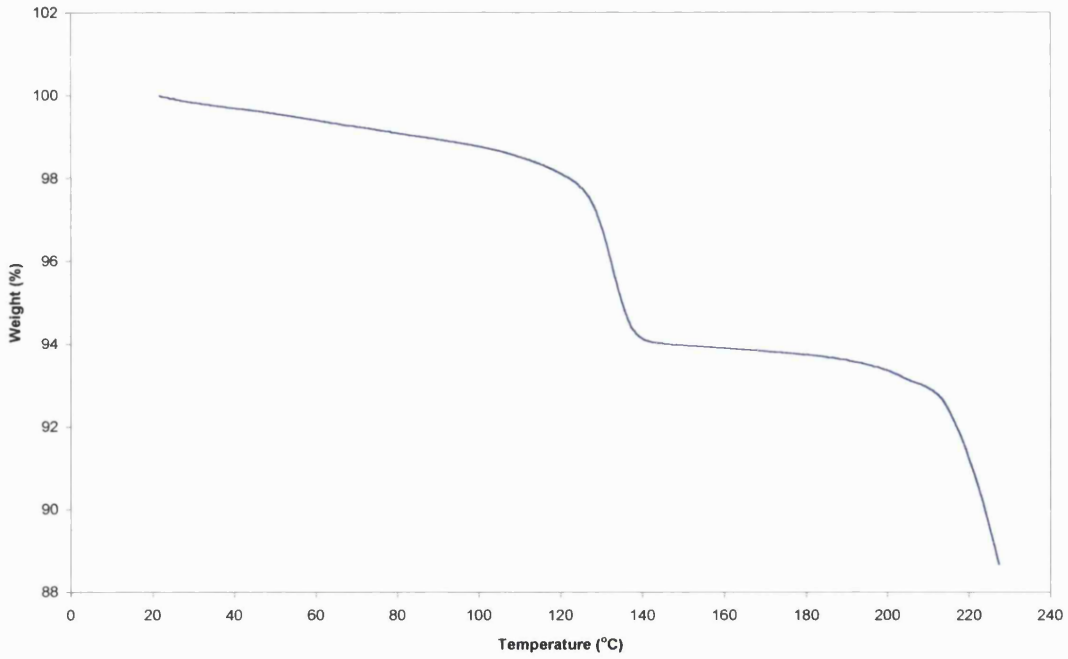

Figure 4.5 *Typical TGA curve for spray-dried lactose after fluid-bed drying at 50°C for 30 minutes (without the addition of water)*

Figure 4.5 shows a typical TGA weight loss curve for spray-dried lactose after fluid-bed drying. It shows a loss of 1.3% +/- 0.3 (n = 3) water below 100°C, and 4.7% +/- 0.3 (n = 3) between 100°C and 150°C. The 4.7% water loss above 100°C can be attributed to the removal of water of crystallisation. Relating this to the theoretical water loss of 5% for a full monohydrate, the % α-lactose monohydrate was calculated as 94.0% +/- 5.8 (n = 3). This value of 94% α-lactose monohydrate suggests that the percentage has increased from the 90.0% +/- 0.2 for the as received material. However, the standard deviation for the fluid-bed dried sample is far greater, at 5.8%, suggesting that there is large variation in the amorphous content between samples and is not as uniform as the as received material.

4.4.5 Differential Scanning Calorimetry (DSC) investigation

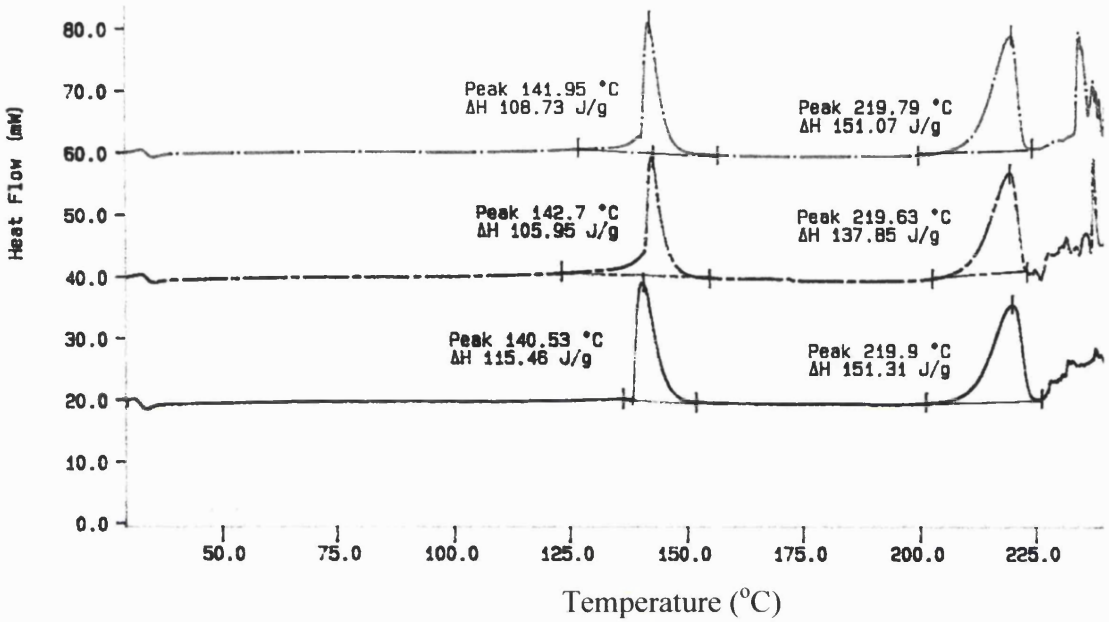

Figure 4.6 *DSC traces for fluid-bed dried spray-dried lactose showing a dehydration peak and α-lactose melting peak*

Figure 4.6 shows three DSC scans for fluid-bed dried spray-dried lactose. It shows a dehydration peak at 141.7°C +/- 0.9 (n = 3) and a α-lactose melting peak at 219.8°C +/- 0.1 (n = 3). These peak temperatures are essentially the same as the as received material. When the areas under the curves (AUC) are considered it is found that the dehydration enthalpy of the fluid-bed spray-dried lactose is 110.1 J/g +/- 4.0 (n = 3), whilst that for the as received spray-dried lactose is 100.2 J/g +/- 3.4 (n = 3). There is a higher AUC for the fluid-bed dried sample compared to the as received material, suggesting a higher proportion of crystal hydrate water. However, since no water has been introduced into the system, it seems likely that the differences are due to differences in drying of the sample. Ampoule microcalorimetry also showed that the amount of amorphous material is unchanged from the as received spray-dried lactose.

4.4.6 Conclusion

Ampoule microcalorimetry showed that fluid-bed drying of spray-dried lactose without the addition of water appears to have no effect on the amount of amorphous material. However, there appears to be a greater variation in the thermal properties of the fluid-bed dried sample that may be due to the fluid-bed dried sample being non-uniform relative to the as received spray-dried lactose.

4.5 INVESTIGATION OF WETTING AND FLUID-BED DRYING OF SPRAY DRIED LACTOSE

4.5.1 Introduction

Spray-dried lactose was mixed with 11% water using a planetary mixer for 10 minutes. The wet mass was then transferred to the laboratory fluid-bed drier. The drying conditions used were a temperature of 50°C and a drying time of 30 minutes.

4.5.2 Ampoule microcalorimetry investigation

The same method was used as for the ampoule microcalorimetry investigation of the as received spray-dried lactose described above. The microcalorimtery investigation did not produce a recrystallisation peak indicating the absence of amorphous material. This is what would have been expected since the 10.8% amorphous material in the starting material would have been recrystallised by the water used in the wetting stage of the process.

4.5.3 Thermogravimetric analysis (TGA) investigation

Figure 4.7 shows a TGA trace for the spray-dried lactose sample that has been wetted and fluid-bed dried. It shows loss of hydrate water between 100°C and 150°C, with a hydrate weight loss of 4.7% +/- 0.04 (n = 3). A full α-lactose monohydrate has a theoretical hydrate weight loss of 5%. The 4.7% weight loss for the wetted and dried sample then equates to 94.0% α-lactose monohydrate in the wetted and dried sample. The sample has already been shown by microcalorimetry to contain no detectable amorphous material. The remaining ca. 6% of the sample may then possibly be due to α-anhydrous or anhydrous β-lactose in the sample. This was then considered further by using DSC.

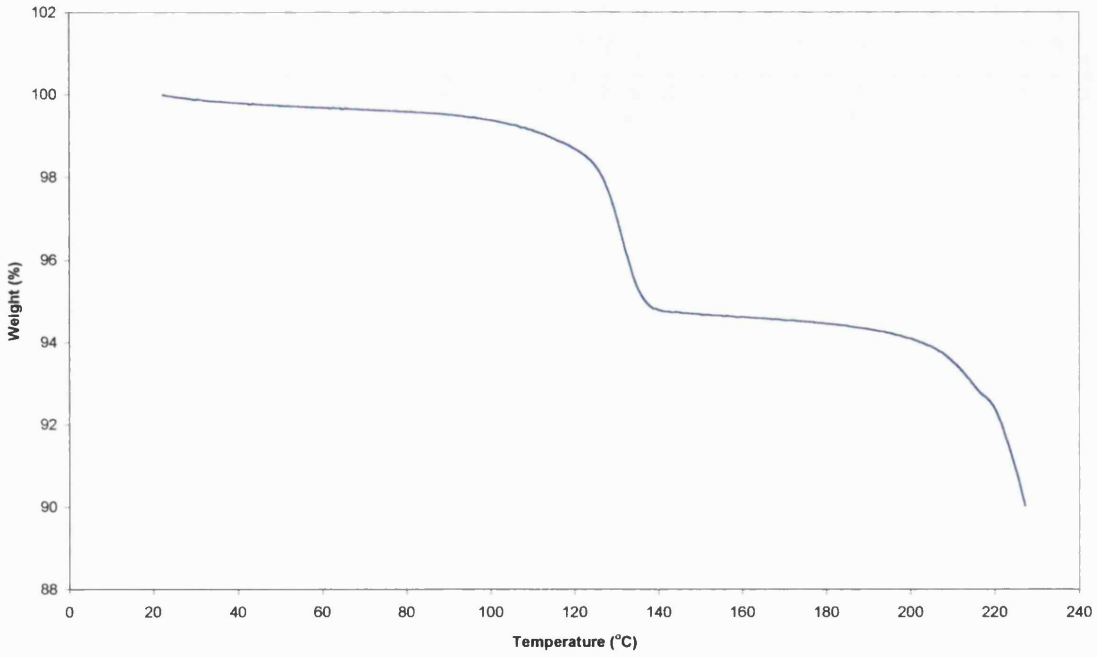

Figure 4.7 *TGA trace for spray-dried lactose after wetting and fluid-bed drying at 50°C for 30 minutes*

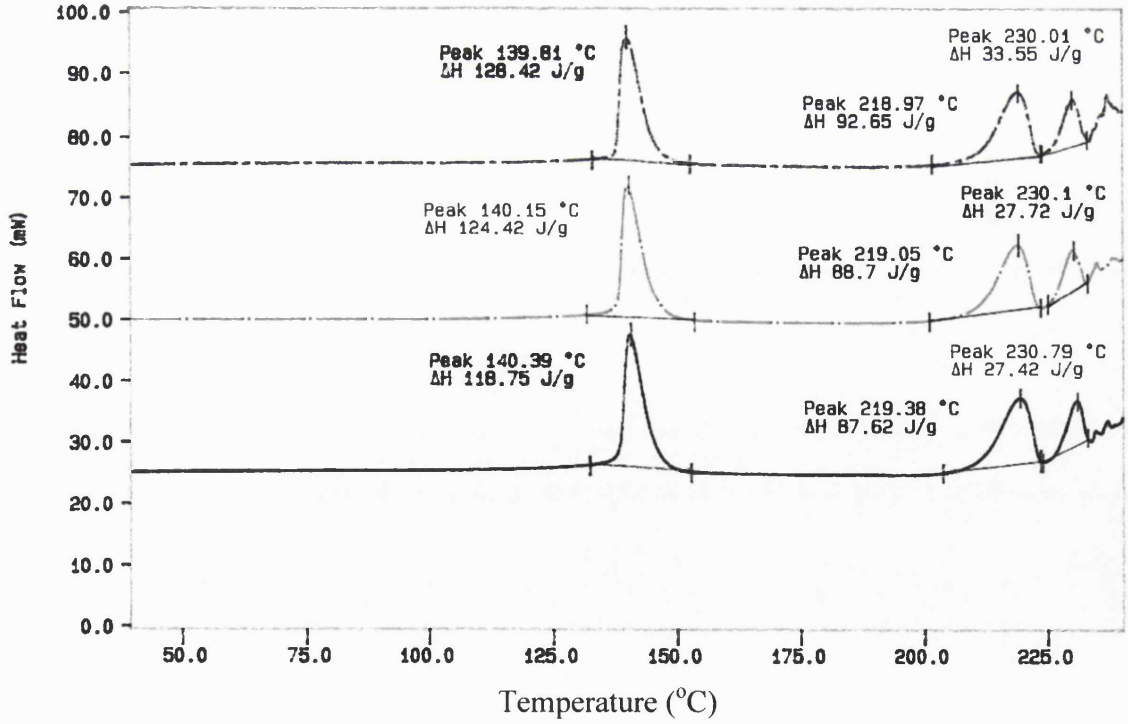

Figure 4.8 *DSC traces for spray-dried lactose wetted and fluid-bed dried at 50°C for 30 minutes*

4.5.4 Differential Scanning Calorimetry (DSC) investigation

Figure 4.8 shows three DSC scans for the wetted and fluid-bed dried lactose sample. It shows a typical dehydration peak at 140.1°C +/- 0.2 (n = 3), an α-lactose melting peak at 219.1°C +/- 0.2 (n = 3), and a β-lactose melting peak at 230.3°C +/- 0.3 (n = 3). The presence of a β-lactose melting peak shows that crystalline β-lactose is present in the sample. Microcalorimetric analysis showed that the sample did not contain detectable amounts of amorphous material. The β-lactose detected using DSC is likely to be due to crystallisation of the amorphous material during wetting and fluid-bed drying of the sample. DSC has not been used to provide a quantitative analysis of the proportions of α- and β-lactose in the sample since it is known that mutarotation can occur during heating of the sample in the DSC (Olano et al, 1983). However, gas chromatography (GC) was employed to investigate the presence of α- and β-lactose further. It was found using GC that the sample contained 93.1% +/- 0.7 (n = 3) α-lactose and 6.9% +/- 0.7 (n = 3) β-lactose. The 6.9% β-lactose is similar to the 6% anhydrous lactose calculated from TGA above, taking into account experimental error. Sebhatu et al (1994a) and Briggner et al (1994) found that crystallisation of amorphous spray-dried lactose can lead to a mixture of α- and β-lactose. Therefore, it appears that the 10.8% amorphous lactose in the as received spray-dried lactose has crystallised into a mixture of approximately equal amounts of α- and β-lactose.

4.5.5 Conclusion

The amorphous portion of the wetted and fluid-bed dried sample of spray-dried lactose has been shown to have crystallised. TGA has shown that 94% of the sample is now α-lactose monohydrate. The remaining 6% was shown using GC to be due to anhydrous β-lactose.

4.6 CONCLUSIONS

- The as received spray-dried lactose consists of ca. 90% α-lactose monohydrate and ca. 10% amorphous lactose.

- Fluid-bed drying of spray-dried lactose without the addition of water does not appear to change the amorphous content present in the starting material.

- Wetting and fluid-bed drying has the expected effect of crystallisation of the amorphous lactose. TGA and GC show that the amorphous lactose crystallised into a mixture of α- and β-lactose.

Chapter 5

Interaction of water with maltodextrins

5.1 INTRODUCTION

The maltodextrins are carbohydrate ingredients that are obtained by controlled starch hydrolysis with acid and/or enzyme (Li and Peck, 1990). They are defined as having a dextrose equivalent (DE) value of upto 20 (Mollan and Celik, 1993). The DE value is measured as the amount of reducing sugars present and is expressed as percentage of dextrose on a dry weight basis. The maltodextrins are composed of glucose polymers, the chain length depending on the degree of starch hydrolysis. They are amorphous materials that have been used in the food industry to retard crystallisation, increase viscosity, and reduce the stickiness and hygroscopicity of dried materials. They are also used in the pharmaceutical industry as diluents, binders, viscosity-inducing agents, and drying aids. It is well known that various amorphous materials such as poly (vinyl pyrrolidone) (PVP) absorb large amounts of water due to uptake in to the bulk of the amorphous material rather than being restricted to particle surfaces. Absorption of water into the material can affect the physico-chemical properties of the material such as chemical stability, powder flow properties, compaction, and dissolution rate (Zografi and Kontny, 1986).

Maltodextrins can be used as excipients in pharmaceutical formulation where they can form a large proportion of the formulation and it is therefore important to have knowledge of the effect that moisture sorption can have on the maltodextrins.

The main aims of this investigation were:

- To investigate the effect of humidity on the glass transition temperature and moisture content of the maltodextrins

- To investigate the effect of humidity on the collapse phenomena for the maltodextrins

- To establish critical humidity levels which would be a useful guide to conditions that may cause physical changes to occur

5.2 INVESTIGATION OF THE GLASS TRANSITION TEMPERATURE (Tg)

5.2.1 Introduction

The glass transition temperature (Tg) of an amorphous material determines its physical stability, chemical stability, and viscoelastic properties. The Tg usually becomes a critical parameter when it is approached or exceeded (Hancock and Zografi, 1994). This usually occurs when the operating temperature exceeds the Tg, or by plasticisation of the Tg to below the operating temperature (Oksanen and Zografi, 1990). In this study, the absorption of water by the maltodextrins and its effects on the glass transition temperature are investigated.

5.2.2 Methods

The gravimetric studies were carried out using Dynamic Vapour Sorption (DVS) as described in Chapter 2. A sample mass of 15mg was weighed into aluminium foil boats placed in the quartz sample pan for all DVS investigations. A foil boat was used rather than weighing directly onto the sample pan since it was anticipated that the maltodextrins would change to a sticky material that would be difficult to remove from the quartz sample pan. The method used for the samples was 0% RH to 90% RH in steps of 10% RH. The condition for changing from one step to the next was a dm/dt of 0.001 (%/min) for a minimum time of 10 minutes. This ensured that the water absorption at each step had come to equilibrium before proceeding to the next step in the method. Figure 5.1 shows that the mass equilibrated at each step, with the exception of the 80% and 90% RH responses. This is due to a maximum time limit at each step of 360 minutes. This procedure was carried out in duplicate for each of the maltodextrins investigated.

5.2.3 Results

Figure 5.1 shows a plot of change in mass (%) and target RH as a function of time (minutes). Figure 5.1 shows a steady increase in weight up to 50% RH. From 60% RH onwards the weight increases are greater, suggesting that a physical change may be occurring in the sample. The large amount of water taken up by the sample is characteristic of amorphous materials, which are known to absorb large amounts of water into amorphous regions (Hancock and Shamblin, 1998).

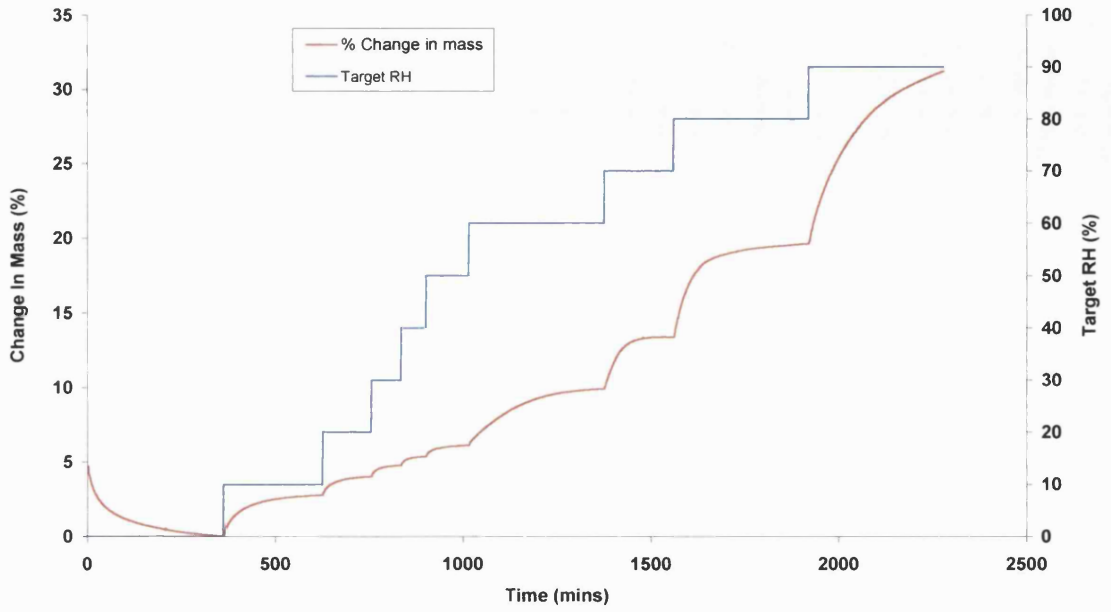

Figure 5.1 *DVS moisture sorption and target RH data for Maltrin M150 maltodextrin*

5.2.4 Calculation of glass transition temperatures (Tg) for the maltodextrins

5.2.4.1 The Gordon and Taylor equation

The glass transition temperature of compatible polymer mixtures can be calculated using equation (5.1) (Gordon and Taylor, 1952). This equation has also been used for the Tg calculation of polymer-water mixtures (Roos, 1993b, Hancock and Zografi, 1994).

$$Tg = \frac{w_1 Tg_1 + k w_2 Tg_2}{w_1 + k w_2} \qquad (5.1)$$

In equation (5.1), Tg is the glass transition temperature of the mixture (maltodextrin-water), Tg_1 and Tg_2 are the glass transition temperatures of components 1 (maltodextrin) and 2 (water), w_1 and w_2 are the weight fractions of components 1(maltodextrin) and 2 (water), and k is a constant.

The constant k from equation (5.1) was calculated using equation (5.2) as used by Roos (1993b). Equation (5.2) was developed by Roos (1993a) by plotting k against Tg for a number of carbohydrates and calculating the regression equation from the data.

$$k = 0.0293\ Tg + 3.61 \qquad (5.2)$$

The k values for the maltodextrins used are shown in Table 5.1. The constant k in equation (5.1) can be considered as a ratio of the free volumes of the two components (Hancock and Zografi, 1994).

5.2.4.2 Establishing anhydrous Tg values for the maltodextrins

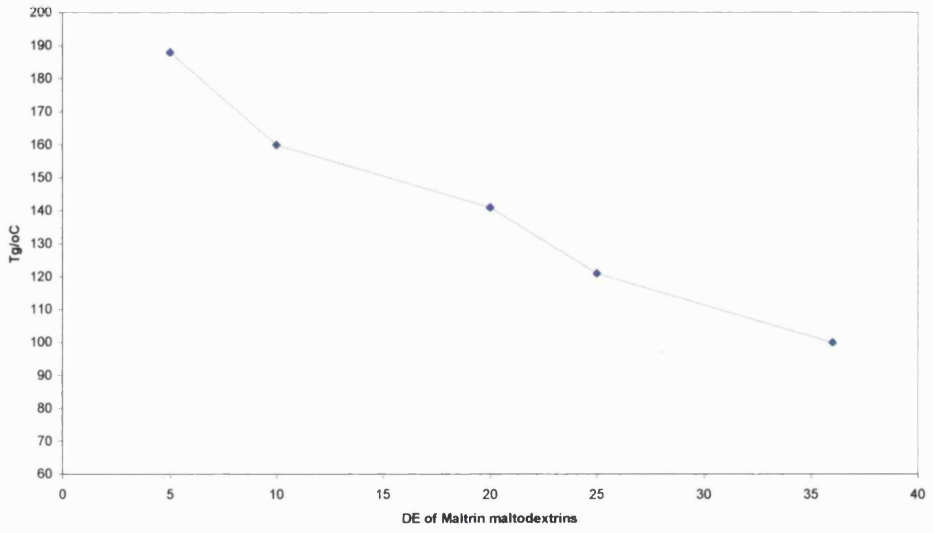

Figure 5.2 *Glass transition data for Maltrin maltodextrins (using data from Roos and Karel, 1991a)*

DE of maltodextrin	k	Tg(°C)	Source of Tg value
5	9.118	188	Roos and Karel (1991a)
10	8.298	160	Roos and Karel (1991a)
15	8.034	151	Estimated from Figure 5.2
20	7.741	141	Roos and Karel (1991a)

Table 5.1 *Glass transition temperatures (Tg) and k values for the maltodextrins*

Figure 5.2 shows a plot of Tg against the DE value of the Maltrin maltodextrins. The Tg values for maltodextrins with DE values of 5, 10, and 20 are plotted in Figure 5.2. The Tg value for the maltodextrin with a DE value of 15 (Maltrin M150) has been estimated graphically from Figure 5.2. Table 5.1 shows the Tg values and their sources for the maltodextrins studied.

5.2.4.3 Glass transition (Tg) data for the maltodextrins

Table 5.2 shows the moisture content (m) obtained from the DVS experiments and corresponding Tg values calculated using equation (5.1). The Tg of water was taken as –135°C.

DE	DE 5		DE 10		DE 10		DE 15		DE 20	
Maltrin	M040		M100		M500		M150		M200	
% RH	m (g/100g dry)	Tg (°C)	m (g/100g dry)	Tg (°C)	m (g/100g dry)	Tg (°C)	m (g/100g dry)	Tg (°C)	m (g/100g dry)	Tg (°C)
0	0.0	188.0	0.0	160.0	0.0	160.0	0.0	151.0	0.0	141.0
10	4.0	99.0	2.9	101.6	2.7	104.2	2.9	96.3	2.2	99.6
20	5.7	73.8	4.4	79.1	4.5	77.2	4.1	77.6	3.4	81.5
30	6.8	58.5	5.3	66.7	5.7	61.1	4.9	67.8	4.2	71.4
40	8.0	45.5	5.9	58.5	6.7	49.5	5.4	60.6	4.7	65.2
50	9.6	29.7	6.7	49.6	7.7	39.7	6.3	50.9	5.2	59.1
60	11.5	12.9	9.1	26.0	9.0	26.8	10.0	16.0	8.3	27.5
70	14.2	-6.1	13.1	-4.1	12.5	0.0	13.6	-8.6	13.2	-8.3
80	18.0	-27.2	18.7	-33.4	17.4	-27.6	19.8	-39.0	18.9	-36.7
90	27.6	-62.8	28.9	-67.6	27.7	-64.4	31.9	-74.9	31.3	-74.0

Table 5.2 *Moisture content and glass transition temperature (Tg) for the maltodextrins with DE between 5 and 20. Moisture contents (m) are given in g/100g dry matter and Tg in °C*

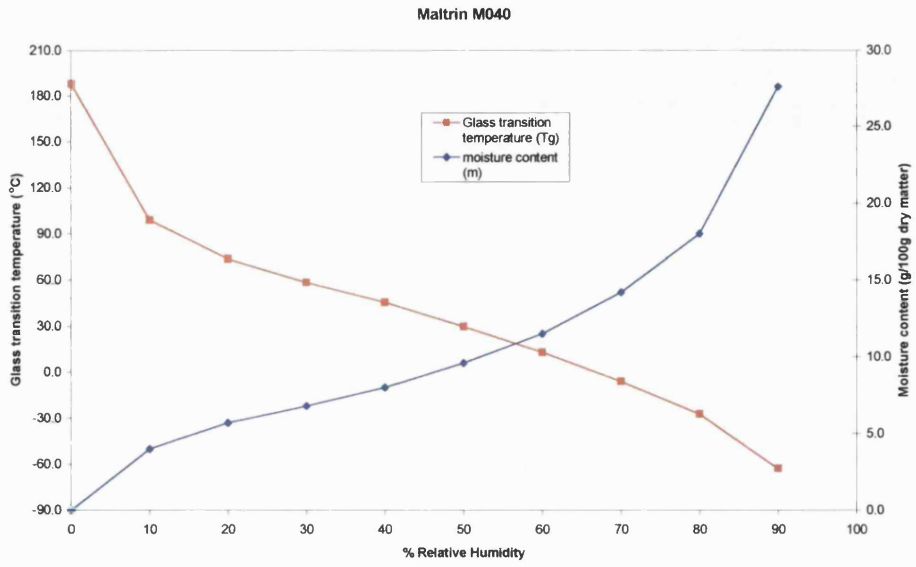

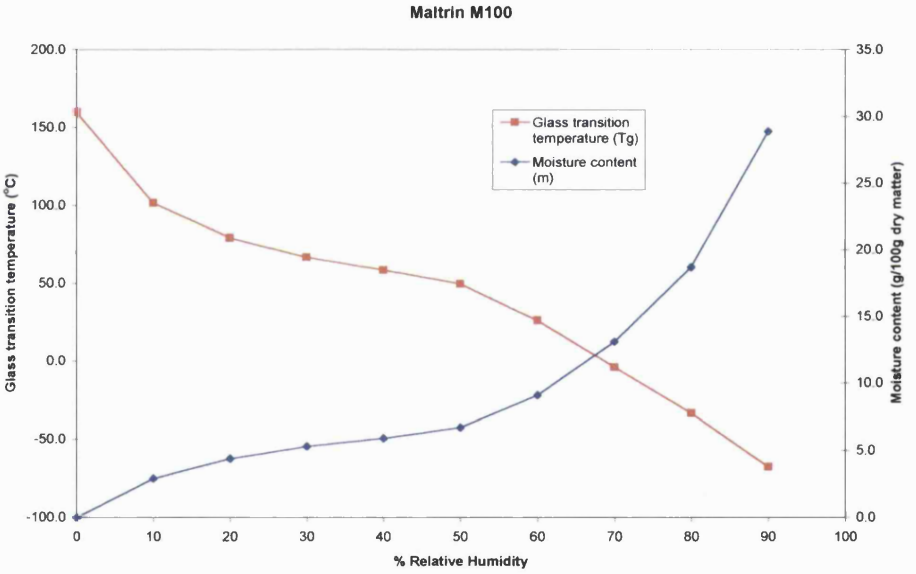

Figure 5.3 *Absorption isotherms showing the effect of moisture sorption on the Tg for M040 and M100 maltodextrins at 25°C*

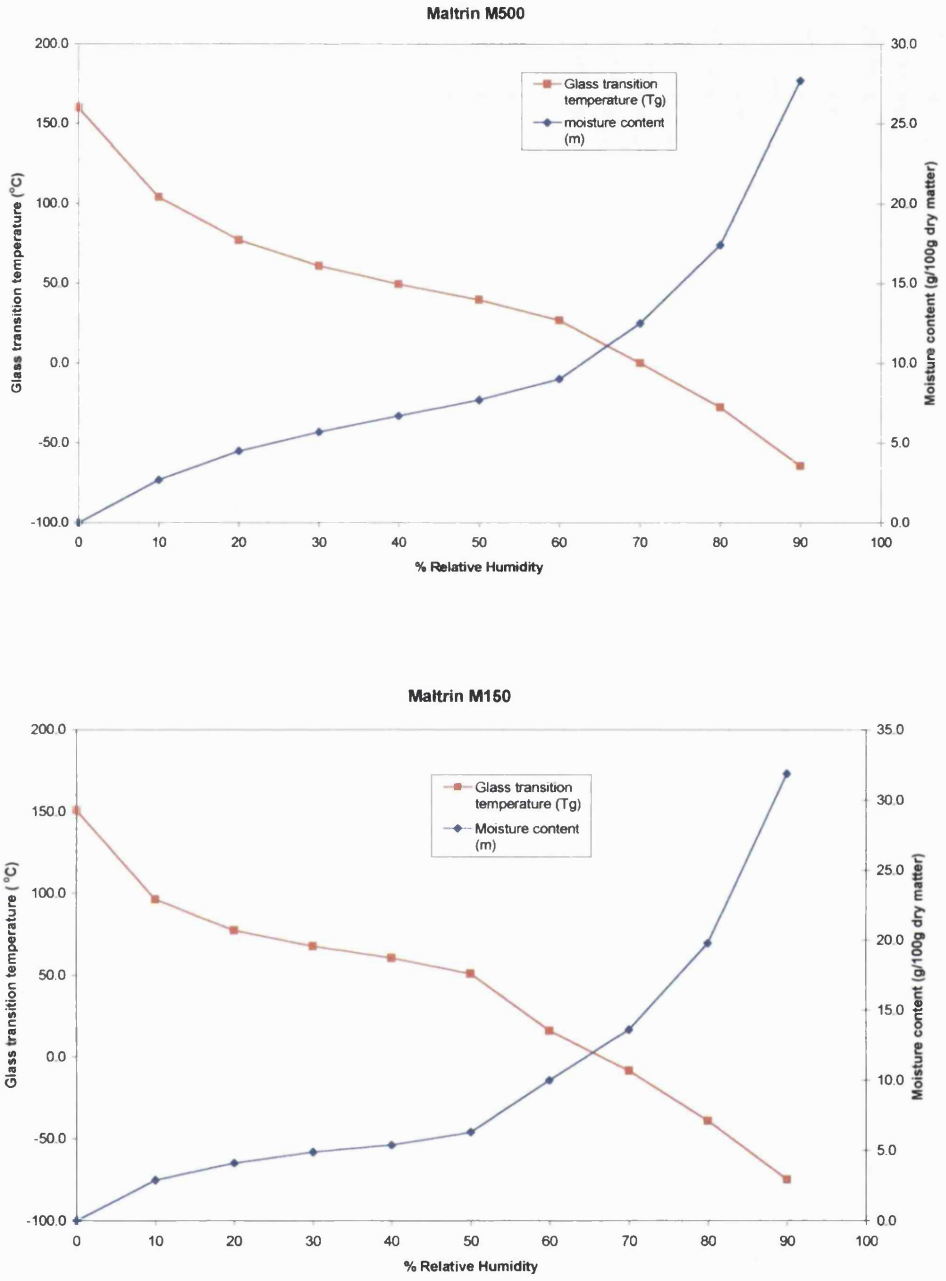

Figure 5.4 *Absorption isotherms showing the effect of moisture sorption on the Tg for M500 and M150 maltodextrins at 25°C*

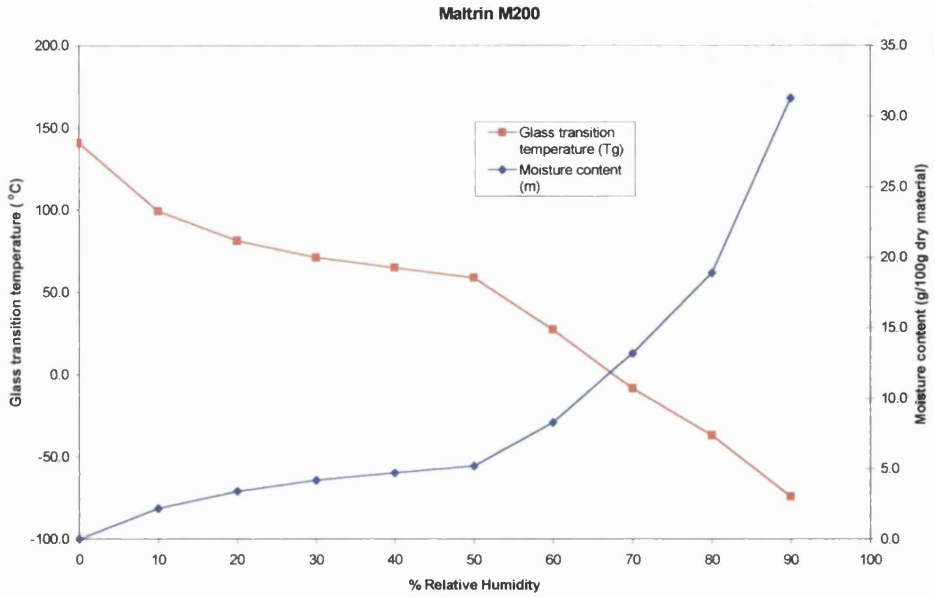

Figure 5.5 *Absorption isotherm showing the effect of moisture sorption on the Tg for M200 maltodextrin at 25°C*

The absorption and glass transition data shown in Figures 5.3 to 5.5 were used to find out the critical % RH and moisture content, when the Tg is lowered to 25°C, the operating temperature of the dynamic vapour sorption (DVS) experiments carried out. The critical % RH and moisture content for the maltodextrins are shown in Table 5.3.

DE	DE 5	DE 10	DE 10	DE 15	DE 20
Maltrin	M040	M100	M500	M150	M200
% RH at Tg of 25°C	53%	60%	61%	58%	61%
Critical moisture content (g/100g dry matter)	10.1	9.1	8.5	9.1	8.5

Table 5.3 *Critical % RH and moisture content at a glass transition temperature of 25°C*

Figures 5.3 to 5.5 show the plots of Tg and moisture content against % RH for the maltodextrins studied. They show that the maltodextrins studied all have a sigmoidal moisture sorption profile. Figures 5.3 to 5.5 show that as the RH is increased beyond 50% RH, water sorption increases significantly. This upward inflection in the water sorption profile is thought to be due to the glass-to-rubber transition occurring at Tg, as the absorbed water plasticises the Tg to below the operating temperature (Oksanen and Zografi, 1990). Inspection of the critical % RH values shown in Table 5.3 show that the Tg is lowered to T (the operating temperature) between 50% and 60% RH for the maltodextrins, which corresponds to the points on the sorption curves where the upward inflection occurs. Levine and Slade (1988a) suggest that water plasticisation of glassy polymers close to the Tg leads to increasing permeability of the substrate to gases and vapours, due to increasing segmental mobility as the Tg decreases towards T, the operating temperature. They also suggest that in the rubbery state, when Tg is below T, polymer free volume increases sharply and this is known to cause a dramatic increase in the permeability to gases and vapours.

Water absorption into amorphous materials has been studied with regard to the state of water in the amorphous solid. It has been suggested that a certain proportion of the water absorbed is in a 'tightly bound' state and amounts absorbed in addition to this value are present in a 'solvent-like' state (Khan and Pilpel, 1987). Oksanan and Zografi (1990) investigated the absorption isotherm for PVP, a water-soluble amorphous polymer. They found that the water content where the water appears to be 'tightly bound' coincided with the weight of water required to form a single layer of molecules on the surface of the solid (W_m) that is commonly used for crystalline materials. They also found that at a definitive multiple of W_m a second critical point occurred in the isotherm. For starches this second critical point occurs at 3 times W_m, whereas for celluloses it occurs at 5 times W_m (Zografi and Kontny, 1986). This point appeared to correspond to when the water takes on a 'solvent-like' state (Oksanen and Zografi, 1990). However, despite the evidence for the different states of water associated with the amorphous solid, it has been suggested that the change in the apparent states of water absorbed may be a result of the change in the physical state of the amorphous material as plasticisation occurs (Levine and Slade, 1988a). They suggest that the 'tightly bound' state of water may be due to the immobility that is present in the high viscosity glassy state. Also, the 'solvent-like' state of water may be a result of the much reduced viscosity of the rubbery state of the amorphous polymer above the Tg. Oksanen

and Zografi (1990) studied the water absorption isotherms for PVP at different temperatures. They calculated Wg values, which are the water content (W) values of the amorphous material at the point where the Tg is plasticised to T. They found that when the Wg value had not been reached, the shape of the isotherm was without the upward inflection in water absorption that is characteristic of the sigmoidal shape for water-soluble amorphous polymers. Below the Wg value, the polymer/water mixture is in a highly viscous state, whereas above the Wg value, the polymer/water system has been changed to the rubbery state with the corresponding increased molecular mobility (Oksanen and Zografi, 1993). The 'solvent-like' state of water in amorphous polymers appeared to be a complex combination of water and polymer existing in a rubbery amorphous state (Oksanen and Zografi, 1990). Oksanen and Zografi (1993) calculated diffusion coefficients of water, which reflect the translational and rotational motions of molecules (Shalaev and Zografi, 1996), for PVP/water mixtures. They found that at water contents below Wm, the water molecules still possessed a high degree of translational mobility, and were not in a 'tightly bound' or an 'immobilised' state in the glassy polymer. Also noted was the diffusion coefficients of water above the Wg values, where the molecular mobility was more than one order of magnitude below that expected for the free diffusion of bulk water. Proton NMR relaxation studies also showed that the absorbed water in PVP never attains the mobility of pure water even at the highest water contents. It was suggested that the water molecules even at the higher water contents are still restricted by the polymer structure (Oksanen and Zografi, 1993).

5.3 INVESTIGATION OF COLLAPSE PHENOMENA

5.3.1 Introduction

Levine and Slade (1988a) considered the collapse phenomena in amorphous materials to include stickiness, agglomeration, caking, flow of amorphous powders, and structural collapse. The schematic in Figure 5.6 represents the 'humidity caking' mechanism that is most commonly encountered in food powders (Peleg, 1983). The most common caking mechanism is due to water sorption and subsequent interparticle fusion (Peleg, 1983). Caking of amorphous powders results from the change of the material from a glassy to the less viscous liquid-like state, thus allowing liquid flow between particles and formation of liquid bridges between particles (Roos, 1995). Moistening of the particle's surface leads to surface plasticisation of the amorphous material (Roos, 1995) and a reduction in the surface viscosity of the particles (Downton et al, 1982). Humidity caking is a consequence of an increasing water content, plasticisation, and depression of Tg to below the ambient temperature (Roos, 1995). The caking mechanism is described as a surface wetting process (Roos, 1995).

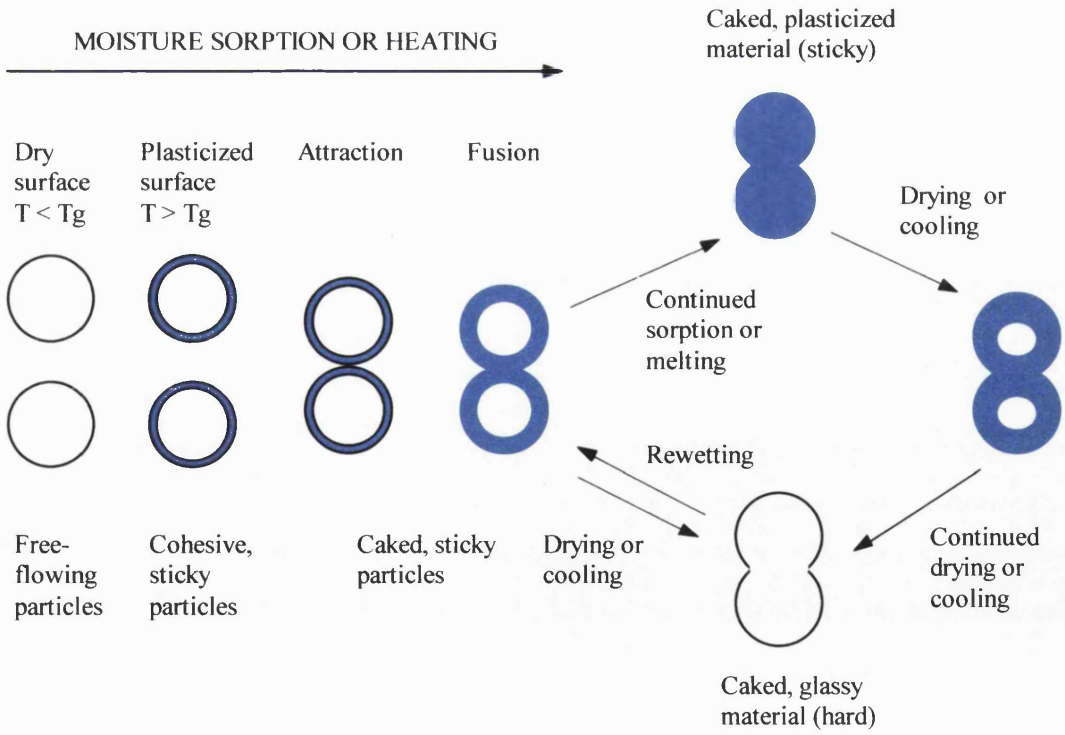

Figure 5.6 *Schematic representation of the humidity caking mechanism in food powders (reproduced from Peleg, 1983)*

5.3.2 Methods

5.3.2.1 Ampoule microcalorimetry

The maltodextrin samples were weighed (30mg) into 3ml glass ampoules and a durham tube containing a saturared salt solution was placed inside the glass ampoule to produce a given RH. The saturated salt solutions used were sodium nitrite (65% RH), sodium chloride (75% RH), and potassium chloride (85% RH) at 25°C. Samples were placed in the equilibration position for 30 minutes for all samples before lowering into the measuring site. Calculation of the area under the power-time curve (AUC) was carried out using Origin 3.5 (Microcal). The first point for AUC analysis was taken as the start of the peak, and the end point was when the peak reached the baseline. For the responses that did not reach the baseline, the following procedure was used. As shown in Figure 5.7, a straight line was superimposed onto the sloping baseline using Origin 3.5, and the point where the curve deviated from the straight line (shown by a red arrow in Figure 5.7) was taken as the second point in the AUC calculation.

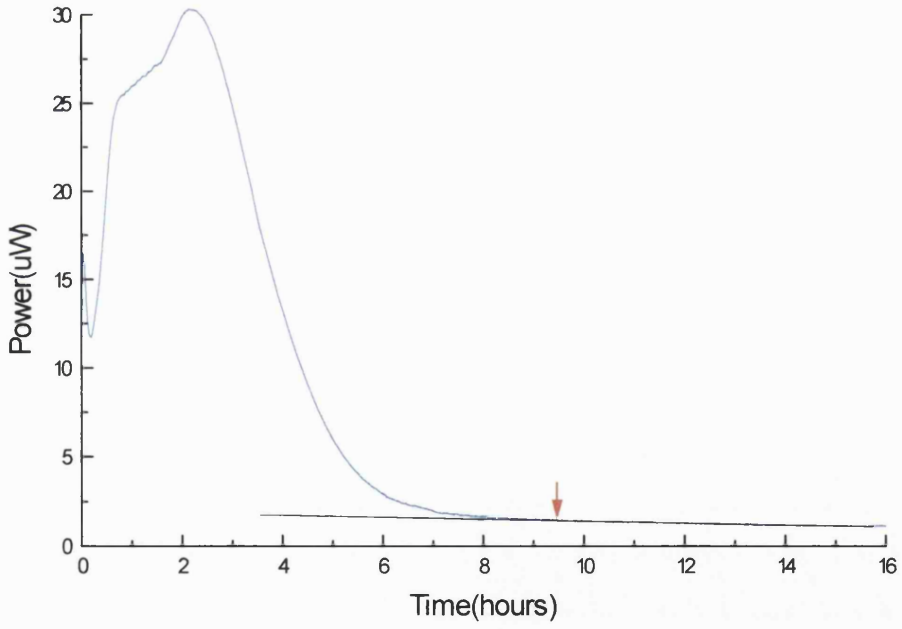

Figure 5.7 *Ampoule microcalorimetry response for Maltrin M500, showing the method used to calculate the AUC for responses that did not reach the baseline*

5.3.2.2 Dynamic Vapour Sorption (DVS)

To investigate collapse of the maltodextrins, Dynamic Vapour Sorption was used. A method was created with the RH set at 0% RH for 400 minutes, then 75% RH for 1200 minutes, and 0% RH for 400 minutes. The starting materials were the as received materials and investigations were carried out in duplicate for each of the maltodextrins.

5.3.2.3 Scanning Electron Microscopy (SEM)

To investigate the effect of humidity on the appearance of the maltodextrins, SEM was employed. This involved analysing samples of the maltodextrins before and after being exposed to 75% RH using sodium chloride saturated salt solution. The SEM work was carried out by Mr D McCarthey in the Microscopy Unit.

5.3.2.4 Light microscopy

This involved viewing samples of maltodextrins using a light microscope before and after exposing them to 75% RH using sodium chloride saturated salt solution.

5.3.3 Calculation of the collapse temperature (Tc)

Roos (1995) correlated collapse temperature (Tc) data from Tsourouflis et al (1976) and glass transition (Tg) data from Roos and Karel (1991a) and Roos (1993b) to obtain a linear relationship with Tc values about 40 to 70°C above the corresponding Tg value for the maltodextrins studied (Roos, 1995). Roos (1995) used regression analysis to obtain an equation for the linear relationship between Tc and Tg values for the maltodextrins, equation (5.3). The Tc values determined by Tsourouflis et al (1976) were for freeze-dried maltodextrins where visual determination of collapse was used, defined as a change in the sample's surface appearance, as the temperature of the humidified samples was increased.

$$Tc = 1.15\ Tg + 42.02 \qquad (5.3)$$

Equation (5.3) was used to calculate the Tc values for the maltodextrins analysed in this study, using the Tg values already calculated in the previous section using the Gordon and Taylor equation.

DE	DE 5		DE 10		DE 10		DE 15		DE 20	
Maltrin	M040		M100		M500		M150		M200	
% RH	m (g/100g dry)	Tc (°C)	m (g/100g dry)	Tc (°C)	m (g/100g dry)	Tc (°C)	m (g/100g dry)	Tc (°C)	m (g/100g dry)	Tc (°C)
0	0.0	258.2	0.0	226.0	0.0	226.0	0.0	215.7	0.0	204.2
10	4.0	155.9	2.9	158.9	2.7	161.9	2.9	152.8	2.2	156.6
20	5.7	127.0	4.4	133.0	4.5	130.8	4.1	131.3	3.4	135.7
30	6.8	109.3	5.3	118.7	5.7	112.3	4.9	120.0	4.2	124.1
40	8.0	94.3	5.9	109.3	6.7	98.9	5.4	111.7	4.7	117.0
50	9.6	76.2	6.7	99.1	7.7	87.7	6.3	100.6	5.2	110.0
60	11.5	56.9	9.1	71.9	9.0	72.8	10.0	60.4	8.3	73.6
70	14.2	35.0	13.1	37.3	12.5	42.0	13.6	32.1	13.2	32.5
80	18.0	10.7	18.7	3.6	17.4	10.3	19.8	-2.8	18.9	-0.2
90	27.6	-30.2	28.9	-35.7	27.7	-32.0	31.9	-44.1	31.3	-43.1

Table 5.4 *Moisture content (m) and collapse temperature (Tc) values for the maltodextrins with DE between 5 and 20. Moisture contents (m) are given in g/100g dry matter and Tc in °C*

The absorption and collapse data in Figures 5.8 to 5.10 were used to find out the critical % RH and moisture content, when the Tc is lowered to 25°C. The critical % RH and moisture content for the maltodextrins are shown in Table 5.5.

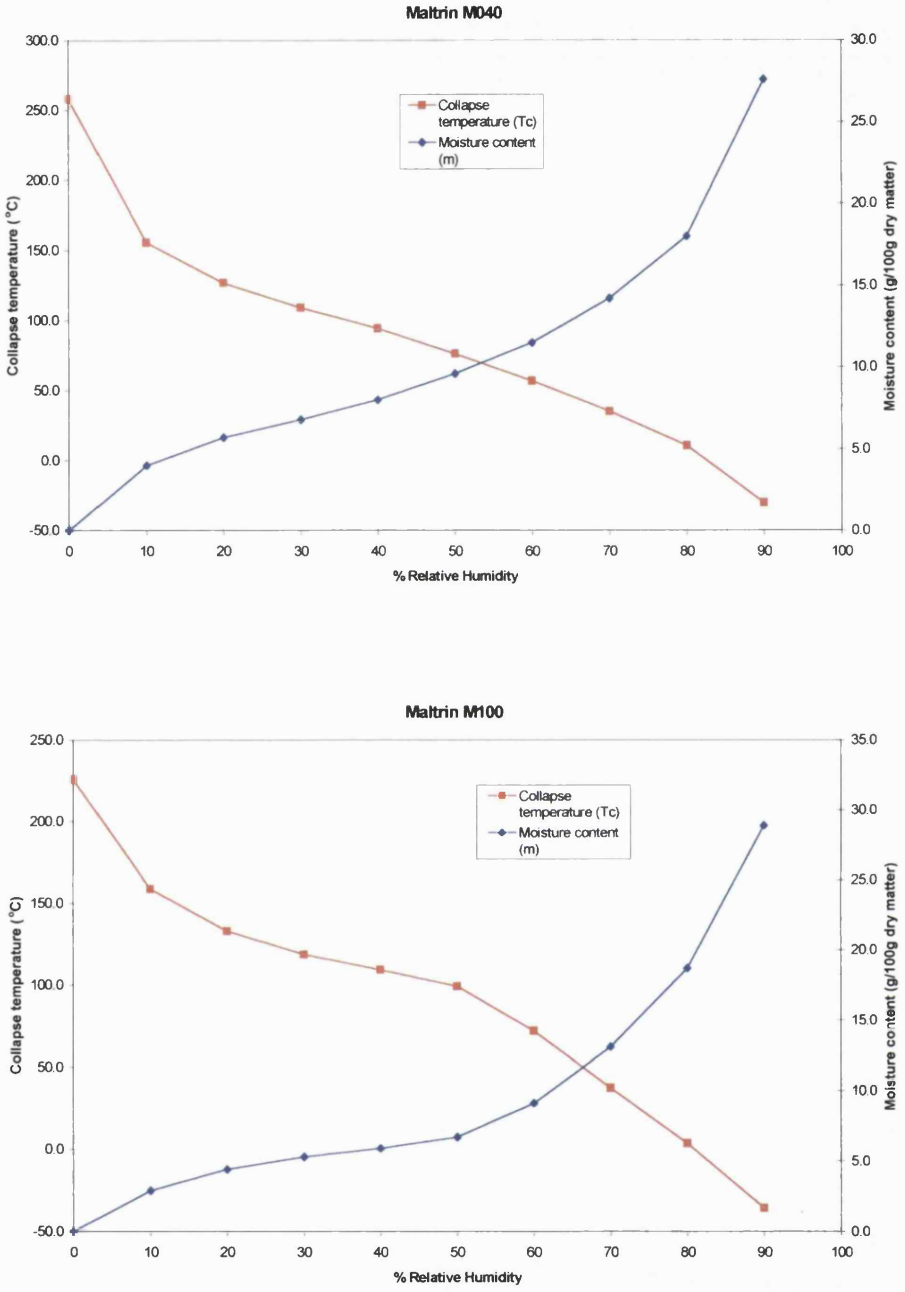

Figure 5.8 *Absorption isotherms showing the effect of moisture content on the collapse temperature (Tc) for Maltrin M040 and M100 maltodextrins at 25°C*

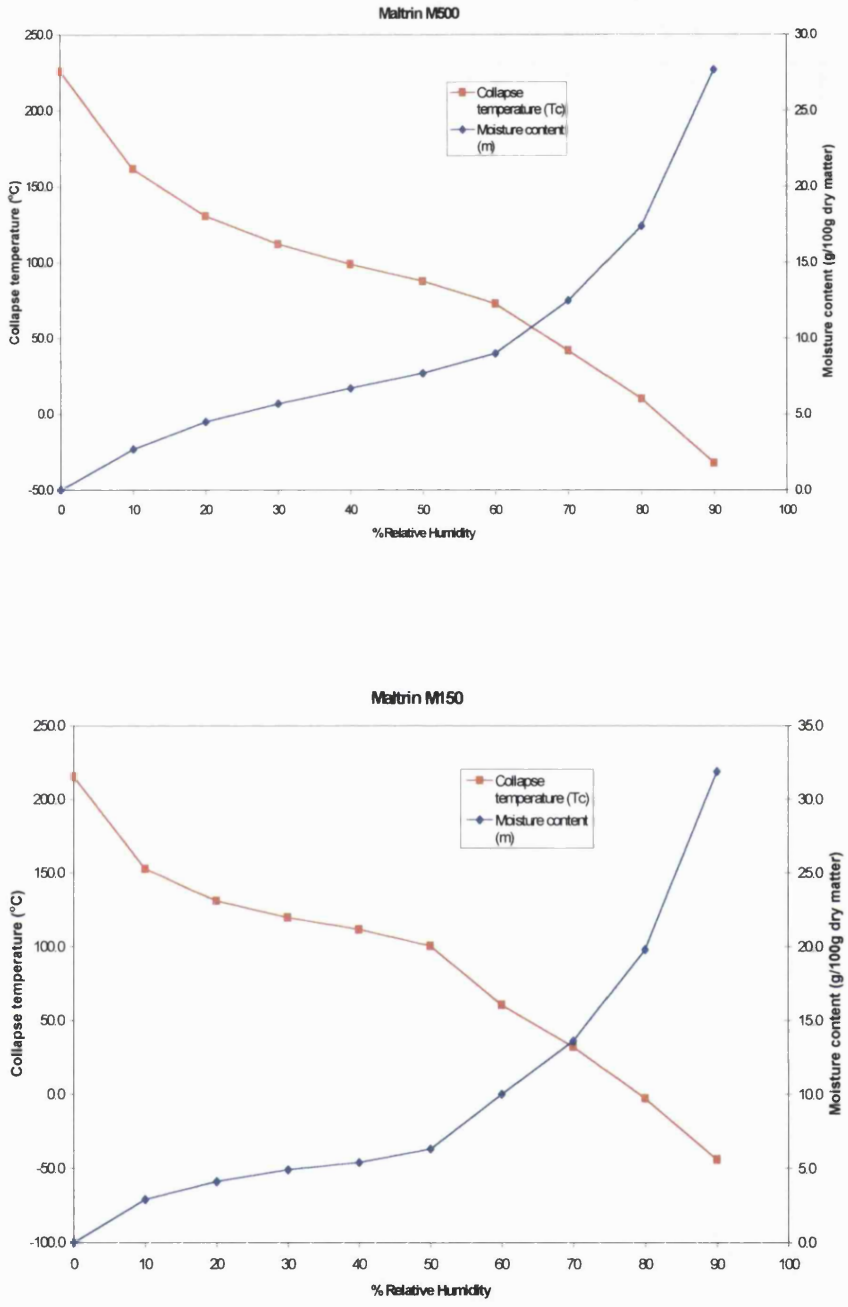

Figure 5.9 *Absorption isotherms showing the effect of moisture content on the collapse temperature (Tc) for Maltrin M500 and M150 maltodextrins at 25°C*

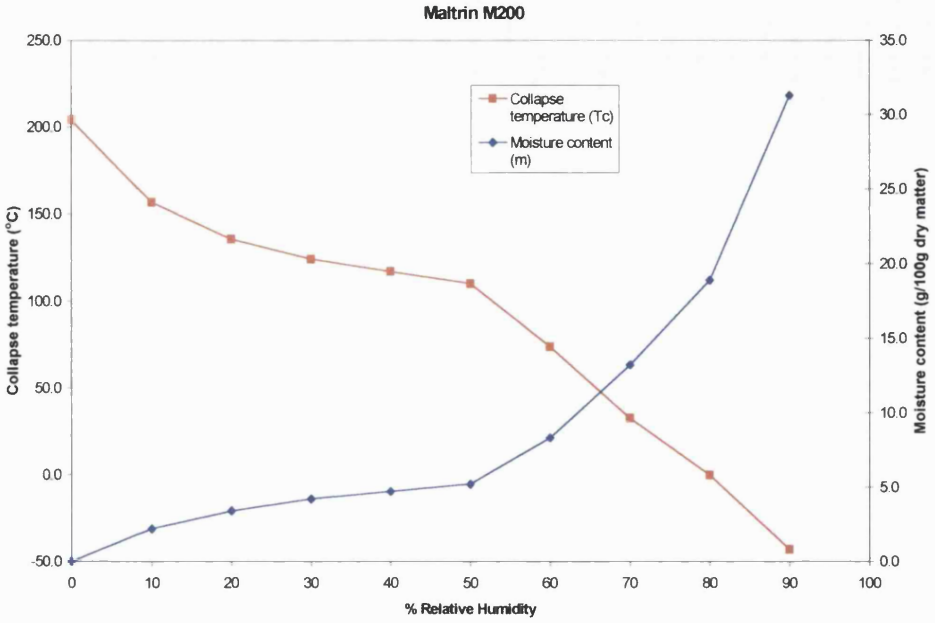

Figure 5.10 *Absorption isotherm showing the effect of moisture content on the collapse temperature for Maltrin M200 maltodextrin at 25°C*

DE	DE 5	DE 10	DE 10	DE 15	DE 20
Maltrin	M040	M100	M500	M150	M200
% RH at Tc of 25°C	75	74	76	72	72
Critical moisture content (g/100 dry matter)	16.0	15.2	15.2	14.8	14.5

Table 5.5 *Critical % RH and moisture content at a collapse temperature of 25°C*

5.3.4 Results and discussion

5.3.4.1 Investigation of Maltrin M040

Maltrin M040 has an approximate DE value of 5. Figure 5.11 shows a power-time curve of typical responses for M040 at 75% and 85% RH. Figure 5.11 shows that the initial response at both 75% and 85% RH is a sharp peak. For the 75% RH peak, this is then followed by a return to the baseline. Following the sharp initial peak at 85% RH, the curve declines in a similar way to the 75% RH response at first but then has a

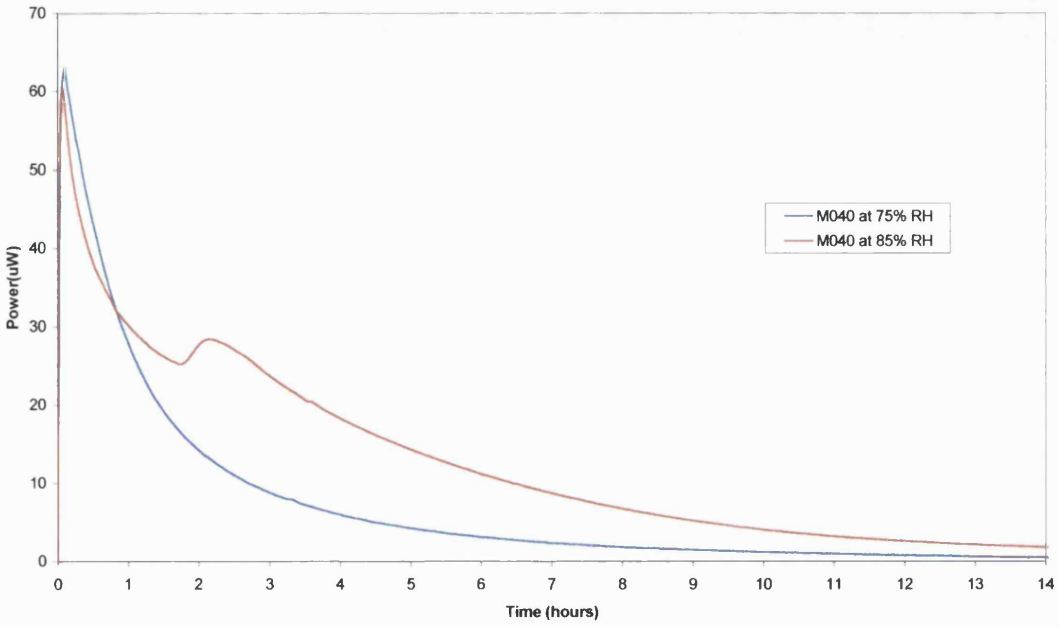

Figure 5.11 *Ampoule microcalorimetry response for Maltrin M040 at 75% and 85% RH*

second broad peak between 2 and 3 hours before then declining towards the baseline. The AUC for the 75% RH peak is 12.4 mJ/mg +/- 2.0 (n = 3) and for the 85% RH peak is 17.8 mJ/mg +/- 1.8 (n = 3). The presence of the second broad peak and the higher AUC associated with the 85% RH response suggests that a physical change is occurring in the sample. Observations of the samples at the end of the ampoule experiments showed that after the 75% RH experiment, the sample remained a white and free-flowing powder. However, for the 85% RH experiment, the sample appeared to be a white, caked material that was not free-flowing. Roos and Karel (1991a) stated that water plasticisation of the maltodextrins has an effect on the physical properties, which is observable above the Tg of the maltodextrins by a structural change from powder to a clear paste. Tables 5.3 and 5.5 show that M040 has a Tg critical RH of 53% and a Tc critical RH of 75% both at 25°C. The ampoule experiment at 75% RH would then be expected to lower the Tg and Tc of M040 to below 25°C. However, the ampoule data at 75% RH and observations following the ampoule experiment that the sample remained a white, free-flowing powder suggest that the sample has not undergone a physical change. However, the ampoule data at 85% RH, with the higher AUC, a second broad

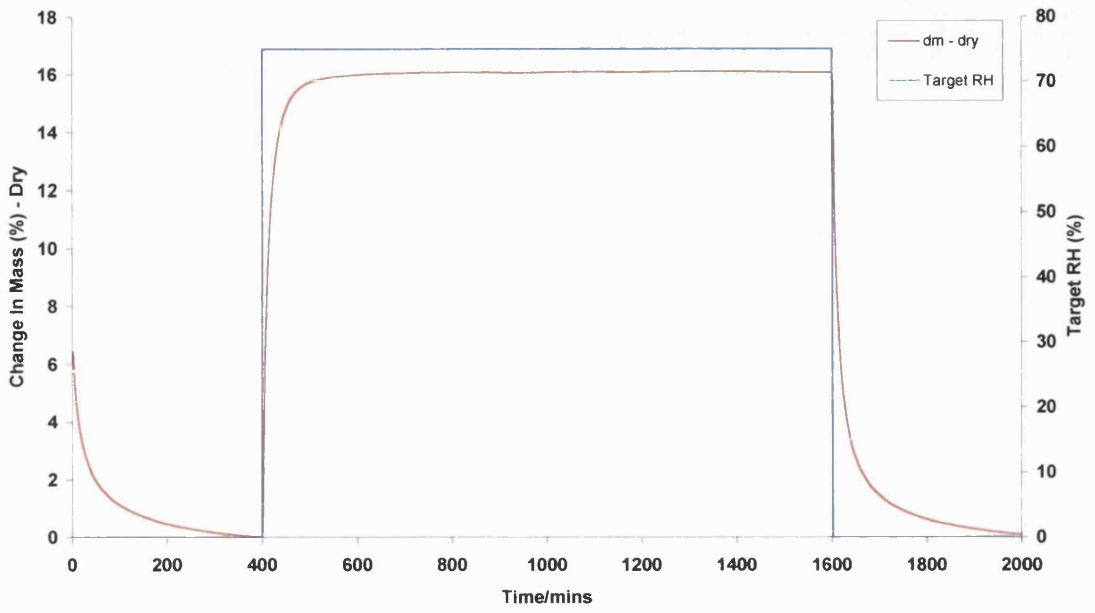

Figure 5.12 *DVS data for M040 on exposure to 0% RH for 400 minutes, 75% RH for 1200 minutes, and 0% RH for 400 minutes*

peak present and the observations after the experiment that the sample had changed to a white, caked material suggest that the sample has undergone a physical change that may be due to the Tg and Tc being plasticised by water to below 25°C. Figure 5.12 shows a dynamic vapour sorption (DVS) plot for M040 with the sample exposed to 0% RH for 400 minutes, 75% RH for 1200 minutes, and 0% RH for 400 minutes. It shows that when the RH is set to 0% RH, the M040 loses 6.5% of its initial weight. After changing the RH to 75% RH the weight can be seen to rise sharply initially and then more slowly as it reaches a moisture content of 16% w/w. During the time that the RH remains at 75% RH, the weight does not change significantly. This may be due to the equilibrium water uptake having been attained at 75% RH. After the RH is changed back to 0% RH, the sample is seen to rapidly lose the moisture and returns towards the zero level during the final 400 minutes of the experiment.

Observations after the DVS experiment showed that M040 remained a white, free-flowing powder. This is similar to the observations after the ampoule experiment carried out at 75% RH. DVS data for M040 shows that moisture is rapidly sorbed and desorbed,

suggesting that the response being measured by the ampoule experiment for M040 at 75% RH is a wetting response and that measurable physical changes are not occurring.

5.3.4.2 Investigation of Maltrin M100

Maltrin M100 has an approximate DE of 10. Figure 5.13 shows a power-time plot for Maltrin M100 at 75% and 85% RH. M100 at 75% and 85% RH have similar shape peaks. However, M100 at 85% shows a larger initial sharp peak compared to the 75% RH peak, as would be expected with a greater amount of water available. The AUC for the 75% RH peak is 16.1 mJ/mg +/- 0.6 (n = 3) and for the 85% RH response is 14.6 mJ/mg +/- 2.3 (n = 3).

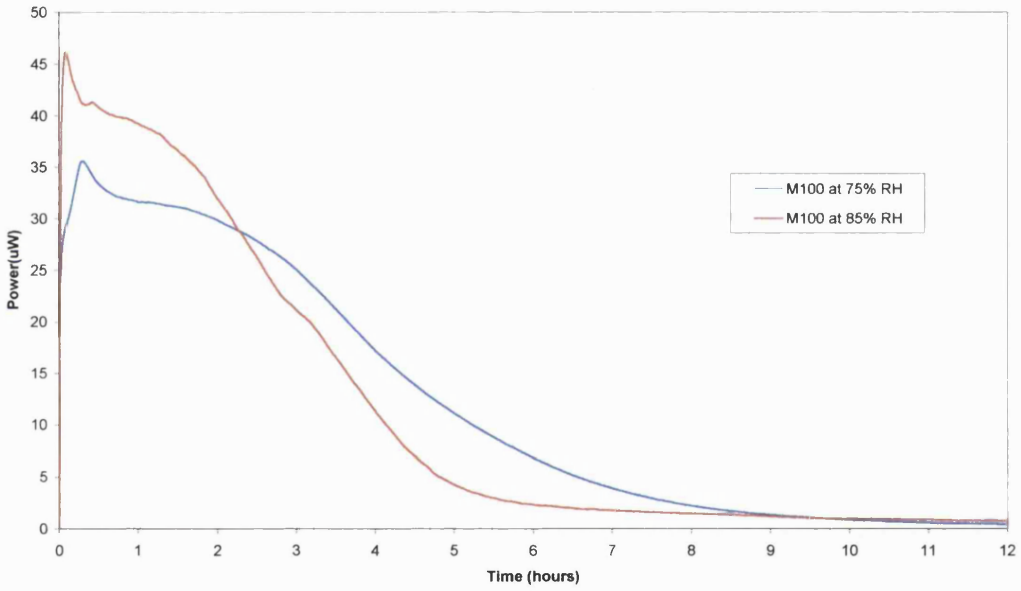

Figure 5.13 *Ampoule microcalorimetry response for Maltrin M100 at 75% and 85% RH*

Tables 5.3 and 5.5 show that M100 has a critical Tg RH of 60% and critical Tc RH of 74% both at 25°C. At the ampoule experiment where 75% RH is used, the Tg should have been lowered to below 25°C and collapse should also have been induced by an RH of 75%. Comparison of the ampoule data for M100 and M040 at 75% RH (Figures 5.13 and 5.11 respectively) shows that both samples have the initial sharp peak. However, whereas for M040 the curve then returns to the baseline, the ampoule data shows that for M100 the initial peak is then followed by a broad shoulder that then declines

towards the baseline. Observations after the ampoule experiments showed that M040 remained a white, free-flowing powder whereas M100 had changed to a hard, white

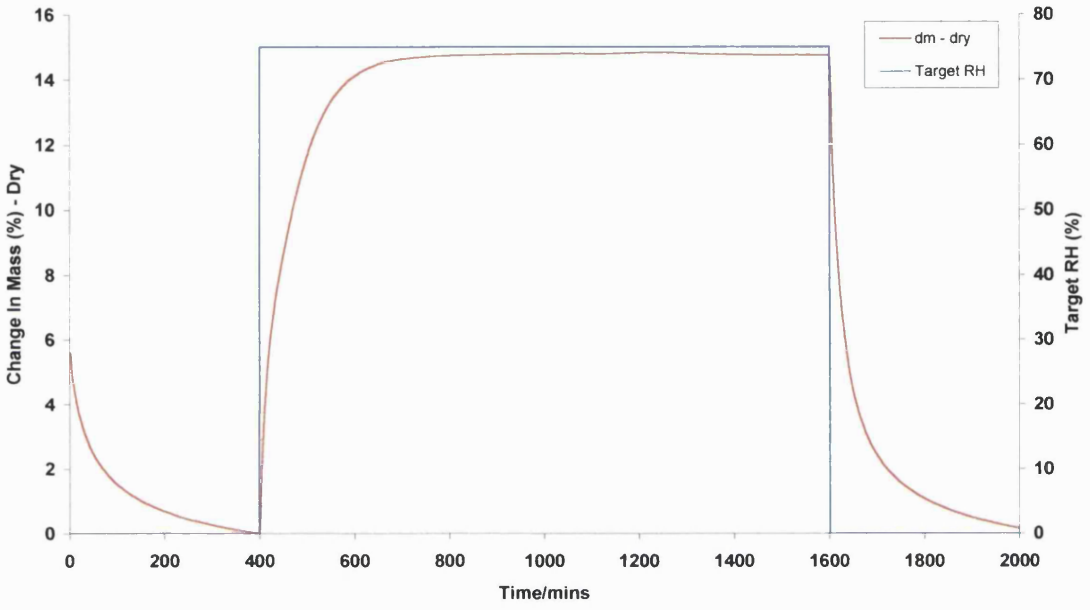

Figure 5.14 *DVS data for M100 on exposure to 0% RH for 400 minutes, 75% RH for 1200 minutes, and 0% RH for 400 minutes*

caked material. This indicates that the difference in the ampoule response between M040 and M100 at 75% RH is due to this change in physical form. The maltodextrins are water soluble materials and the changes being detected by microcalorimetry could at least in part be due to dissolution of the maltodextrins. After the 85% RH ampoule experiment, M100 had changed to a soft gel-like material. It was thought that the gel-like appearance of the material observed after the 85% RH ampoule experiment may be due to a process similar to starch gelatinisation, since the maltodextrins are starch hydrolysis products. Starch gelatinisation is caused by heating of the sample in the presence of water (Roos, 1995). The starch gelatinisation process can lead to formation of a gel that is caused by the 3-dimensional networking of the linear amylose molecules (Borchard, 1983). However, the water content needs to be 60% (w/w) for complete gelatinisation to occur (Lund, 1984). Starch gelatinisation does occur at lower water

contents of 30-40% (w/w) but then this requires higher temperatures to induce gelatinisation (Roos, 1995). Table 5.4 shows that the highest water content for M100 is below 30g/100g dry matter (30% w/w) at the experimental temperature of 25°C, suggesting that a process similar to starch gelatinisation does not occur for the maltodextrins studied due to the higher water content and temperature required for the process to occur. A standard procedure for starch gelatinisation is the heating of a 5% w/w starch suspension in a water bath at 100°C (Van den Berg, 1975). The maltodextrins used in this investigation are derived from corn starch. The gelling of potato starch-derived maltodextrins has been reported. However, this requires a 10-35% w/w aqueous solution of the maltodextrin for the gelling process to occur (Vorwerg et al, 1988).

Figure 5.14 shows DVS data for M100, showing that on changing the RH from 0% to 75% RH the response is immediate, although water uptake in this case is more prolonged in relation to M040 (Figure 5.12). However, like M040, once it has reached its maximum water content at 75% RH no further significant increase in weight is seen. On changing the RH back to 0% RH, the weight for M100 decreases rapidly back towards the zero level.

Visual observations after the microcalorimetry and DVS experiments at 75% RH showed the same change in physical form occurred for M100 from a free-flowing white powder to a hard, white, caked material with loss of free-flowing properties. Figure 5.14 showed DVS data for M100 with the weight returning to the same level as before exposure to 75% RH, suggesting that the change in physical form is not detected by DVS. The microcalorimetry data in Figure 5.13 showed M100 had a broad shoulder at 75% RH. It appears that microcalorimetry is able to detect the changes in physical form, perhaps due to differences in the heat capacity resulting from the change in physical form of the maltodextrins on exposure to high humidity conditions. Observations following the microcalorimetry experiment for M040 at 75% RH showed that it remained a free-flowing white powder. The ampoule response for M040 at 75% RH in Figure 5.11 showed the initial wetting peak but no subsequent broad shoulder or peaks. If the broad shoulder/peaks are due to the change in physical form of the maltodextrins, then the absence of a broad shoulder/peak for M040 at 75% RH when the sample does not change in physical form (by visual observation) appears consistent with this.

Figure 5.15 shows SEM images for M100 before and after exposure to 75% RH using sodium chloride saturated salt solution. As part of the production process of the

maltodextrins by starch hydrolysis, a refined solution is spray-dried to give a white powder (Kennedy et al, 1995). The top SEM image in Figure 5.15 shows that for the as received M100, the particles are smooth, spherical, have a porous structure that consists of particles that are easily distinguished. After exposure to 75% RH, the particles appear to be agglomerated with adjacent particles fused together.

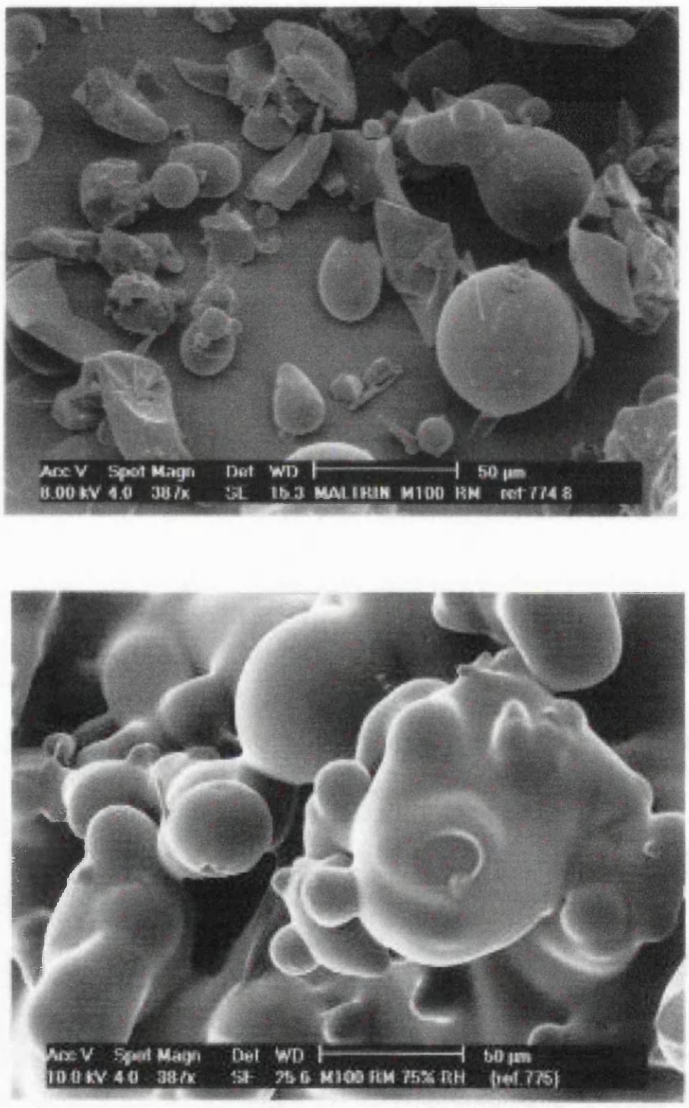

Figure 5.15 *SEM images for M100 before (top) and after (below) exposure to 75% RH*

Figure 5.6 is a schematic representation of the 'humidity caking' mechanism that was proposed by Peleg (1983). It involves the gradual transition of amorphous food powders from a free-flowing powder, through the stages of plasticised surface, attraction, fusion,

and finally a sticky, caked, plasticised material as increasing amounts of moisture are sorbed. For the maltodextrins, the sticky, caked, plasticised material of the humidity caking mechanism appears to manifest itself as a sticky material that is gel-like in appearance. The mechanism begins with plasticisation of the surface of the particles to form cohesive, sticky particles that are still distinct (see Figure 5.6). This then progresses to the attraction stage where the particles are caked and sticky. The next stage is fusion between the sticky particles, involving the formation of liquid bridges between particles. Continued moisture sorption results in a sticky, caked, plasticised material (Peleg, 1983). The SEM for M100 after exposure to 75% RH shows that particle agglomeration is taking place. The changes in physical form observed after the microcalorimetry and DVS experiments may be due to the humidity caking mechanism explained above. This further indicates that the broad shoulders/peaks shown for the microcalorimetry responses are due to the changes in physical form taking place as a result of the humidity caking mechanism. In the humidity caking mechanism, the migration of moisture to the interior of the particles may be slow, resulting in the surface of the particles remaining sticky while the central parts are still dry (Peleg and Mannheim, 1977). The water that plasticises the particle surface would then form a saturated solution of the soluble components at the surface of the particle, which then allows the formation of liquid bridges between particles. Dissolution of the maltodextrins in the sorbed water is likely due to the water soluble nature of the materials. The microcalorimetry response may therefore also include an enthalpy of solution for the maltodextrins.

5.3.4.3 Investigation of Maltrin M150

Maltrin M150 has a DE value of approximately 15. Figure 5.16 shows a power-time plot for M150 at 75% and 85% RH. It shows that both curves have broad shoulders, however, the curve for 85% RH also has a second shoulder between 2 and 3 hours. The AUC for the 75% RH peak is 16.4 mJ/mg +/- 0.2 (n = 3) and 17.5 mJ/mg +/- 0.8 (n = 3) for the 85% RH peak.

These values are essentially the same allowing for experimental error, suggesting that a similar process is being measured by the microcalorimeter. Tables 5.3 and 5.5 show that

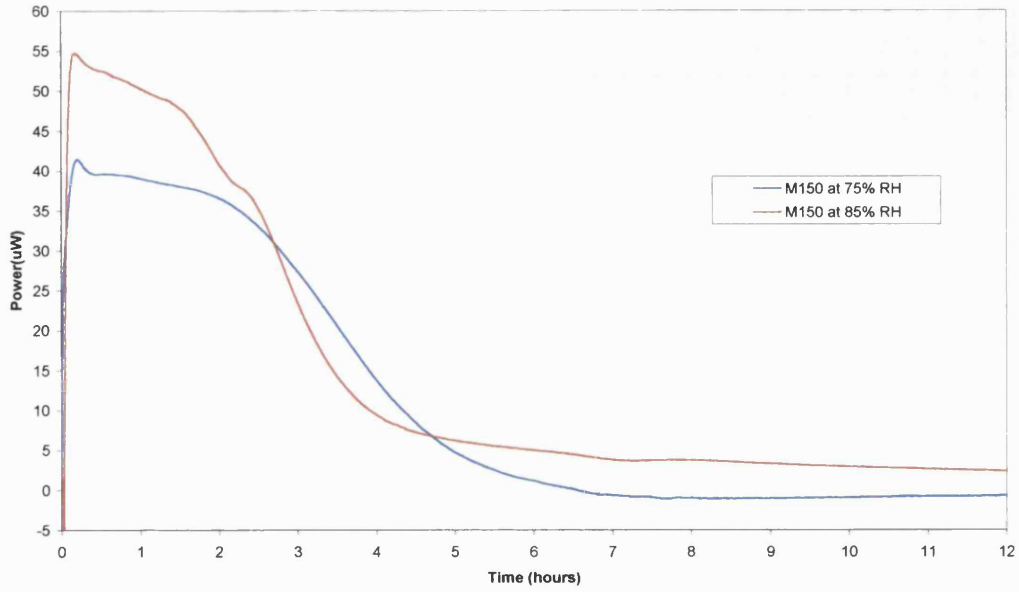

Figure 5.16 *Ampoule microcalorimetry response for M150 at 75% and 85% RH*

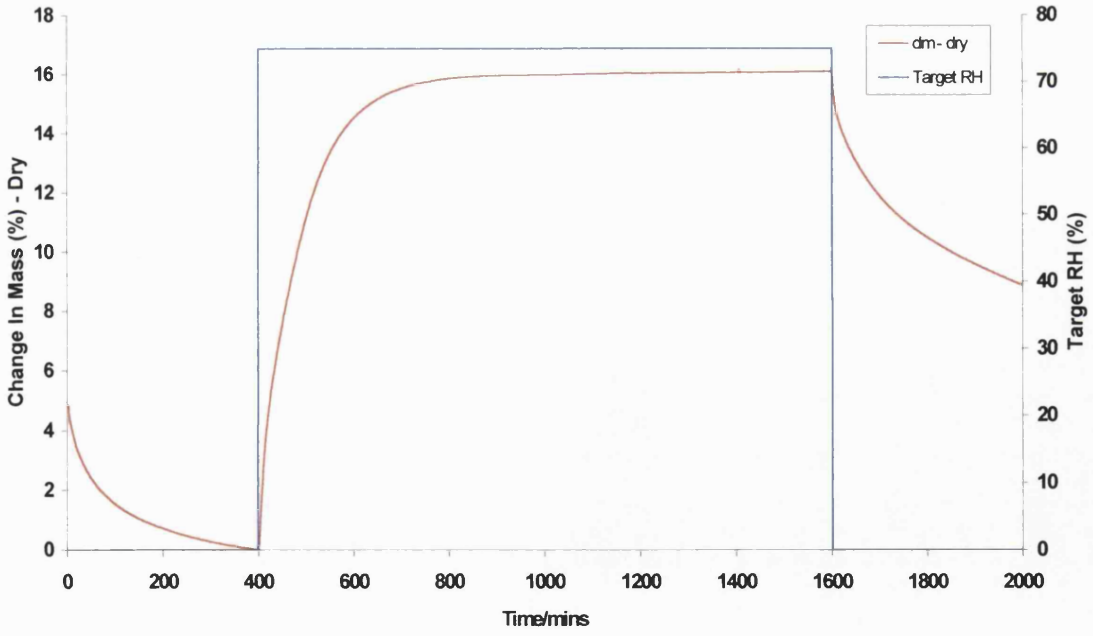

Figure 5.17 *DVS data for Maltrin M150 on exposure to 0% RH for 400 minutes, 75% RH for 1200 minutes, and 0% RH for 400 minutes*

M150 has a Tg critical RH of 58% and a Tc critical RH of 72%. For the ampoule experiment at 75% RH, the sample would therefore be expected to be at the early stages of collapse, whereas at 85% RH the sample would be expected to be at a more advanced stage of the collapse process since the Tc critical RH would have been far exceeded at 85% RH. The observations after the ampoule experiment at 75% RH show that the sample had changed to a hard white caked material. This may correspond to the fusion stage in the schematic in Figure 5.6, since the material remained white and formation of a solid cake was evident. After the 85% RH ampoule experiment, the sample was observed to have changed to a soft opaque material that was gel-like in appearance. This may represent the caked, plasticised material in the model shown in Figure 5.6.

Figure 5.17 shows DVS data for M150 at 0% RH for 400 minutes, followed by a weight increase up to 16% w/w on changing the RH from 0% to 75% RH. When the RH is reduced back to 0% RH, the DVS plot shows that the moisture is lost rapidly at first but this is then followed by a slower rate of moisture loss. At the end of the 400 minutes desorption at 0% RH, Figure 5.17 shows that 9% w/w moisture remains in the sample. Observations after the DVS experiment showed that M150 had changed from a free-flowing white powder to a hard opaque material. The presence of an amorphous material in a collapsed or non-collapsed amorphous state has an effect on desorption of water from the material (Buckton and Darcy, 1996). Buckton and Darcy (1996) investigated the effect of holding amorphous lactose for various times at 50% RH, followed by a return to 0% RH. They found that samples held at 50% RH for one hour or less showed rapid desorption of water from the amorphous material. However, as the exposure time at 50% RH increased, it was observed that the desorption of water from the amorphous material was not rapid and became increasingly slow as the time held at 50% RH was increased up to 3 hours. This was due to the amorphous lactose changing to a partially collapsed and then a totally collapsed amorphous material at 3 hours exposure to 50% RH. In a non-collapsed state, amorphous lactose is able to rapidly desorb water on environmental changes of RH. However, when amorphous lactose is in a collapsed state then water desorption is diffusion-controlled, and not readily responsive to environmental changes (Darcy and Buckton, 1997). The DVS data for M040 and M100 (Figures 5.12 and 5.14 respectively) showed rapid desorption of water following a change in the RH from 75% RH to 0% RH, indicating that the desorption is controlled by the environmental RH (in this case 0% RH). This indicates that following exposure to 75% RH, M040 and M100 are in a non-collapsed amorphous state.

However, the DVS data for M150 in Figure 5.17 shows that desorption following the change from 75% to 0% RH is slow, indicating that desorption is diffusion-controlled rather than dependent on the environmental RH. This indicates that for M150 following exposure to 75% RH, a collapsed amorphous material is produced.

5.3.4.4 Investigation of Maltrin M200

Maltrin M200 has an approximate DE value of 20. Figure 5.18 shows microcalorimetry power-time curves for M200 when exposed to 65%, 75%, and 85% RH. It shows that for M200 at 65% RH, the initial wetting response is followed by a decline towards the baseline, followed by a second broad peak which is distinct from the sharp initial peak. After the ampoule experiment at 65% RH, the sample had changed from a free-flowing white powder to a hard white caked material, which could be broken into smaller pieces.

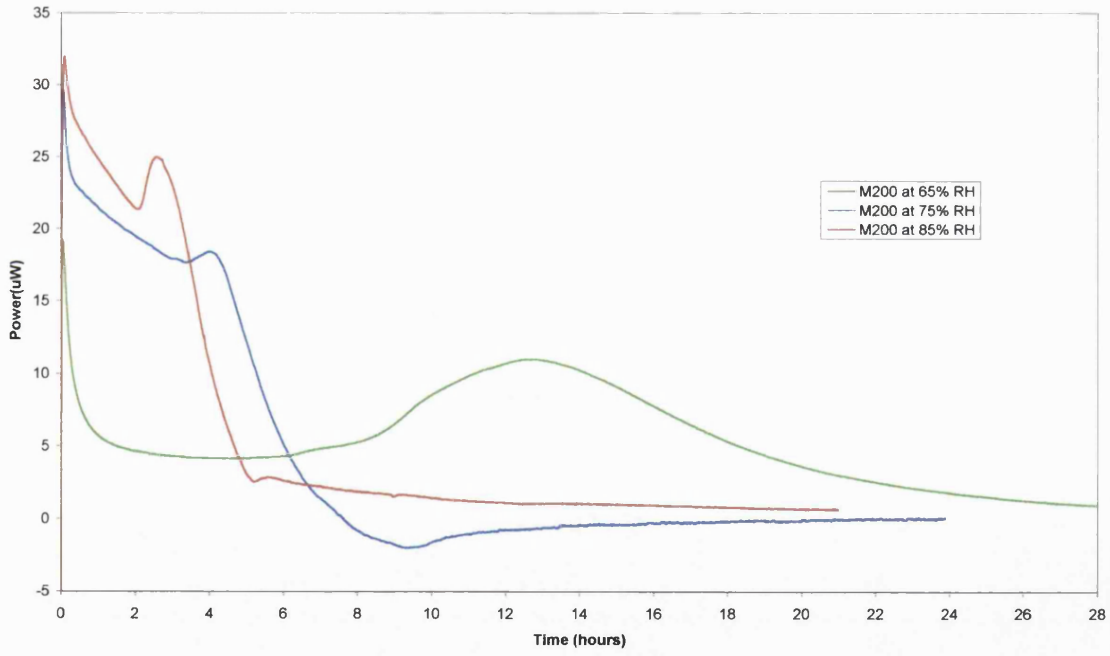

Figure 5.18 *Ampoule microcalorimetry response for M200 at 65%, 75% and 85% RH*

The AUC for M200 at 65% RH is 20.6 mJ/mg +/- 1.8 (n = 3). Figure 5.18 shows that M200 at 75% RH has the sharp initial response, which is followed by a broad shoulder and a second broad peak between 4 and 5 hours. The AUC for M200 at 75% RH is 10.8 mJ/mg +/- 2.7 (n = 3). Figure 5.18 also shows that M200 at 75% RH has a broad

endothermic peak starting at approximately 7.5 hours before returning to the baseline. This may be due to swelling of M200 maltodextrin. Swelling is an endothermic process that involves breaking of solid-solid bonds and therefore requires energy (Wurster et al, 1984).

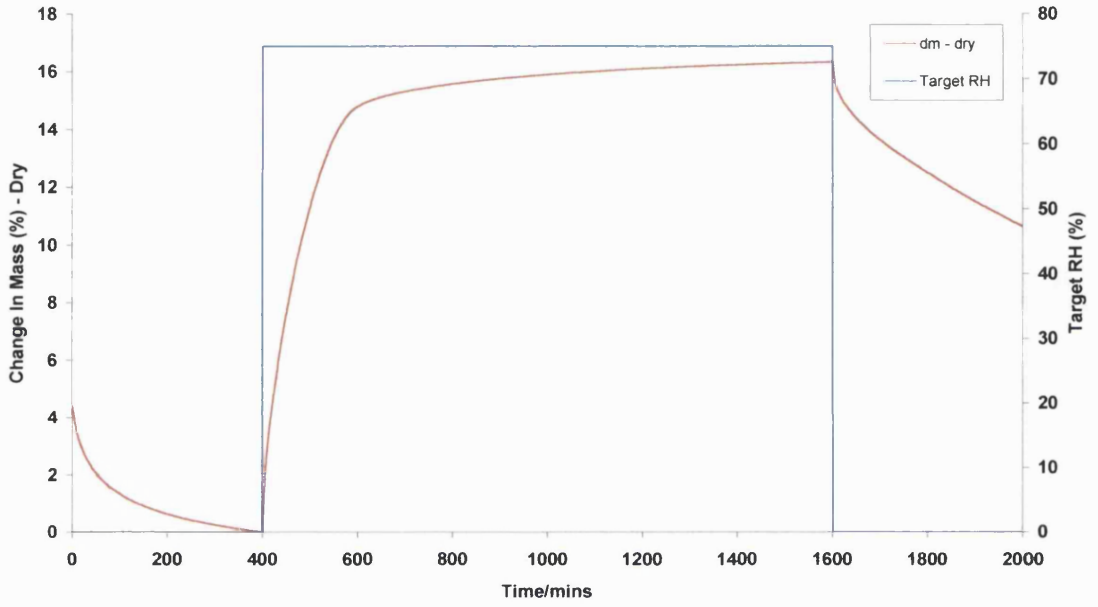

Figure 5.19 *DVS data for Maltrin M200 on exposure to 0% RH for 400 minutes, 75% RH for 1200 minutes, and 0% RH for 400 minutes*

The other maltodextrins investigated may also undergo swelling on water sorption. However, since microcalorimetry measures the overall heat flow, perhaps the exothermic responses (broad shoulders/peaks) occurring due to changes in physical form of the maltodextrins may outweigh the endothermic swelling process. After the 75% RH ampoule experiment, the sample was observed to have changed to a soft opaque material that was gel-like in appearance. The ampoule response at 85% RH shows that following the sharp initial peak, a broad shoulder is present which is then followed by a second broad peak occurring at 3 hours, then a sharp decline towards the baseline. The AUC for M200 at 85% RH is 9.9 mJ/mg +/- 1.7 (n = 3). The sample was observed to have changed to a soft gel-like material.

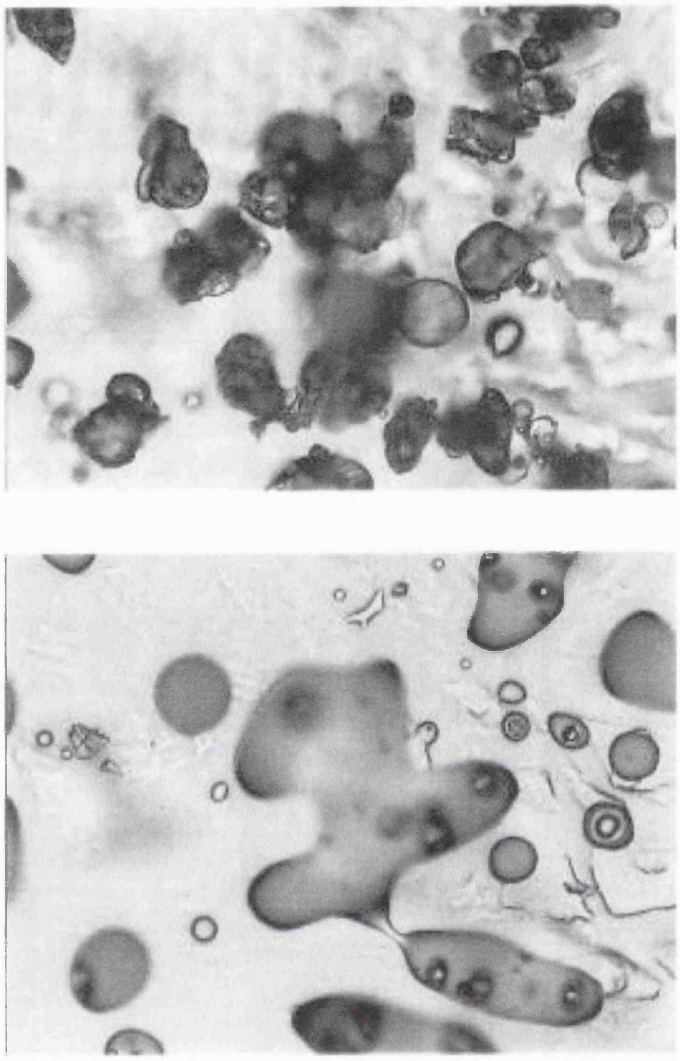

Figure 5.20 *Light microscopy images (10x) for M200 before (top) and after (bottom) 4 hours exposure to 75% RH*

Figure 5.19 shows DVS data for M200. When the RH is changed from 0% to 75% at 400 minutes, the weight rapidly increases to 15% w/w, and then continues to increase to 16% w/w. On changing the RH back to 0% at the end of the 75% RH holding phase, the weight loss is initially rapid following the change in RH, but is then immediately followed by a slower rate of weight loss. At the end of the DVS experiment the sample was observed to have changed to a hard opaque material. It appears that as reported by Darcy and Buckton (1996) for amorphous lactose, this slow desorption of water from M200 is due to collapse of the amorphous maltodextrin sample at 75% RH. Figures 5.17 and 5.19 show that M150 retained 9% w/w moisture and M200 retained 11% w/w

moisture at the end of the 0% RH phase. This indicates that in line with the collapse of amorphous lactose investigated by Darcy and Buckton (1996), M200 may have undergone a higher degree of collapse than M150 at 75% RH.

Figure 5.20 shows light microscopy images for M200 before and after exposure to 75% RH for 4 hours. The image for M200 after exposure to 75% RH shows coalesced particles (bottom image). The origin of these particles can clearly be seen in the image for M200 before 75% RH exposure (top image). Figure 5.20 shows shrinkage of M200 after exposure to 75% RH, which is consistent with structural collapse and is due to viscous flow of the material resulting from reduced viscosity (To and Flink, 1978b).

DE	5	10	15	20	10
Maltrin	M040	M100	M150	M200	M500
Average MW	3600	1800	1200	900	1800
Average DP	22.1	11.1	7.4	5.6	11.1

Table 5.6 *Average molecular weight (MW) and degree of polymerisation (DP) data for the maltodextrins (obtained from manufacturer)*

The maltodextrins investigated vary in their DE value. Table 5.6 shows that M040 (DE = 5) has a high average molecular weight and degree of polymerisation (DP), whereas M200 (DE = 20) has a lower average molecular weight and degree of polymerisation (DP). M100 and M150 have intermediate values for average molecular weight and DP. The collapse of amorphous materials is the result of a reduction in the viscosity of the material when it becomes too low to support its own weight against flow (To and Flink, 1978b). Tsourouflis et al (1976) found that the decrease in viscosity allowing sufficient flow of the amorphous material for collapse to occur could be achieved by various combinations of water content and temperature. In the present study, all investigations were carried out at a constant temperature of 25°C, therefore the main determinant of collapse is the water content (or the RH). Tsourouflis et al (1976) measured the viscosity of the maltodextrins studied. They found that for M100 the viscosity was 6.2 cP, decreasing to 3.4 cP for M150, and 3.3 cP for M200. The viscosity of M150 and M200 are similar, and both are about half the viscosity of M100. The differences in the composition between the maltodextrins, with decreasing average DP with increasing DE

value appears to affect the collapse of the maltodextrins. For M150 and M200, the lower DP and viscosity appear to be sufficient, at 75% RH, to induce collapse of the amorphous materials. Table 5.5 showed Tc critical % RHs for the maltodextrins. These were 72% RH for both M150 and M200, 75% RH for M040, and 74% RH for M100. DVS data in Figures 5.17 and 5.19 showed that M150 and M200 appear to be in a collapsed amorphous state following exposure to 75% RH. This appears to agree with the Tc critical % RHs for M150 and M200 (72% RH for both). Furthermore, Figures 5.12 and 5.14 showed that M040 and M100 following exposure to 75% RH are in a non-collapsed amorphous state. Once again this appears to agree with the Tc critical % RH values for M040 and M100 (75% and 74% RH respectively). However, RHs higher than 75% RH may be sufficient to induce collapse in M040 and M100. Below the Tc critical % RHs, the physical changes occurring appear to be due to the humidity caking mechanism. The effects of the humidity caking mechanism may represent an early stage of the collapse process in the maltodextrins that is then followed by structural collapse above a critical moisture content or % RH.

5.3.4.5 Investigation of an agglomerated maltodextrin

Maltrin M500 is a maltodextrin of the same DE as M100 (DE = 10) which has been fluid-bed agglomerated using water by Grain Processing Corporation (GPC). This results in the production of a material that has better flow properties, good physical strength, and reduces the production of dust due to fine particles (Papadimitriou et al, 1992). The physical form of M500 is a granular white powder whereas that of the non-agglomerated M100 (DE = 10) is a white powder.

Figure 5.21 shows ampoule data for M500 at 75% and 85% RH. The curve for M500 at 75% RH shows the initial wetting response followed by declining of the signal towards the baseline. This is then followed by a second distinct broad peak that reaches its maximum at 3 hours, followed by a slow decline towards the baseline. The visual observation after this experiment was that M500 remained a white free-flowing powder. This is in contrast to the non-agglomerated M100 where observations after the 75% RH ampoule experiment showed that the sample had changed to a hard white, caked material with loss of free-flowing properties. However, Figure 5.21 does show a broad peak suggesting that a change in physical form may be occurring that is not detected by visual observation following the microcalorimetry experiment at 75% RH.

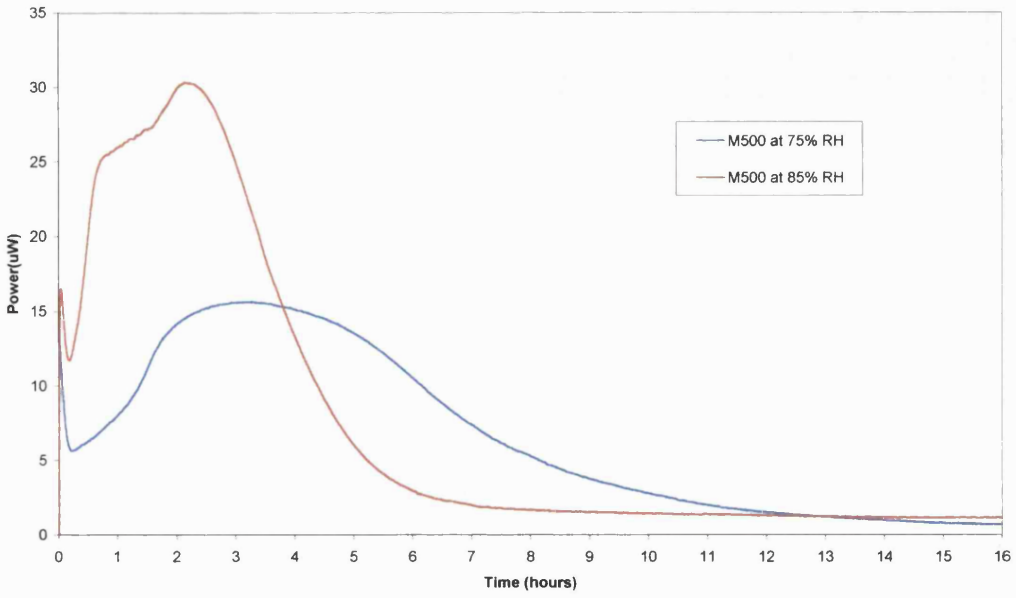

Figure 5.21 *Ampoule microcalorimetry response for M500 at 75% and 85% RH*

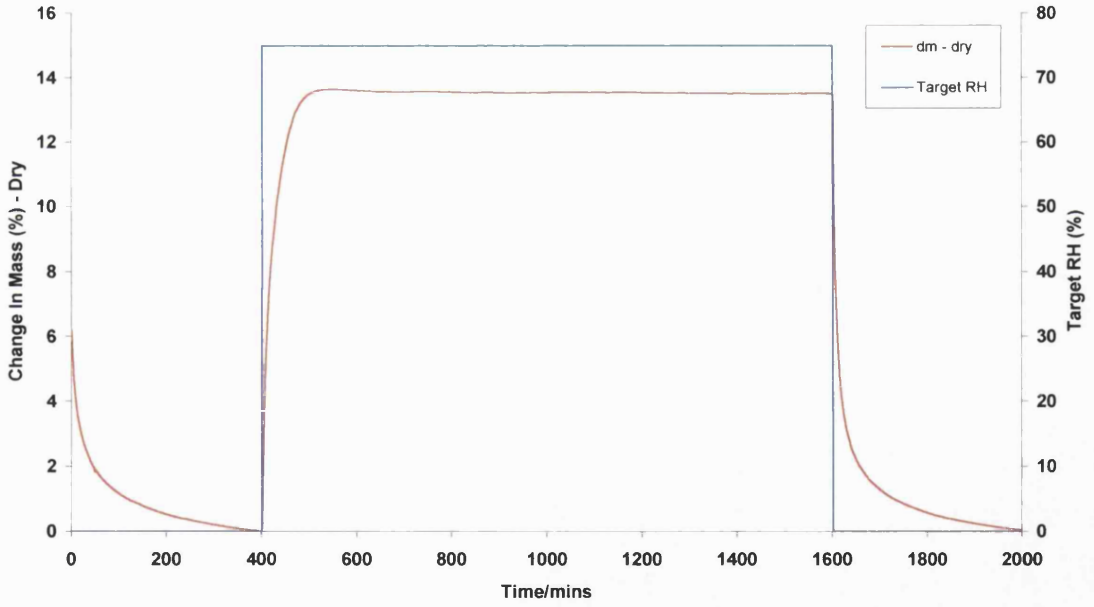

Figure 5.22 *DVS data for M500 on exposure to 0% RH for 400 minutes, 75% RH for 1200 minutes, and 0% RH for 400 minutes*

Figure 5.21 shows the 85% RH response for M500 is different to the 75% RH peaks for M500. Once again it begins with the initial wetting response which declines slightly towards the baseline, and is followed by a second broad peak which itself has a shoulder during the inclining part of the peak. The broad response peaks between 2 and 2.5 hours and following this there is a rapid decline towards the baseline. Observations after the 85% RH ampoule experiment showed that the sample had changed to a soft material that was gel-like in appearance. It was also noted that the durham tube which houses the saturated salt solution inside the glass ampoule was sticking to the sample. Tables 5.3 and 5.5 show that the Tg critical RH for M500 is 61% and the Tc critical RH is 76%. According to these values, for the 75% RH ampoule experiment, the sample would have had its Tg lowered to below 25°C, but the collapse temperature (Tc) would not have been lowered to 25°C. This is also suggested by the observation after the 75% RH ampoule experiment that the sample remains a white, free-flowing powder. For the 85% RH ampoule experiment, the sample would have had its Tg and Tc lowered to below 25°C. Observations after the 85% RH ampoule experiments showed that the sample had changed to a soft gel-like material, indicating a change in physical form for M500 at 85% RH.

Figure 5.22 shows DVS data for M500 with the percentage change in mass and target RH shown against time. It shows that M500 rapidly takes up moisture, which starts to plateau 100 minutes after the change to 75% RH. Between 100 and 1200 minutes at 75% RH, the sample mass is constant although a slight decrease in mass can be seen in Figure 5.22. When the RH is changed back to 0% RH, the sample mass decreases rapidly to the zero level. This suggests that M500 after exposure to 75% RH is in a non-collapsed amorphous state (Darcy and Buckton, 1996). Observations of the sample after the DVS experiment showed that the sample remained a white, free-flowing powder. This is consistent with the observations for M500 after the 75% RH ampoule experiment and suggests that there is no apparent change in physical form for M500 at 75% RH (by visual observation). DVS data for M100, the non-agglomerated form, in Figure 5.14, showed that M100 at 75% RH is also in a non-collapsed amorphous state. However, the SEM images showed that agglomeration of M100 takes place after exposure to 75% RH, and observations following the microcalorimetry experiments showed that a change in physical form to a hard, caked material with loss of free-flowing properties occurred.

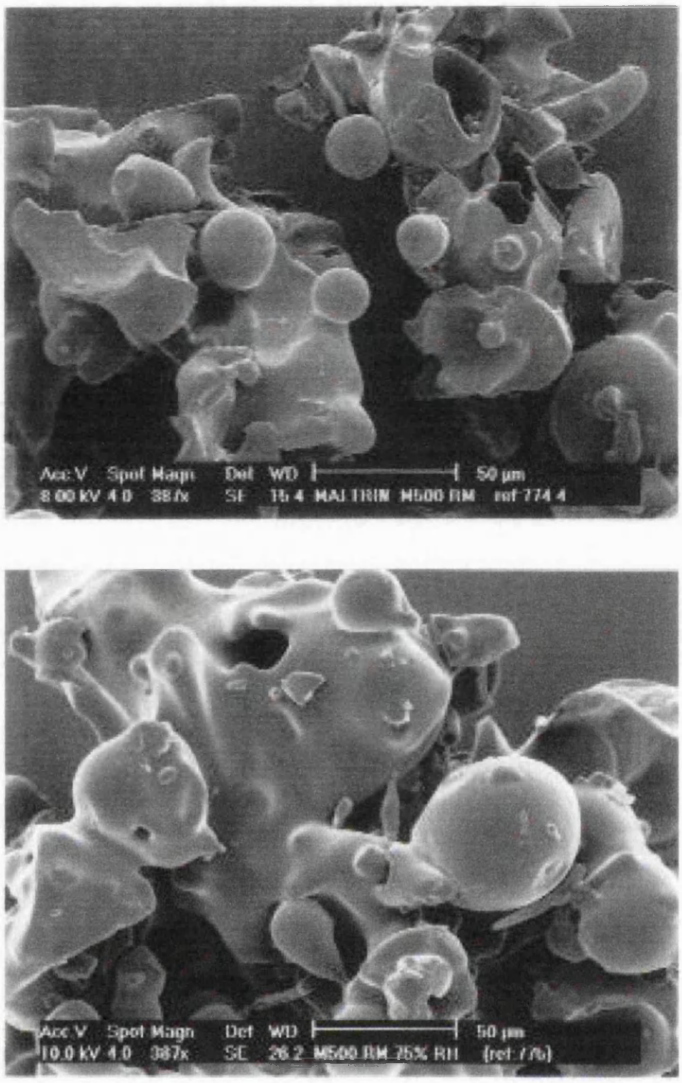

Figure 5.23 *SEM images for M500 before (top) and after (bottom) exposure to 75% RH*

Figure 5.23 shows SEM images for M500 before and after exposure to 75% RH. Figure 5.23 shows that there is only a small observable difference between the samples. This is in contrast to the SEM images for the non-agglomerated M100 (Figure 5.15) where it is clearly evident that agglomeration is taking place between M100 particles. During the process of agglomeration, the surface of the powder is uniformly wetted and then dried to the desired moisture content (Masters and Stoltze, 1973). From a comparison of the agglomerated M500 and non-agglomerated M100 data, M500 appears to have greater stability against physical changes occurring at high humidity conditions relative to M100, perhaps due to the prior agglomeration and drying during the production of M500.

5.4 The glass transition (Tg) and collapse (Tc) temperatures

To and Flink (1978b) found significant similarities between the collapse temperature and the glass transition temperature of polymers. They found that the molecular weight and composition dependence of the glass transition temperature also applied to the collapse temperature. They concluded that collapse and glass transition are phenomenologically similar events.

Levine and Slade (1988b) proposed that Tg and Tc are fundamentally equivalent. Chuy and Labuza (1994) measured Tsc (surface caking) and Tac (advanced caking). The Tsc is also referred to as the collapse temperature (Tc) and the Tac as the sticky point temperature. They suggested that the temperature difference between the glass transition and collapse temperatures is due to the difference between the experimental time scales of measurement. They explained that the Tg is measured by a change in the heat capacity of a small sample using DSC, whereas the collapse temperature is measured using visual or mechanical methods. If the changes were observed at each temperature by holding for a long time at almost zero heating rate then it may be observed that the onset Tsc is very close to the Tg. Tsourouflis et al (1976) commented that for a dynamic process such as the flow of viscoelastic materials, the determination of collapse depends on the length of time allowed for observation. For their studies, they found that holding at each temperature for 45 minutes was sufficient time for collapse to be observed.

Downton et al (1982) pointed out that the sticky point temperature (Tac) is higher than the collapse temperature (Tsc). Both measure the same physical phenomena, related to the glass transition, but are observations of a different degree of collapse. The Tsc is a measurement of initial clumping, while Tac measures an advanced stage of collapse. The collapse temperature or surface caking (Tsc) temperature is usually measured visually. An example is the method used by Tsourouflis et al (1976) where the sample contained in an ampoule is placed in a water bath. The bath temperature is raised slowly until collapse in the sample occurs, defined as a change in the appearance of the surface of the sample. Visual determination of Tsc (or Tc) can also be achieved using optical microscopy with a heating stage. The Tc of a sample is then determined by heating the sample at a fixed rate and recording the temperature when sample shrinkage is first observed (To and Flink, 1978a). The sticky point temperature (Tac) is typically measured using the method of Lazar et al (1956) where the sample is contained in a test tube immersed in a water bath. The water bath temperature is then slowly raised while the powder is periodically stirred by hand by a small propeller that is embedded in the

sample. The sticky point temperature (Tac) is determined as the water bath temperature that causes a sharp increase in the force required to manually turn the stirrer. Brennan et al (1971) used a similar method where sample stirring was carried out mechanically using a stirrer motor, instead of manually as described above. At the sticky point temperature (Tac), the current to the stirrer motor increased sharply. The various threshold temperatures are fundamentally equivalent since they result from the viscous flow in the rubbery region above Tg. The difference between the Tsc and Tac has been explained by different extents of collapse being measured. The sticky point is measured by a mechanical change in the sample, whereas the surface caking temperature is measured using visual observation of initial clumping of the sample. However, they represent different extents of the same collapse process and are thus detected at different temperatures.

Franks (1982) stated that whenever the glass transition and resultant structural collapse occur on the same time scale, the Tg is the minimum onset temperature for the collapse phenomena. A system is stable against collapse, within the period of experimental measurements of Tg and Tc, at T<Tg (Levine and Slade, 1988b). Chuy and Labuza (1994) also stated that Tg measures the onset of the physical change, whereas the Tsc is observed only after a larger physical change (collapse) occurs.

5.5 Effects of collapse phenomena on the maltodextrins

The change in physical form for the maltodextrins under high humidity conditions could explain the adverse effect that humidity has on the flow properties of the maltodextrins. Mollan and Celik (1995) found that the flow rate for M500 changed from 162g/min at 11.3% RH to 140g/min at 70.9% RH. The humidity caking mechanism shows that as the moisture content is increased, there is loss of free-flowing properties as the particle surface is plasticised. M500, an agglomerated maltodextrin, has been investigated above. It was found that following the 75% RH microcalorimetry experiment, the sample remained (by visual observation) a free-flowing material. However, the study by Mollan and Celik (1995) mentioned above shows that the flow rate of M500 is adversely affected at 70.9% RH. Figure 5.21 showed that microcalorimetry detected a broad peak for M500 at 75% RH. The decrease in flow rate for M500 measured by Mollan and Celik (1995) may be due to surface plasticisation of M500 particles leading to the production of cohesive, sticky particles as shown in Figure 5.6. Microcalorimetry appears to be able to detect this early stage in the humidity caking mechanism, before

visual observation of a physical change occurs. Flow properties are important for the maltodextrins since they can be used as direct compression excipients. It would therefore be recommended that the use of maltodextrins takes place in a humidity and temperature controlled environment to prevent the detrimental changes that take place on moisture sorption.

The presence of an amorphous material in a collapsed or non-collapsed state may affect other formulation ingredients. As described by Darcy and Buckton (1997) for amorphous lactose, water loss below 100°C attributed to the loss of absorbed water occurs from the non-collapsed amorphous material. However, for a collapsed amorphous material water loss may occur above 100°C. For the collapsed amorphous lactose investigated by Darcy and Buckton (1997), water loss was shown to occur between 70°C and 130°C. This has implications for pharmaceutical manufacturing since collapse of the maltodextrins on exposure to high humidity conditions may lead to water being released over the lifetime of a pharmaceutical product, perhaps leading to problems for other formulation components.

To prevent the collapse phenomena occurring in the maltodextrins, it is recommended that they are processed and stored at low humidity and temperature conditions. The Tc critical % RHs are a useful guide for the humidity level when the maltodextrins undergo structural collapse. However, from the above discussion about the glass transition and collapse temperatures, it is apparent that the Tg marks the onset of the collapse phenomena. For the maltodextrins, below the Tc critical % RHs, humidity caking of the free-flowing materials occurs. It is recommended that the **Tg** critical % RHs are used as critical humidity levels above which the physical changes due to collapse of the maltodextrins can occur. Table 5.3 shows that these critical values are between 53% and 61% RH for the maltodextrins studied (DE between 5 and 20). Therefore, storage and processing of the maltodextrins below 50% RH at 25°C may prevent the collapse phenomena occurring.

5.6 CONCLUSIONS

- Absorption isotherms for the maltodextrins at 25°C display the characteristic sigmoidal shape for amorphous polymers. The calculated glass transition temperature (Tg) values were found to be greatly plasticised by water sorption in to the maltodextrins. The upward inflection in water sorption appears to occur in the region where the Tg is plasticised to 25°C (the operating temperature).

- The maltodextrins undergo a change in physical form on increasing humidity from a free-flowing, white powder through a hard, white, caked material to a sticky, viscous gel-like material. It was shown that this change in physical form for the maltodextrins is due to a 'humidity caking mechanism'. Dissolution of the maltodextrins in the sorbed water is likely due to the water-soluble nature of the materials.

- It was shown that microcalorimetry is able to detect the changes in physical form for the maltodextrins through broad shoulders/peaks following the initial wetting peak. It was suggested that these broad shoulders/peaks for the maltodextrins are due to differences in the heat capacity of the materials due to changes in their physical form brought on by water uptake.

- DVS data showed that for M150 and M200 following a change in RH from 75% RH to 0% RH, water is not fully desorbed for these maltodextrins. It was shown this these was due to M150 and M200 being in a collapsed amorphous state following exposure to 75% RH. Light microscopy images showed shrinkage of M200 following exposure to 75% RH. DVS data showed that M200 retained a greater amount of moisture than M150 after exposure to 75% RH, indicating a greater extent of collapse for M200.

- Investigation of M500 (DE 10), an agglomerated form of M100, showed that M500 has a greater resistance to changes in physical form due to water sorption when compared to the non-agglomerated M100. It is therefore recommended that when the maltodextrins are used as direct compression excipients, the

agglomerated forms are used to minimise the effects of humidity on the change in physical form of the maltodextrins.

- Critical humidity levels above which changes in physical form of the maltodextrins may occur were considered. It is recommended that Tg critical % RHs are used, above which changes in physical form may occur. These critical humidity levels were between 53% RH and 61% RH for the maltodextrins with DE between 5 and 20. It is recommended that storage and processing of the maltodextrins occurs below 50% RH at 25°C to prevent the collapse-related phenomena occurring.

Chapter 6

Calculation of thermodynamic parameters for the maltodextrins

6.1 INTRODUCTION

Calculation of the thermodynamics of absorption for the maltodextrins allows the absorption process to be characterised in thermodynamic terms and the mechanism of water sorption to be investigated.

In the previous chapter, the effect of moisture on glass transition and collapse phenomena for the maltodextrins was discussed. In this chapter, the thermodynamic parameters of enthalpy, free energy, and entropy of absorption for the maltodextrins are reported in order to obtain a greater understanding of the mechanism of interaction of water with the maltodextrins.

The calculation of thermodynamic parameters for starches (Van den Berg et al, 1975 and Wurster et al, 1984) and cellulose (Khan and Pilpel, 1987) have provided valuable quantitative information on the interaction of water with these materials.

In this chapter, perfusion microcalorimetry and dynamic vapour sorption (DVS) data are used to obtain the thermodynamic parameters of enthalpy, entropy, and free energy of absorption.

The main aims of this investigation were

- To calculate the free energy of absorption using dynamic vapour sorption data
- To calculate enthalpy and entropy of absorption using perfusion microcalorimetry and dynamic vapour sorption data
- To investigate the mechanism of water interaction with the maltodextrins

6.2 METHODS

6.2.1 Perfusion microcalorimetry

The general method was as described in Chapter 2. Perfusion microcalorimetry using a step method where the RH was increased in steps of 10% RH starting from 10% RH up to 90% RH. The conditions for increasing the RH from one step to the next was set at either a heat flow between –2.000μW and +2.000μW for 60 minutes, or a maximum time limit of 2000 minutes. A sample mass of 5mg was weighed into an eppendorff tube. An eppendorff tube was used rather than weighing the maltodextrin sample directly into the steel ampoule since it was anticipated that the maltodextrins would change from a free flowing white powder to a sticky, plasticised material which would prove difficult to remove from the steel ampoule. Perfusion microcalorimetry investigations were carried out in duplicate for each of the maltodextrins studied. The eppendorff tube covered the lower two-thirds of the steel ampoule, thus also reducing the possible interaction of water vapour with the steel ampoule. The presence of the eppendorff tube on water sorption was tested by running the blank experiment with and without the eppendorff tube inserted. It was found that the eppendorff tube had no significant effect on the enthalpy values.

6.2.2 Dynamic Vapour Sorption (DVS)

The general method was as described in Chapter 2. DVS was used to determine the amount of water taken up at each RH from 10% RH to 90% RH in steps of 10% RH. This set of experiments has already been used in calculating the absorption isotherms and Tg values described in Chapter 5.

6.3 THERMODYNAMIC THEORY

6.3.1 Calculation of Gibbs free energy of absorption (ΔG)

The method of calculating ΔG was that used by Buckton et al (1986, 1988), which is summarised as follows. ΔG is given by equation (6.1)

$$\Delta G = - RT \ln K_{abs} \qquad (6.1)$$

Where R is the gas constant (= 8.314 J K^{-1} mol^{-1}), T is the temperature in Kelvin and K_{abs} is the equilibrium constant for absorption. K_{abs} is obtained by first defining a standard state, as for the method used by Buckton et al (1986). The standard state used was defined as the equilibrium uptake (mg) into 10.000 mg of powder (d) at the vapour pressure for the RH being used at 298K (P), see equation (6.2). Equilibrium uptake was obtained from the average of two DVS experiments from 10% RH to 90% RH in steps of 10% RH.

$$K_{abs} = d/P \qquad (6.2)$$

The experimental temperature was 298K, and the vapour pressure at each RH used was calculated using a linear increase in the vapour pressure from zero Pascals (Pa) at 0% RH to 3167.2 Pa at 100% RH (Rankell et al, 1986 and Buckton et al, 1986), using the S.I. unit for pressure (Pascal).

6.3.2 Calculation of enthalpy of absorption (ΔH)

The enthalpy of absorption values were calculated using the average of two perfusion microcalorimetry experiments between 10% RH and 90% RH in steps of 10% RH for each of the maltodextrins studied. The areas under the curve for the blank response was subtracted from the area under the curve for the maltodextrin sample to obtain a value in Joules (J). This value was then converted to J/mol of water absorbed into that weight of maltodextrin sample. The amount of water absorbed by each maltodextrin was obtained from the average of two dynamic vapour sorption (DVS) experiments for each maltodextrin sample.

6.3.3 Calculation of entropy of absorption (ΔS)

The entropy change, ΔS was calculated using equation (6.3) and the ΔG and ΔH values already calculated above.

$$\Delta G = \Delta H - T\Delta S \qquad (6.3)$$

6.3.4 Calculation of BET monolayer value

The BET monolayer value is the amount of water that is sufficient to cover the adsorbing surface with one layer of water molecules (Brunauer et al, 1938). For the maltodextrins, water is absorbed due to their amorphous nature. However, the significance of the BET monolayer value for the maltodextrins will be discussed later. The Brunauer-Emmett-Teller (BET) adsorption model of Brunauer et al (1938) can be written in the form of a straight line (Roos, 1993b) as shown in equation (6.4)

$$\frac{a_w}{m(1-a_w)} = \frac{(K-1)\ a_w}{m_m K} + \frac{1}{m_m K} \qquad (6.4)$$

Where a_w is the water activity (a_w = RH/100), m_m is the BET monolayer value, and K is a constant.

Equation (6.4) may be expressed as equation (6.5) where b and c are constants.

$$\frac{a_w}{m(1-a_w)} = b\,a_w + c \qquad (6.5)$$

Where $b = (K-1) / m_m K$ and $c = 1 / (m_m K)$

Linear regression of the experimental data from an a_w of 0.1 to 0.3 (n = 3) was carried out to obtain values for b and c in equation (6.5). This a_w range was used since amorphous polymers only fit the BET equation up to an a_w of 0.3 to 0.4 (Zografi and Kontny, 1986). Then equation (6.6) was used to calculate the BET monolayer value (Roos, 1993b).

$$m_m = \frac{1}{b+c} \qquad (6.6)$$

6.4 RESULTS

Figure 6.1 shows a typical perfusion microcalorimetry response for Maltrin M500. The general shape of the response is the same for all of the maltodextrins studied. It shows that responses for RHs up to 70% RH are sharp peaks which are typical of wetting responses. However, for the 80% RH peak, a larger initial response is followed by a broad shoulder. This was also seen for the ampoule microcalorimetry results, shown in the previous chapter. The 90% RH peak consists of a larger initial sharp peak followed by a more rapid decline towards the baseline than for the 80% RH peak.

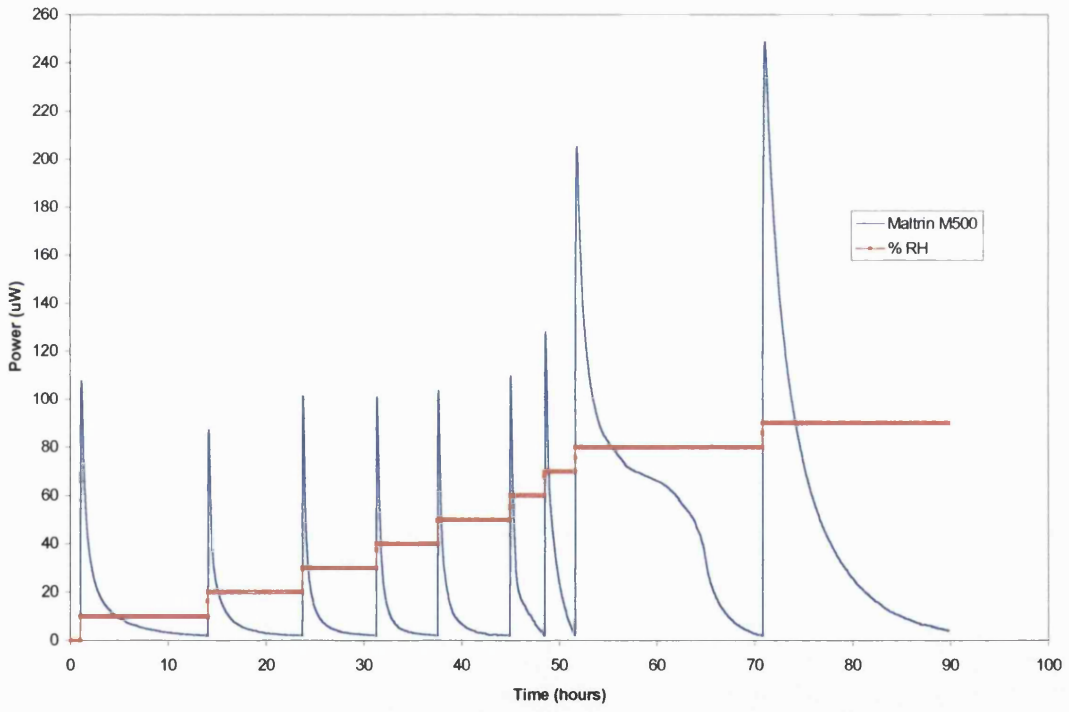

Figure 6.1 *Perfusion microcalorimetry data for Maltrin M500 maltodextrin, using the method 10% RH to 90% RH in steps of 10% RH*

Maltrin M040	Moisture Content	Thermodynamic parameters		
% RH	moles/100g dry matter	ΔH (kJ mol^{-1})	ΔG (kJ mol^{-1})	ΔS (J $mol^{-1}K^{-1}$)
10	0.22	-44.1	16.5	-203.4
20	0.31	-17.0	17.4	-115.2
30	0.38	-11.4	17.9	-98.3
40	0.44	-10.5	18.3	-96.4
50	0.53	-9.3	18.4	-92.7
60	0.64	-8.9	18.4	-91.3
70	0.79	-8.4	18.2	-89.3
80	1.00	-120.9	18.0	-465.9
90	1.53	-130.7	17.2	-496.4

Table 6.1 *Enthalpy, free energy, and entropy of absorption data for Maltrin M040 maltodextrin*

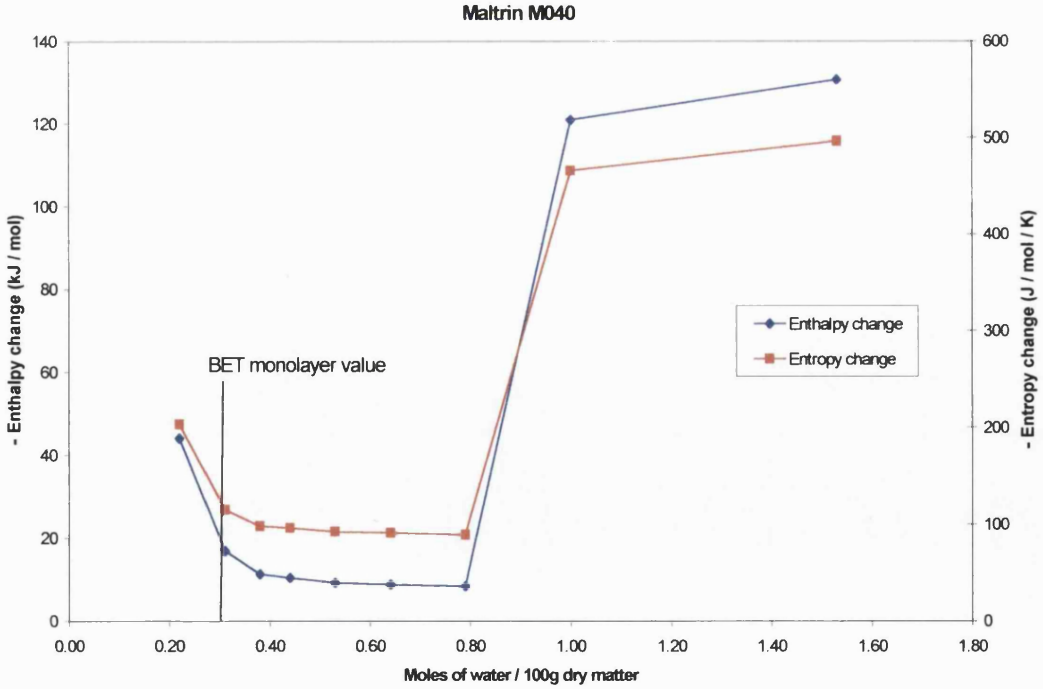

Figure 6.2 *Enthalpy and entropy of absorption changes (non-cumulative) against moisture content for Maltrin M040 maltodextrin*

Maltrin M100	Moisture content	Thermodynamic parameters		
% RH	moles/100g dry matter	ΔH (kJ mol^{-1})	ΔG (kJ mol^{-1})	ΔS (J $mol^{-1}K^{-1}$)
10	0.16	-51.9	17.3	-232.4
20	0.24	-17.6	18.0	-119.6
30	0.29	-14.2	18.6	-109.8
40	0.33	-10.7	19.0	-99.7
50	0.37	-10.9	19.2	-101.1
60	0.51	-7.9	18.9	-89.9
70	0.73	-10.8	18.4	-98.1
80	1.04	-71.4	17.9	-299.6
90	1.61	-39.0	17.1	-188.1

Table 6.2 *Enthalpy, free energy, and entropy of absorption data for Maltrin M100 maltodextrin*

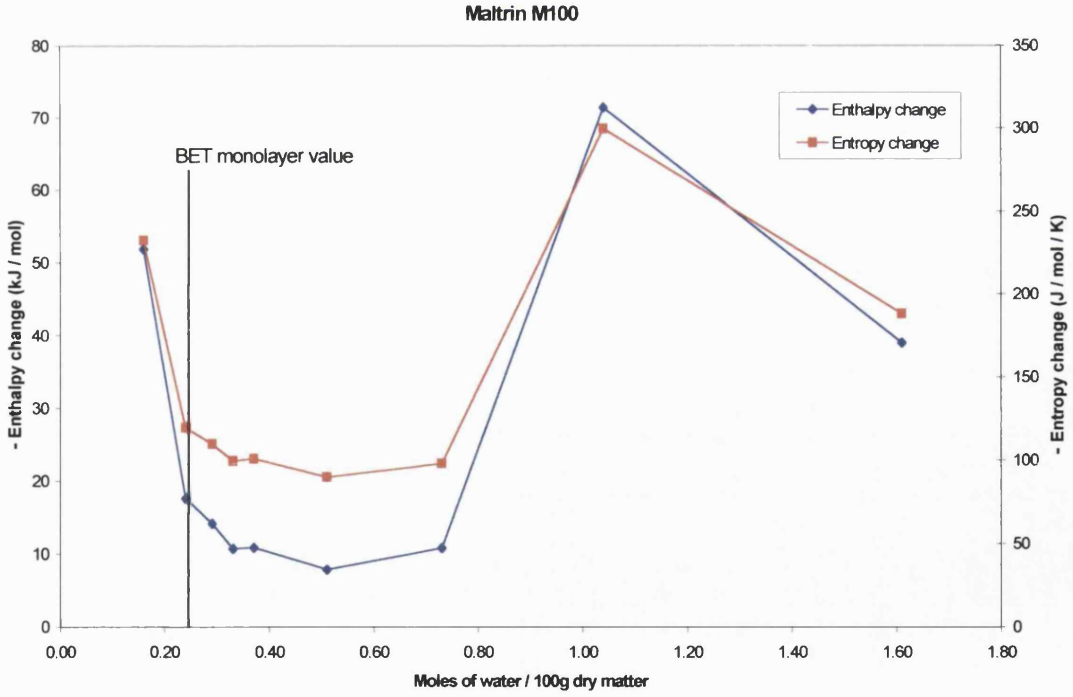

Figure 6.3 *Enthalpy and entropy of absorption changes (non-cumulative) against moisture content for Maltrin M100 maltodextrin*

Maltrin M500	Moisture content	Thermodynamic parameters		
% RH	moles/100g dry matter	ΔH (kJ mol^{-1})	ΔG (kJ mol^{-1})	ΔS (J $mol^{-1}K^{-1}$)
10	0.15	-60.2	17.5	-260.6
20	0.25	-19.7	18.0	-126.4
30	0.32	-12.7	18.4	-104.1
40	0.37	-9.4	18.7	-94.1
50	0.43	-9.8	18.9	-96.5
60	0.50	-9.2	19.0	-94.5
70	0.69	-8.1	18.5	-89.3
80	0.97	-68.1	18.0	-289.1
90	1.54	-35.3	17.2	-176.0

Table 6.3 *Enthalpy, free energy, and entropy of absorption data for Maltrin M500 maltodextrin*

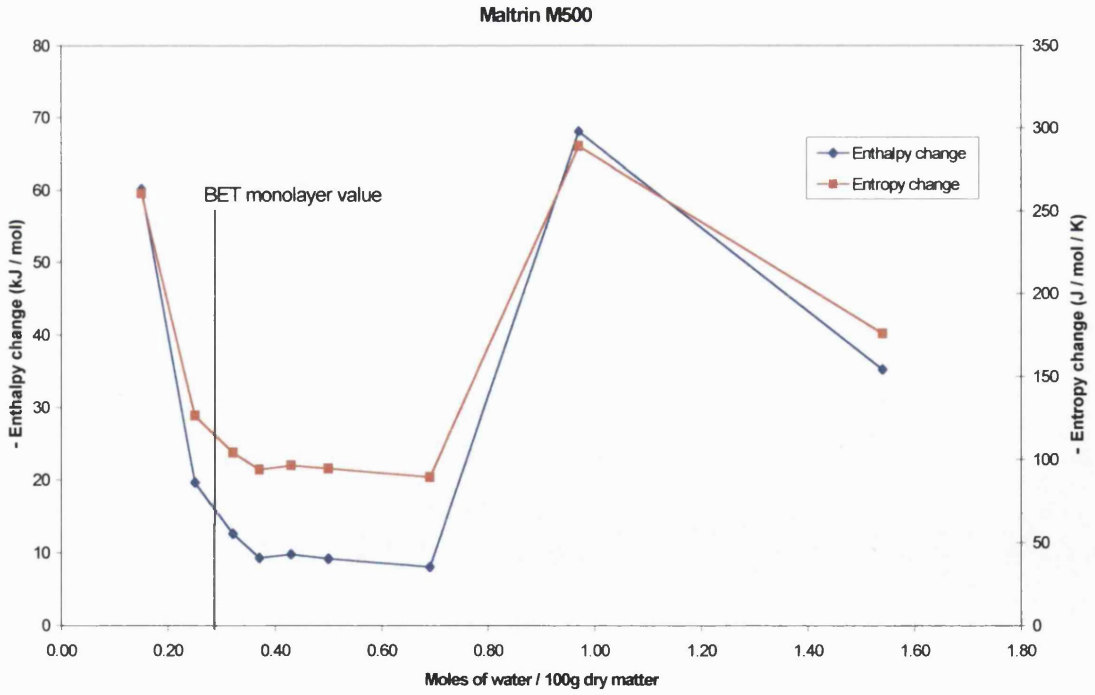

Figure 6.4 *Enthalpy and entropy of absorption changes (non-cumulative) against moisture content for Maltrin M500 maltodextrin*

Maltrin M150	Moisture content	Thermodynamic parameters		
% RH	moles/100g dry matter	ΔH (kJ mol^{-1})	ΔG (kJ mol^{-1})	ΔS (J $mol^{-1}K^{-1}$)
10	0.16	-55.6	17.4	-244.8
20	0.23	-17.8	18.2	-120.7
30	0.27	-11.5	18.8	-101.5
40	0.30	-8.5	19.2	-93.0
50	0.35	-8.1	19.4	-92.4
60	0.56	-7.6	18.7	-88.3
70	0.75	-12.8	18.3	-104.3
80	1.10	-59.4	17.7	-258.8
90	1.77	-30.9	16.9	-160.3

Table 6.4 *Enthalpy, free energy, and entropy of absorption data for Maltrin M150 maltodextrin*

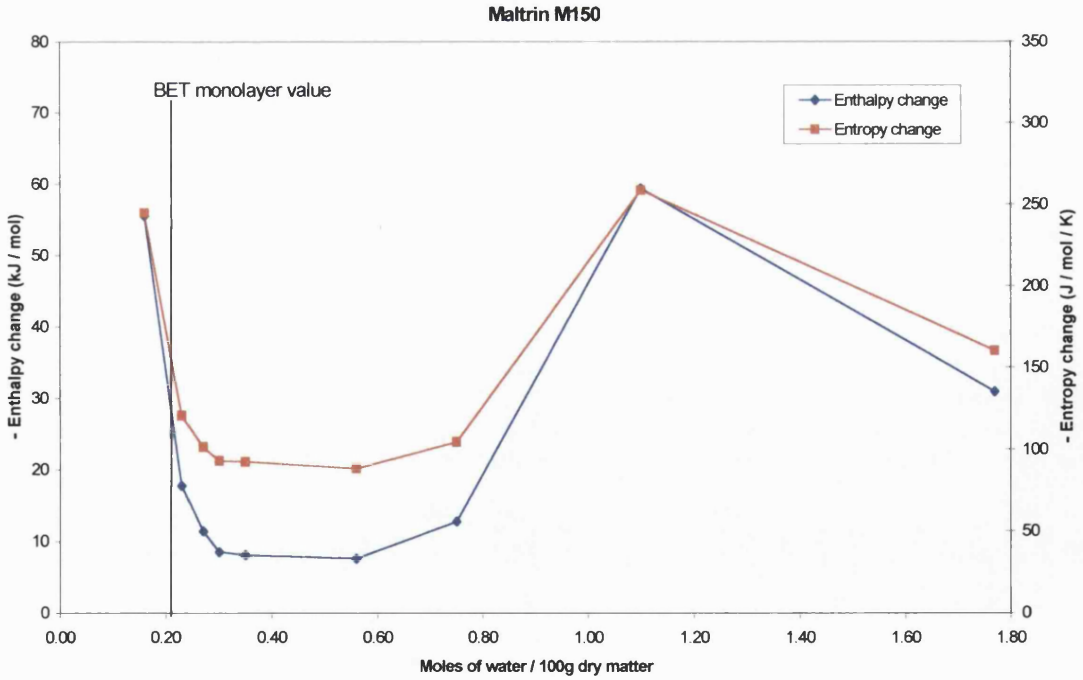

Figure 6.5 *Enthalpy and entropy of absorption changes (non-cumulative) against moisture content for Maltrin M150 maltodextrin*

Maltrin M200	Moisture content	Thermodynamic parameters		
% RH	moles/100g dry matter	ΔH (kJ mol^{-1})	ΔG (kJ mol^{-1})	ΔS (J $mol^{-1}K^{-1}$)
10	0.12	-63.1	18.0	-272.0
20	0.19	-20.7	18.6	-131.9
30	0.23	-11.5	19.2	-103.0
40	0.26	-8.8	19.6	-95.2
50	0.29	-8.3	19.9	-94.6
60	0.46	-9.6	19.2	-96.6
70	0.73	-14.3	18.4	-109.8
80	1.05	-60.1	17.8	-261.6
90	1.74	-28.6	16.9	-152.6

Table 6.5 *Enthalpy, free energy, and entropy of absorption data for Maltrin M200 maltodextrin*

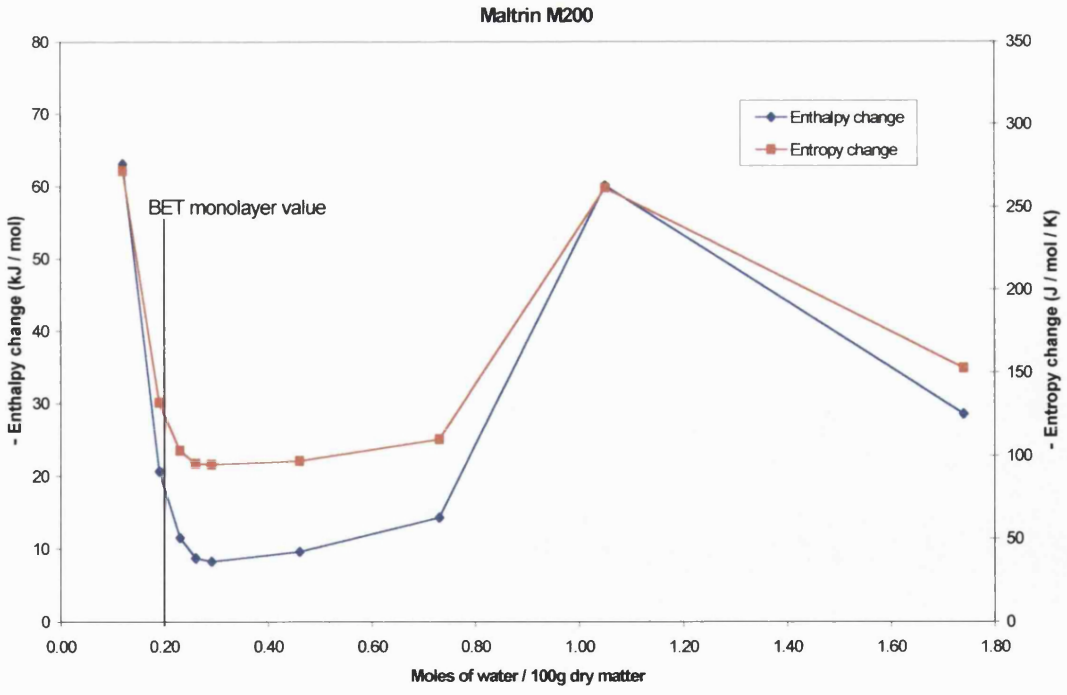

Figure 6.6 *Enthalpy and entropy of absorption changes (non-cumulative) against moisture content for Maltrin M200 maltodextrin*

6.5 DISCUSSION

6.5.1 Investigation of Gibbs free energy of absorption (ΔG)

Tables 6.1 to 6.5 show that the ΔG values increase up to a maximum at 50% or 60% RH, and then decrease up to 90% RH. For a spontaneous process such as water absorption, the Gibbs free energy change (ΔG) must be negative. However, the ΔG values in Tables 6.1 to 6.5 are all positive values suggesting that the process of water absorption is not spontaneous. This discrepancy lies in the calculation of the ΔG values by selection of a standard state. As stated above, the standard state used in calculating ΔG was the equilibrium uptake (mg) into 10.000mg of powder at the vapour pressure for the RH being used at 298K. The values obtained using this standard state results in ΔG values that can only be used relative to other values that have been obtained from the same standard state. In this case, as all the ΔG values are positive, the lowest number for the ΔG is the most favoured process (Buckton, 1995). The decreasing ΔG values from 50% or 60% RH up to 90% RH (Tables 6.1 to 6.5) suggest that the water vapour sorption becomes more favourable. Table 5.3 in Chapter 5 showed that Tg critical RHs (the RH when the Tg is plasticised by water to the operating temperature, 25°C) were between 53% and 61% RH for the maltodextrins studied. Above the Tg, a much greater amount of water is absorbed in to the maltodextrins, as shown by the upward inflection in the sorption isotherms for the maltodextrins in Figures 5.3 to 5.5 (Chapter 5). The ΔG values appear to reflect these changes in water absorption, as would be expected from the choice of standard state. For the maltodextrins, the most favourable in terms of free energy is absorption at 10% RH for M040 and 90% RH for the other maltodextrins. Between the different DE maltodextrins, the ΔG values are almost identical. This is due to the total amount of water absorbed by the maltodextrins being almost the same (Buckton and Beezer, 1988). However, Tables 6.1 to 6.5 do show that between the maltodextrins, a high moisture content corresponds to the lowest ΔG values, as would be expected as a result of the method of calculation of ΔG values. For example, M040 has the highest moisture content of all the maltodextrins at 10% RH and therefore has the lowest ΔG value at 10% RH. Also, M150 and M200 have the highest moisture content at 90% RH and therefore the lowest ΔG values at 90% RH of all the maltodextrins studied.

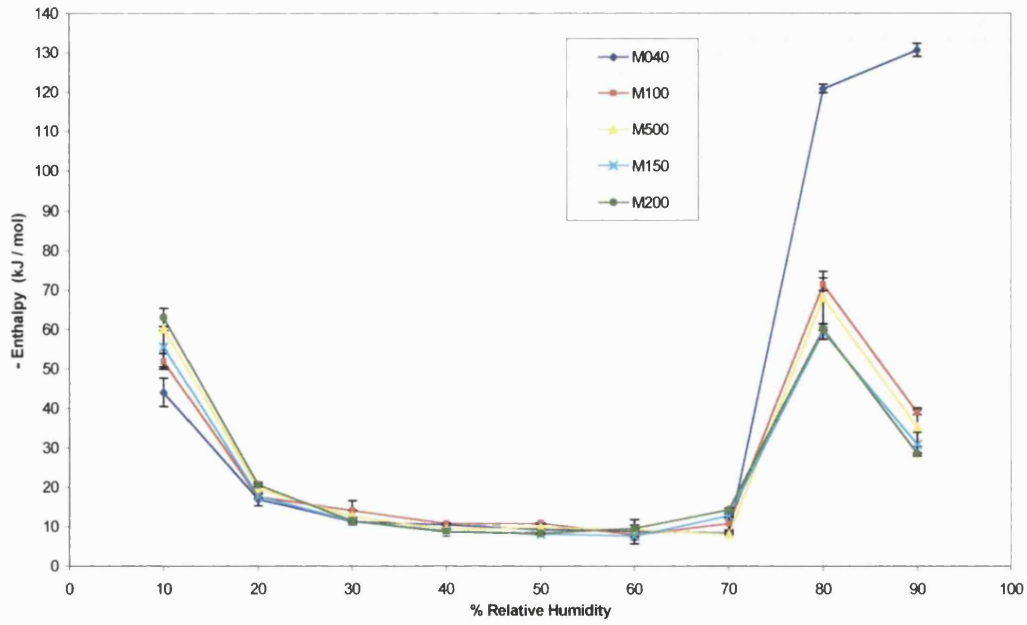

Figure 6.7 *Enthalpy of absorption changes (non-cumulative) against % relative humidity for the maltodextrins between 10% and 90% RH*

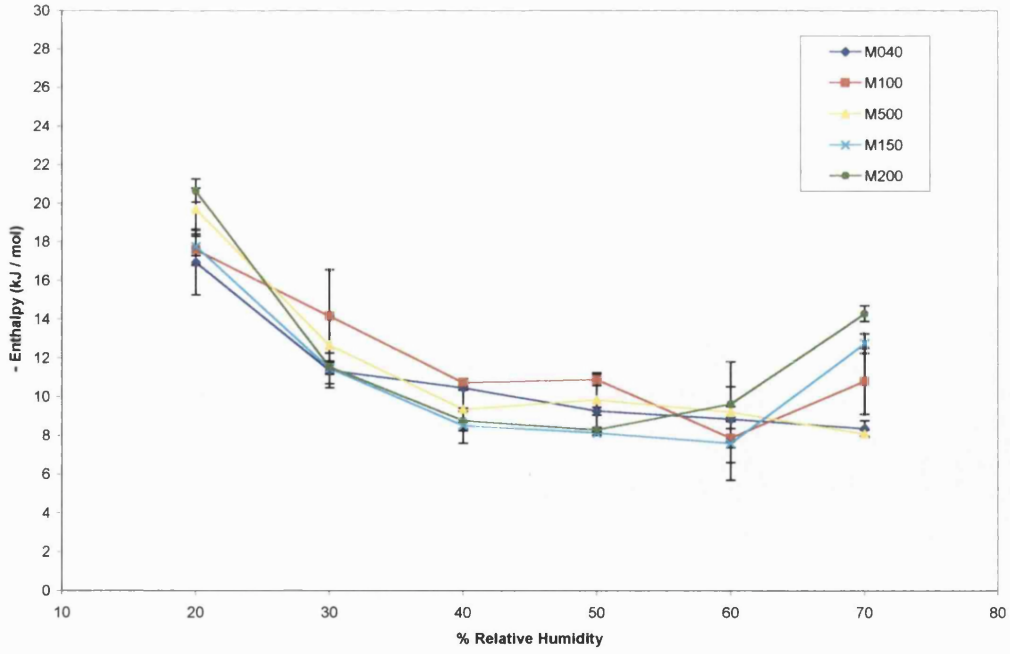

Figure 6.8 *Enthalpy of absorption changes (non-cumulative) against % relative humidity for the maltodextrins between 20% and 70% RH*

6.5.2 Investigation of enthalpy (ΔH) and entropy (ΔS) of absorption

Table 6.1 shows that the enthalpically most favoured absorption process occurs at 90% RH for M040 (the most negative ΔH value). However, Table 6.1 also shows that at 90% RH, the ΔS value is the most negative value (not favoured direction) suggesting the imposition of greatest amount of order in the system. Entropically the most favoured process is the most positive ΔS value, which for M040 occurs at 70% RH, with entropy being the dominant component (Buckton and Beezer, 1988). However, whereas Buckton and Beezer (1988) calculated thermodynamic parameters for the adsorption of water vapour onto the surface of the barbiturates, the parameters calculated for the maltodextrins represents the absorption of water vapour in to the solid, swelling of the polymer (endothermic process), and the physical changes occurring due to the humidity caking mechanism described in Chapter 5. Tables 6.2 to 6.5 show that for all the other maltodextrins studied, the enthalpically most favoured absorption process occurs at 80% RH, except for M200. However, once again, the enthalpically most favoured corresponds to the entropically least favoured process.

A comparison between the maltodextrins at 10% RH shows that M040 is the most entropically and the M200 the least entropically favoured at 10% RH. This suggests that M040 has a higher affinity for water at 10% RH and M200 has a relatively low affinity for water at 10% RH. However, when the ΔS values are compared for 80% and 90% RH it is found that the entropic values become more positive from M040 to M200. This suggests that water absorption at 80% and 90% RH becomes more energetically favourable as we move from M040 to M200. The relative order for the affinity for water appears to depend on the RH being considered. At very low RHs, M040 has the greatest affinity for water, whereas at high RHs M200 appears to be more hygroscopic.

The ΔS values are all negative values in Tables 6.1 to 6.5 suggesting that water sorption is not entropically favoured. Water vapour sorption introduces order into the system thus causing the ΔS value for the system to decrease (not the favoured direction). However, the total entropy change is the sum of the entropy change for the system and the surroundings. Since water vapour sorption is an exothermic process, heat is released into the surroundings. This has the effect of causing a large increase in the entropy of the surroundings, so that the total change in entropy is above zero.

DE	5	10	10	15	20
Maltrin	M040	M100	M500	M150	M200
BET monolayer value (mols)	0.30	0.24	0.29	0.21	0.19
Average MW	3600	1800	1800	1200	900
Average DP	22.1	11.1	11.1	7.4	5.6

Table 6.6 *BET monolayer values, molecular weight (MW) and degree of polymerisation (DP) for the different dextrose equivalent (DE) maltodextrins*

6.5.3 Investigation of mechanism of water sorption

The general model for water sorption into starches and celluloses is as follows (Zografi and Kontny, 1986):

(1) At low RHs, water is bound directly to anhydroglucose units with a ratio of one water molecule per anhydroglucose unit.
(2) At intermediate RHs, upto about 60% RH, polymer-polymer hydrogen bonds are caused to break allowing more primary binding sites for water sorption to become available. Water also binds to other water molecules that are already bound to anhydroglucose units.
(3) At higher RHs, further primary binding sites can become available, and water can bind to other water molecules, including those not bound to primary sites, resulting in a more loosely bound region of sorbed water.

Figures 6.2 to 6.6 show plots of enthalpy and entropy change against the moisture content in moles / 100g dry matter. The initial enthalpy values for the maltodextrins vary between –44.1 kJ/mol for M040 to –63.1 kJ/mol for M200. The enthalpy of formation of a hydrogen bond is in the order of –5 to –30 kJ/mol (Blair et al, 1990). The initial enthalpy values for the maltodextrins appear higher than that attributed to the formation of one hydrogen bond between water and each anhydroglucose unit of the

maltodextrin. Khan and Pilpel (1987) proposed that the first stage involved the first water molecules forming two hydrogen bonds per water molecule to the cellulose studied. The enthalpy values for the initial water absorption by the maltodextrins are in the region of twice the enthalpy of formation of a hydrogen bond. It appears that initial water absorption involves each water molecule forming two hydrogen bonds with the maltodextrin.

The BET monolayer value when applied to gas adsorption represents the weight of gas required to completely cover the available surface with a monolayer (Brunauer et al, 1938). The physical meaning of the BET monolayer value for water absorption into amorphous materials is unclear. However, it has been suggested that it refers to the absorption of one water molecule per sorption site on the solid (Zografi and Kontny, 1986). Maltodextrins are glucose polymers with the repeating unit being anhydroglucose, with an empirical formula $(C_6H_{10}O_5)_n$. The theoretical amount of water corresponding to a ratio of one water molecule per anhydroglucose unit can then be calculated as 18g water in 162g anhydroglucose (ratio 1:1). The theoretical amount of water corresponding to 100g anhydroglucose is 11.1g water. So to obtain a ratio of one water molecule per anhydroglucose unit would require the uptake of 11.1g (0.62 mols) water per 100g anhydroglucose or dry matter. Table 6.6 and Figures 6.2 to 6.6 show the calculated BET monolayer values for the maltodextrins. The BET monolayer values are below the 0.62 moles level corresponding to a ratio of 1:1 between water and each anhydroglucose unit. This shows that the BET monolayer value for water absorption by the maltodextrins appears not to represent the sorption of one water molecule per anhydroglucose unit, but instead may represent the amount of water that is directly bound to the solid (Zografi, 1988).

Figures 6.2 to 6.6 show that up to the BET monolayer values for the maltodextrins, the negative enthalpy values decrease. However, if the sites of sorption are identical upto "monolayer coverage", then the enthalpy values should remain constant up to the "monolayer value". The most likely site for absorption is the carbon-6-hydroxyl (6-OH) which is most exposed (Khan and Pilpel, 1987). The sites of absorption up to "monolayer coverage" are likely to be identical since all of the polar groups in maltodextrins are hydroxyls and there are no unsaturations in the molecule (Wurster et al, 1984). However, the enthalpy values for all of the maltodextrins clearly show a sharp decline in the negative enthalpy values. This discrepancy was also observed for water

sorption by corn starch, where it was suggested that the falling negative enthalpy values up to "monolayer coverage" are due to the swelling of the solid before the approach of "monolayer coverage" (Wurster et al, 1984). Swelling involves the breaking of solid-solid bonds that requires energy and is thus an endothermic process. This makes the water-solid interaction appear to be less exothermic than it actually is (Wurster et al, 1984).

Van den Berg et al (1975) noted that the first 10% of moisture sorption for potato starch corresponded with a constant differential heat of sorption and a strong decrease in entropy, suggesting that the first water molecule is highly immobile. Entropy represents the degree of order or disorder of a system. An increase in entropy is the favoured direction since this equates to a decrease in order. The entropy up to monolayer formation would be expected to decrease since the sorption of the first water imposes order on the system. However, Figures 6.2 to 6.6 show that for all the maltodextrins, the entropy increases (the negative entropy decreases) up to the "monolayer value". Swelling results in the disturbance of the solid surface as the solid-solid bond breaking process is occurring. This disturbance in the solid surface causes the entropy to increase since disorder is being introduced as a result of swelling (Wurster et al, 1984).

Following the "monolayer value", Figures 6.2 to 6.6 show that the enthalpy values continue to decrease rapidly at first but then more slowly. Khan and Pilpel (1987) reported that the second stage of water sorption into cellulose involved the breaking of some of the hydrogen bonds between water and cellulose, and the hydrogen bonding of additional water molecules to the newly vacated anhydroglucose units. Zografi and Kontny (1986) reported that at RHs upto 60% RH, polymer-polymer hydrogen bonds are caused to break causing an increase in primary binding sites for more water to bind. The amount of water accounting for one water molecule per anhydroglucose unit is 0.62 mols as explained above. For all the maltodextrins studied this occurs during the phase where the enthalpy values are decreasing more slowly as the moisture content increases. The observation that the enthalpy values are more stable at the intermediate RHs than before the "monolayer value" supports the proposal that hydrogen bond breaking as well as hydrogen bond formation is taking place during this phase. It is likely that one of the two hydrogen bonds between water and anhydroglucose formed during the first stage is broken, making way for more water molecules to hydrogen bond to the hydroxyl groups.

The final stage of water sorption is thought to involve hydrogen bonding between water molecules, to form a region of loosely bound water (Khan and Pilpel, 1987 and Zografi and Kontny, 1986). This loosely bound region of water results in the negative enthalpy and entropy values decreasing (Van den Berg et al, 1975 and Wurster et al, 1984). However, Figures 6.2 to 6.6 show that following the second stage of water sorption, the negative enthalpy values increase sharply.

In Chapter 5, the 'humidity caking' mechanism and collapse were indicated for the maltodextrins studied at higher relative humidities. The humidity caking mechanism was proposed by Peleg (1983) and involves the gradual transition of amorphous food powders from a free-flowing powder, through the stages of plasticised surface, attraction, fusion, and finally a sticky, caked, plasticised material as increasing amounts of moisture are sorbed. The mechanism begins with plasticisation of the surface of the particles to form cohesive, sticky particles. This then progesses to the attraction stage where the particles are caked and sticky. Next is the fusion stage, involving the formation of liquid bridges between the particles. The main reason for the stickiness is the plasticisation of particle surfaces, which allows a sufficient decrease in the surface viscosity for adhesion between particles to take place (Roos, 1995). The water that plasticises the particle surfaces would form a saturated solution on the surface of the particle, which then causes the particles to become sticky and capable of forming liquid bridges between particles (Downtown et al, 1982). The source of the liquid bridges between particles are sticky particle surfaces that may be produced by moisture sorption. It should be noted that it is not necessary for the liquefaction of the whole particle to initiate the humidity caking mechanism; it is enough for the surface to become wet to initiate the agglomeration (Peleg, 1983).

In Chapter 5, it was shown that the maltodextrins studied have Tc critcal RHs (the RH when the collapse temperature (Tc) decreases to 25°C) from 75% RH for M040 decreasing to 72% RH for M200. Collapse is the result of a reduction in the viscosity of the material when it becomes too low to support its own weight against flow (To and Flink, 1978b). Figure 6.7 shows a plot of negative enthalpy against % relative humidity. It shows that the largest increases in the negative enthalpy occur for the 80% RH responses. At this RH the Tc critical RHs for all of the maltodextrins studied would be exceeded so the collapse phenomena would be expected to have started.

For the ampoule microcalorimetry experiments discussed in the previous chapter it was observed that the presence of a broad shoulder or broad peak in addition to the initial sharp wetting peak could be attributed to the humidity caking mechanism. This shows that changes occurring due to the humidity caking mechanism are likely to be producing changes in the enthalpy response as measured by microcalorimetry. The plasticisation of the particle surface leading to the formation of saturated solution at the surface of the particle would suggest that the enthalpy values include an enthalpy of solution of the particle surface. The enthalpy values at 80% and 90% RH appear to reflect the physical changes occurring during the humidity caking mechanism.

Figure 6.7 shows that M040 has the largest negative enthalpy values at 80% and 90% RH relative to the other maltodextrins studied. Figure 6.8 highlights the data in Figure 6.7 between 20% and 70% RH. It shows that for M040, the negative enthalpy continues to decrease up to 70% RH, before increasing sharply as shown in Figure 6.7. Table 6.6 shows that M040 has the highest average molecular weight and degree of polymerisation. Tsourouflis et al (1976) investigated the effect of molecular weight on the Tc, and found that increasing molecular weight led to an increase in the Tc value. M040 with the highest molecular weight of all the maltodextrins studied appears to have a higher resistance to collapse relative to the other maltodextrins. M200 with the lowest average molecular weight and degree of polymerisation of the maltodextrins studied, has one of the lowest negative enthalpy values at 80% and 90% RH. Figure 6.8 shows that for M200 the negative enthalpy values begin increasing from 50% RH onwards, compared to the decrease mentioned above for M040. It appears that as the DE increases so the resistance to collapse decreases with the molecular weight. This was clearly observed after the ampoule microcalorimetry experiments described in Chapter 5. After the 75% RH ampoule experiment for M040, the sample remained a white free-flowing powder with no broad shoulder or broad peaks evident. However, after the 75% RH ampoule experiment for M200 the sample had changed to a soft opaque plasticised material with a broad shoulder associated with the wetting peak. For M200 after the 65% RH ampoule experiment, the sample had changed to a hard white, caked material, with the presence of a broad peak in addition to the wetting peak. This appears consistent with the negative enthalpy values which show that M040 decreases up to 70% RH whereas for M200, the negative enthalpy values begin increasing from 50% RH onwards. Figure 6.8 also shows that at 70% RH, the order of the negative enthalpy

values reflects the DE value of the maltodextrins, with the exception of M500, with M200 having the highest negative enthalpy value, followed by M150, M100 and M040. M500 is an agglomerated product and is therefore not directly comparable on the basis of DE value.

Despite the higher resistance to collapse for M040 due to its higher average molecular weight, once collapse is initiated then the negative enthalpy values are far higher than the other maltodextrins. This may be due to the high molecular weight and also since up to 70% RH, M040 had resisted collapse; for M200 it is a more gradual process starting at 50% RH, resulting in lower negative enthalpy values at 80% and 90% RH than for M040.

Figures 6.2 to 6.6 show that the negative entropy values increase (decrease in entropy) sharply at the high moisture contents. A decrease in entropy suggests the imposition of order in the system. Peleg and Mannheim (1977) investigated the humidity caking of powdered onion. They found that as the humidity was increased this led to the shrinkage of the powdered onion sample. This decrease in volume during the humidity caking mechanism would impose greater order in the system, which may be responsible for the decrease in entropy observed for the maltodextrins studied.

6.6 CONCLUSIONS

- The calculated Gibbs free energy of absorption (ΔG) values increase up to a maximum at 50% or 60% RH, then decrease up to 90% RH. The ΔG values reflect the absorption of water in to the maltodextrins due to the method of calculation of ΔG using a standard state.

- The calculated enthalpy and entropy of absorption values suggest that the mechanism of water vapour sorption into the maltodextrins is as follows:
  The first water appears to be bound directly to the anhydroglucose unit by 2 hydrogen bonds. During the first stage of water sorption there is a ratio of one water molecule to two anhydroglucose units.
  The next stage appears to involve the breaking of some of the original hydrogen bonds between water and the maltodextrin, followed by sorption of further water

as the moisture content is increased. During this stage there is a ratio of one water molecule to one anhydrogluocse unit.

The third stage shows large increases in the negative enthalpy and entropy of absorption. This may be due to the effects of the humidity caking mechanism where the free-flowing powder changes through a caked material to a fully plasticized sticky material as the moisture content is increased. The surface of the particles forms a saturated solution, so an enthalpy of solution may be involved.

- The calculated BET monolayer values for the maltodextrins lie within the first stage of water sorption explained above. The "monolayer value" for the maltodextrins represents the amount of water that is directly bound to the anhydroglucose units.

- The decrease in negative enthalpy and entropy values up to the BET monolayer values indicate that swelling of the maltodextrins takes place. Swelling is an endothermic process and therefore makes the water-maltodextrin interaction appear less exothermic than it actually is.

Chapter 7

Summary and future work

7.1 SUMMARY

The effect of microwave-vacuum drying on the introduction of amorphous material in to lactose monohydrate was considered in Chapter 3. A standard drying protocol was first established followed by variation of each of the drying parameters in turn to assess the effect on the introduction of amorphous material. The drying parameters that were varied were the jacket temperature, microwave power, vacuum drying (no microwave heating), and the impeller speed during drying. Samples were analysed using ampoule microcalorimetry, DSC, and TGA. It was found that microwave-vacuum drying of lactose monohydrate did not introduce detectable amounts of amorphous material in to the lactose sample. However, endothermic and exothermic peaks between 160°C and 180°C, detected by DSC for the lactose microwave-vacuum dried using a jacket temperature of 50°C, appear to be due to DSC-induced transformation of lactose monohydrate in to unstable anhydrous α-lactose. The starting material used in the microwave-vacuum drying investigation was crystalline α-lactose monohydrate. It was then decided that a material consisting of a small amount of amorphous material in the starting material would be used in further drying investigations. In Chapter 4, commercial spray-dried lactose was chosen as the model substance, since it contains a mixture of amorphous and crystalline lactose. The effect of fluid-bed drying on the level of amorphous material in the spray-dried lactose was considered. The as received spray-dried lactose was found by TGA and ampoule microcalorimetry to contain ca. 90% α-lactose monohydrate and ca. 10% amorphous lactose. The fluid-bed dried lactose (without the addition of water) showed no change in the level of amorphous material in the dried sample. Wetting and fluid-bed drying of the spray-dried lactose resulted in crystallisation of the amorphous lactose. It was found that the amorphous lactose crystallised in to a mixture of α- and β-lactose.

It appears from the above that microwave-vacuum and fluid-bed drying of lactose do not introduce or increase the amount of amorphous material in the sample. Other drying methods that are known to produce amorphous material are spray-drying and freeze-drying. In these drying processes, the solvent (water) is rapidly removed from the solid. This rapid solvent removal means that the stable crystalline form is not allowed sufficient time to form, resulting in the production of amorphous material. In the case of microwave-vacuum and fluid-bed drying, the removal of water may not be fast enough

for amorphous material to form. Since it has been shown that amorphous material is not introduced and the thermal properties of lactose are not significantly altered by microwave-vacuum and fluid-bed drying, it was decided that studying the interaction of water with an amorphous material may be more significant. Maltodextrins, which are starch-hydrolysis products, have been used as binders but are more recently being used as fillers/diluents in direct compression pharmaceutical formulations. This means that they represent a large portion of the formulation and it is therefore important to have knowledge of the effect that moisture sorption can have on the maltodextrins. The effect of water vapour sorption on the physical form of the maltodextrins has not been investigated in the literature. It was therefore decided that since the maltodextrins can form a significant proportion of a pharmaceutical formulation, the interaction of water vapour with the maltodextrins would be investigated.

In Chapter 5, the interaction of water with maltodextrins of different dextrose equivalent (DE) values was investigated. Maltodextrins investigated were the Maltrin series with average DE 5, 10, 15 and 20. Water absorption in to the maltodextrins was studied using dynamic vapour sorption (DVS). Water absorption isotherms showed that the maltodextrins displayed a sigmoidal isotherm shape that is characteristic of amorphous polymers. The glass transition temperature (Tg) for the maltodextrins was calculated using the Gordon and Taylor equation. The high anhydrous Tg values for the maltodextrins were found to be greatly plasticised by water absorption. The absorption isotherms for the maltodextrins showed an upward inflection in the isotherm. This was found to occur in the region where the glass transition temperature (Tg) was reduced to the operating temperature (25°C) by water plasticisation. The effect of the upward inflection is that a significantly greater amount of moisture is absorbed by the maltodextrins. This had a corresponding effect of a sharper decline of the calculated Tg.

The maltodextrins undergo a change in physical form on moisture sorption from a free-flowing white powder through a hard, caked material to a sticky, plasticised material. It was shown that this change in physical form for the maltodextrins is due to a 'humidity caking mechanism' where there is a gradual transition of amorphous powders from a free-flowing powder, through stages of plasticised surface, attraction, fusion between particles, and finally a sticky, caked, plasticised material as increasing amounts of moisture are sorbed. The sticky, caked, plasticised material in the humidity caking mechanism appears to manifest itself as a sticky, plasticised material that is gel-like by

visual observation. The mechanism begins with plasticisation of the surface of the particles to form cohesive, sticky particles. This then progresses to the attraction stage where the particles are caked and sticky. Next is the fusion stage, involving the formation of liquid bridges between particles. Dissolution of the maltodextrins in the sorbed water is likely due to the water solubility of the materials, with solubility increasing with DE value. When the maltodextrins are used as direct compression fillers/diluents, flow properties are important. The change in physical form on increasing humidity can lead to a detrimental effect on the flow rate. It is therefore recommended that processing and storage of the maltodextrins takes place in a low humidity/temperature environment to prevent the changes in physical form occurring.

Microcalorimetry is able to detect the changes in physical form through broad shoulders/peaks following a sharp initial wetting peak. It was suggested that the exothermic broad shoulders/peaks are due to differences in the heat capacity of the materials that result from changes in their physical form brought on by water uptake.

DVS data showed that for M150 and M200 maltodextrins, water desorption on changing the RH from 75% RH to 0% RH was slow and that water was retained at the end of the 0% RH phase, indicating that these maltodextrins are in a collapsed amorphous state after exposure to 75% RH. For M040, M100, and M500 the DVS data showed that desorption on changing from 75% RH to 0% RH was rapid and complete, indicating a non-collapsed amorphous state. In a non-collapsed amorphous state, water desorption is rapid and dependent on the environmental RH. However, for the collapsed amorphous state, water desorption is diffusion controlled, and not readily responsive to environmental RH changes. Collapse is the result of a reduction in the viscosity of the material when it becomes too low to support its own weight against flow, resulting in viscous flow of the material. It was suggested that due to the differences in composition between the maltodextrins, with a lower degree of polymerisation (DP) as the DE increases, the viscosity of M150 and M200 at 75% RH may be sufficiently reduced for collapse to occur. Light microscopy images for M200 showed shrinkage of the material after exposure to 75% RH. This shrinkage occurs in collapse due to viscous flow and a reduction in the macroscopic volume of the material. DVS data showed that M200 retained a greater amount of moisture than M150, suggesting a greater extent of collapse than M150.

An agglomerated maltodextrin M500 (the agglomerated form of M100 with DE 10) was investigated to find out the effect of agglomeration on the collapse-related phenomena. The process of agglomeration, where dry powders are carefully re-wetted to allow them to stick together into clumps, which are then re-dried, is related to the collapse phenomena. It was shown that agglomeration appears to produce a greater resistance to the changes in physical form at high humidies described above compared to the non-agglomerated equivalent. M500 also had the highest critical % RH values for Tg and Tc (where the Tg and Tc are plasticised to 25°C by water), showing that M500 required a higher RH of all the maltodextrins (including the DE 5 M040 maltodextrin) before the humidity-induced changes in physical form take effect. It is therefore recommended that when the maltodextrins are used as direct compression excipients, the agglomerated form of the maltodextrins are used to increase the resistance to changes of physical form, in addition to the usual advantages of agglomeration such as improved flow properties, good physical strength, and reduction of fine particles. However, the storage and processing of agglomerated M500 still requires a humidity and temperature controlled environment since it was shown that even when changes in physical form were not visually observed, microcalorimetry displayed a broad peak at 75% RH indicating a change in physical form. This shows that the high sensitivity of microcalorimetry allows detection of changes in physical form due to moisture uptake in the maltodextrins, and could therefore be used as a tool to verify the physical stability of the maltodextrins under different humidity and temperature conditions.

Establishing critical humidity levels that would be a useful guide to conditions that may cause changes in physical form to occur were considered. It was shown from the literature that the Tg appears to represent the onset temperature for collapse phenomena, and that a system is stable against collapse at $T < Tg$. It was therefore recommended that the Tg critical % RHs are used as guide values, above which changes in physical form may occur. For the maltodextrins studied, these Tg critical % RHs vary between 53% RH and 61% RH at 25°C. Storage and processing of the maltodextrins below 50% RH at 25°C may prevent the collapse-related phenomena occurring. In addition, it may be necessary to use adequate packaging of products containing maltodextrins to prevent moisture sorption during the lifetime of a pharmaceutical product.

In Chapter 6, the enthalpy, entropy, and free energy of absorption were calculated for the maltodextrins using perfusion microcalorimetry and DVS from 10% RH to 90% RH in steps of 10% RH. The calculated Gibbs free energy (ΔG) of absorption values were found to increase up to a maximum at 50% or 60% RH, followed by a decrease up to 90% RH. The ΔG values reflect the absorption of water in to the maltodextrins due to the method of calculating ΔG using a standard state. The calculated enthalpy (ΔH) and entropy (ΔS) of absorption values indicate the following mechanism of water vapour sorption into the maltodextrins. The first sorbed water appears to be bound directly to the anhydroglucose units by two hydrogen bonds. During this first stage of water sorption there is a ratio of one water molecule to two anhydroglucose units. The second stage involves the breaking of some of the original hydrogen bonds between water and the maltodextrin, followed by sorption of further water as the moisture content is increased. During this stage there is a ratio of one water molecule to one anhydroglucose unit. The third stage shows large increases in the negative enthalpy and entropy of absorption values. This may be due to the effects of the humidity caking and collapse of the maltodextrins. Humidity caking involves a change from a free-flowing powder through a caked material to a fully plasticized sticky material as the moisture content is increased. The surface of the particles forms a saturated solution, so an enthalpy of solution may be involved.

The BET monolayer value was calculated and its significance for the maltodextrins investigated. The BET monolayer value for adsorption onto a crystalline material represents the amount of water that is sufficient to cover the adsorbing surface with one layer of water molecules. It was found that the BET monolayer values were below the 0.62 moles of water per 100g dry matter corresponding to a ratio of 1:1 between water and each anhydroglucose unit. The BET monolayer values for the maltodextrins fell within the first stage of water vapour sorption. It appears that for the maltodextrins, the "monolayer value" represents the amount of water that is directly bound to the anhydroglucose units.

It was found that the negative enthalpy and entropy values decreased up to the "monolayer value". It was indicated that this is due to the swelling of the polymer up to "monolayer coverage". Swelling is an endothermic process that would make the exothermic absorption of water in to the maltodextrins appear less exothermic than it actually is. The negative entropy of absorption up to "monolayer coverage" would be

expected to increase due to sorption of the first water imposing order on the system. However, it was found that the negative entropy of absorption for the maltodextrins decreased up to the "monolayer value". The swelling that occurs up to the "monolayer value" causes a disturbance of the solid surface that may be the cause of the decrease in the negative entropy of absorption.

7.2 FUTURE WORK

It was shown above that storage and processing of the maltodextrins below 50% RH at 25°C should prevent collapse and changes in physical form. However, it would be useful in future studies to investigate the effect of humidity levels at and below 50% RH for the maltodextrins over extended time scales. This may provide information about critical humidity levels at 25°C below which the collapse-related phenomena would not occur over the lifetime of a pharmaceutical product (in the order of years). The maltodextrin powders could be stored in humidity chambers containing saturated salt solutions corresponding to the required humidity at 25°C for extended periods of days or weeks. Following exposure to humidity the maltodextrins could be tested for collapse-related phenomena by measuring the flow rate, an important property for a direct compession excipient. Ampoule microcalorimetry has been shown to be sensitive to the changes occurring in physical form of the maltodextrins and could therefore be used to detect any changes. The absence of a broad peak/shoulder may suggest that the change of physical form has occurred during the humidity storage of the maltodextrins. This should then be evident from a decrease in the flow rate investigations for the maltodextrin. The flow properties are important for direct compression excipients in tablet manufacturing. However, even if the collapse-related phenomena are prevented by a controlled humidity and temperature environment, they may still occur during the lifetime of the pharmaceutical product. For maltodextrins used in tablet formulations, changes in physical form may affect dissolution properties and therefore drug release from the dosage form. Future investigations could therefore include the direct compression of the maltodextrins (previously stored at low humidity/temperature conditions) with a model drug. The tablets could then be stored under high humidity conditions (e.g. 50% to 90% RH) in humidity chambers. The effect of changes in the physical form of the maltodextrins, due to humidity storage, on the dissolution properties of the model drug could then be investigated.

It was found using DVS that M150 and M200 were in a collapsed amorphous state following exposure to 75% RH and a return to 0% RH. It would be useful for future studies to investigate the desorption profile for the maltodextrins using DVS at higher RHs e.g. 85% RH. This could be used to determine how the collapse of the maltodextrins varies with DE value on exposure to high humidity conditions.

REFERENCES

Ahlneck, C., 1993.
Chemical and physical stability of drugs in the solid state.
In *Industrial aspects of pharmaceutics.*
Edited by Sandell, E.
Swedish Pharmaceutical Press, Stockholm.

Ahlneck, C., and Zografi, G., 1990.
The molecular basis of moisture effects on the physical and chemical stability of drugs in the solid state.
Int. J. Pharm., 62, 87-95.

Angberg, M., Nystrom, C., and Castensson, S., 1991.
Evaluation of heat-conduction microcalorimetry in pharmaceutical stability studies. III. Crystallographic changes due to water vapour uptake in anhydrous lactose powder.
Int. J. Pharm., 73, 209-220.

Angberg, M., Nystrom, C., and Castensson, S., 1992.
Evaluation of heat-conduction microcalorimetry in pharmaceutical stability studies. V. A new approach for continuous measurements in abundant water vapour.
Int. J. Pharm., 81, 153-167.

Angberg, M., 1995.
Lactose and thermal analysis with special emphasis on microcalorimetry.
Thermochim. Acta, 248, 161-176.

Angell, C.A., Monnerie, L., and Torrell, L.M., 1991.
Strong and fragile behaviour in liquid polymers.
Mat. Res. Soc. Symp. Proc., 215, 3-9.

Angell, C.A., Bressel, R.D., Green, J.L., Kanno, H., Oguni, M., and Sare, E.J., 1994.
Liquid fragility and the glass transition in water and aqueous solutions.
J. Fd. Eng., 22, 115-142.

Atkins, P.W., 1994.
Physical chemistry.
Oxford University Press.

Bakri, A., 1993.
Design, testing and pharmaceutical applications of a gas pressure controller device for solid-gas microcalorimetric titration.
Thermometric Application Note, 22021.

Berlin, E., Kliman, P.G., Anderson, B.A., and Pallansch, M.J., 1971.
Calorimetric measurement of the heat of desorption of water vapor from amorphous and crystalline lactose.
Thermochim. Acta, 2, 143-152.

Blair, T.C., Buckton, G., Beezer, A.E., and Bloomfield, S.F., 1990.
The interaction of various types of microcrystalline cellulose and starch with water.
Int. J. Pharm., 63, 251-257.

Bolhuis, G.K., Reichman, G., Lerk, C.F., van Kamp, H.V., Zuurman, K., 1985.
Evaluation of anhydrous α-lactose, a new excipient in direct compression.
Drug Dev. Ind. Pharm., 11, 1657-1681.

Borchard, W., 1983.
Thermoreversible gelation.
In *Chemistry and technology of water-soluble polymers.*
Edited by Finch, C.A.
Plenum Press, New York, 113-124.

Brennan, J.G., Herrera, J., and Jowitt, R., 1971.
A study of some of the factors affecting the spray drying of concentrated orange juice, on a laboratory scale.
J. Fd. Technol., 6, 295-307.

Briggner, L., 1993.
Microcalorimetric characterization of physical changes in solid-state drugs.
Thermometric Application Note, 22022.

Briggner, L., Buckton, G., Bystrom, K., and Darcy, P., 1994.
The use of isothermal microcalorimetry in the study of changes in crystallinity induced during the processing of powders.
Int. J. Pharm., 105, 125-135.

Brunauer, S., Emmett, P.H., and Teller, E., 1938.
Adsorption of gases in multimolecular layers.
J. Am. Chem. Soc., 60, 309-319.

Buckton, G., 1995.
Interfacial phenomena in drug delivery and targeting.
Harwood Academic, Amsterdam.

Buckton, G., and Beezer, A.E., 1988.
A microcalorimetric study of powder surface energetics.
Int. J. Pharm., 41, 139-145.

Buckton, G., and Darcy, P., 1995.
The influence of additives on the recrystallisation of amorphous spray dried lactose.
Int. J. Pharm., 121, 81-87.

Buckton, G., and Darcy, P., 1996.
Water mobility in amorphous lactose below and close to the glass transition temperature.
Int. J. Pharm., 136, 141-146.

Buckton, G., Beezer, A.E., and Newton, J.M., 1986.
A vacuum microbalance technique for studies on the wettability of powders.
J. Pharm. Pharmacol., 38, 713-720.

Buckton, G., Choularton, A., Beezer, A.E., and Chatham, S.M., 1998.
The effect of the comminution technique on the surface energy of a powder.
Int. J. Pharm., 47, 121-128.

Buckton, G., Darcy, P., Greenleaf, D., and Holbrook, P., 1995a.
The use of isothermal microcalorimetry in the study of changes in crystallinity of spray-dried salbutamol sulphate.
Int. J. Pharm., 116, 113-118.

Buckton, G., Darcy, P., and Mackellar, A.J., 1995b.
The use of isothermal microcalorimetry in the study of small degress of amorphous content of powders.
Int. J. Pharm., 117, 253-256.

Byrn, S.R., 1982.
In *Solid-state chemistry of drugs.*
Edited by Byrn, S.R.
Academic press, Inc. (London) Ltd.

Carstensen, J.T., 1983.
Pharmaceutical principles of solid dosage forms.
Technomic publishing company, Inc.
Pennsylvania, USA.

Chambers, A., Fitch, R.K., and Halliday, B.S., 1989.
Gases in vacuum systems.
In *Basic vacuum technology.*
Bristol: Hilger.

Chatrath, M., and Staniforth, J.N., 1990.
The relative influence of dielectric and other drying techniques in the physico-mechanical properties of a pharmaceutical tablet excipient. Part 1: Compaction characteristics.
Drying Technol., 8, 1089-1109.

Chidavaenzi, O.C., Buckton, G., Koosha, F., and Pathak, R., 1997.
The use of thermal techniques to assess the impact of feed concentration on the amorphous content and polymorphic forms present in spray dried lactose.
Int. J. Pharm., 159, 67-74.

Chuy, L.E., and Labuza, T.P., 1994.
Caking and stickiness of dairy-based food powders as related to glass transition.
J. Fd. Sci., 59, 43-46.

Coleman, N.J., and Craig, D.Q.M., 1996.
Modulated temperature differential scanning calorimetry: a novel approach to pharmaceutical thermal analysis.
Int. J. Pharm., 135, 13-29.

Darcy, P., 1998.
Effects of moisture sorption and temperature on amorphous spray dried lactose.
PhD Thesis.

Darcy, P., and Buckton, G., 1997.
The influence of heating/drying on the crystallisation of amorphous lactose after structural collapse.
Int. J. Pharm., 158, 157-164.

Downton, G.E., Flores-Luna, J.L., and Judson King, C., 1982.
Mechanism of stickiness in hygroscopic, amorphous powders.
Ind. Eng. Chem. Fundam., 21, 447-451.

Doyle, C., and Cliff, M.J., 1987
Microwave drying for highly active pharmaceutical granules.
Manufac. Chem., Feb., 23-25, 32.

Dwivedi, S.K., and Mitchell, A.G., 1989.
Gas chromatographic analysis of anomeric composition of lactose.
J. Pharm. Sci., 78, 1055-1056.

Elamin, A.A., Ahlneck, C., Alderborn, G., and Nystrom, C., 1994.
Increased metastable solubility of milled griseofulvin, depending on the formation of a disordered surface structure.
Int. J. Pharm., 111, 159-170.

Elamin, A.A., Sebhatu, T., and Ahlneck, C., 1995.
The use of amorphous substances to study mechanically activated materials in the solid state.
Int. J. Pharm., 119, 25-36.

Flink, J.M., 1983.
Chapter 17: Structure and structure transitions in dried carbohydrate materials.
In *Physical Properties of Foods.*
Edited by Peleg, M. and Bagley, E.B.
Westport, AVI Publishing.

Flink, J., and Karel, M., 1972.
Mechanisms of retention of organic volatiles in freeze-dried systems.
J. Fd. Technol., 7, 199-211.

Ford, J.L., and Timmins, P., 1989.
Pharmaceutical thermal analysis: techniques and applications.
Ellis Horwood Limited, Chichester.

Fox, T.G., and Flory, P.J., 1950.
Second-order transition temperatures and related properties of polystyrene. I. Influence of molecular weight.
J. Appl. Phys., 21, 581-591.

Franks, F., 1982.
In *Water- A Comprehensive Treatise*, Vol 7, 215.
Edited by Franks, F.
Plenum Press, New York.

Goldblith, S.A., 1967.
Basic principles of microwaves and recent developments.
Adv. Fd. Res., 15, 277-301.

Gordon, M., and Taylor, J.S., 1952.
Ideal co-polymers and the second order transitions of synthetic rubbers. I. Non-crystalline co-polymers.
J. Appl. Chem., 2, 493-500.

Hancock, B.C., and Shamblin, S.L., 1998.
Water vapour sorption by pharmaceutical sugars.
Pharm. Sci. Technol. Today, 1, 345-351.

Hancock, B.C., and Zografi, G., 1994.
The relationship between the glass transition temperature and the water content of amorphous solids.
Pharm. Res., 11, 471-477.

Hancock, B.C., and Zografi, G., 1997.
Characteristics and significance of the amorphous state in pharmaceutical systems.
J. Pharm. Sci., 86, 1-12.

Hancock, B.C., Shamblin, S.L., and Zografi, G., 1995.
Molecular mobility of amorphous pharmaceutical solids below their glass transition temperatures.
Pharm. Res., 12, 799-806.

Handbook of Pharmaceutical Excipients, 1986.
American Pharmaceutical Association, Washington DC.

Huttenrauch, R., Fricke, S., and Zielke, P., 1985.
Mechanical activation of pharmaceutical systems.
Pharm. Res., 2, 302-306.

Huttenrauch, R., and Keiner, I., 1979.
Producing lattice defects by drying processes.
Int. J. Pharm., 2, 59-60.

Itoh, T., Satoh, M., and Adachi, S., 1977.
Differential thermal analysis of α-lactose hydrate.
J. Dairy Sci., 60, 1230-1235.

Kaneniwa, N., and Otsuka, M., 1985.
Effect of grinding on the transformations of polymorphs of chloramphenicol palmitate.
Chem. Pharm. Bull., 33, 1660-1668.

Karel, M., 1985.
Effects of water activity and water content on mobility of food components, and their effects on phase transitions in food systems.
In *Properties of water in foods.*
Edited by Simatos, D., and Multon, J.L.
Dordrecht, Martinus Nijhoff, 153-169.

Kennedy, J.F., Knill, C.J., and Taylor, D.W., 1995.
Chapter 3: Maltodextrins.
Handbook of starch hydrolysis products and their derivatives.
Edited by Kearsley, M.W., and Dziedzic, S.Z.

Khan, F., and Pilpel, N., 1987.
An investigation of moisture sorption in microcrystalline cellulose using sorption isotherms and dielectric response.
Powder Technol., 50, 237-241.

Konno, T., Kinuno, K., and Kataoka, K., 1986.
Physical and chemical changes in medicinals in mixtures with adsorbents in the solid state.
I. Effect of vapor pressure of the medicinals on changes in crystalline properties.
Chem. Pharm. Bull., 34, 301-307.

Krycer, I., and Hersey, J.A., 1981.
Detection of mechanical activation during the milling of lactose monohydrate.
Int. J. Pharm. Tech. Prod. Mfr., 2, 55-56.

Lazar, M.E., Brown, A.H., Smith, G.S., Wong, F.F., and Lindquist, F.E., 1956.
Experimental production of tomato powder by spray drying.
Fd. Technol., 10, 129-133.

Lerk, C.F., Andreae, A.C., and de Boer, A.H., 1984a.
Alterations of α-lactose during differential scanning calorimetry.
J. Pharm. Sci., 73, 856-857.

Lerk, C.F., Andreae, A.C., and de Boer, A.H., 1984b.
Transitions of lactoses by mechanical and thermal treatment.
J. Pharm. Sci., 73, 857-859.

Levine, H., and Slade, L., 1986.
A polymer physico-chemical approach to the study of commercial starch hydrolysis products.
Carbo. Polym., 6, 213-244.

Levine, H., and Slade, L., 1988a.
Water as a plasticiser: physico-chemical aspects of low-moisture polymeric systems.
In *Water Science Reviews*, Vol. 3, 79-185.
Edited by Franks, F.
Cambridge.

Levine, H., and Slade, L., 1988b.
Chapter 9: 'Collapse' phenomena – a unifying concept for interpreting the behaviour of low moisture foods.
In *Food structure – its creation and evaluation.*
Edited by Blanshard, J.M.V., and Mitchell, J.R.
Butterworths, London.

Li, L.C., and Peck, G.E., 1990.
The effect of moisture content on the compression properties of maltodextrins.
J. Pharm. Pharmacol., 42, 272-275.

Lucisano, L.J., and Poska, R.P., 1990.
Microwave technology - fad or future?
Pharmaceutical Technology, April 1990, 38, 40, 42.

Lund, D., 1984.
Influence of time, temperature, moisture, ingredients, and processing conditions on starch gelatinisation.
CRC Crit. Rev. Fd. Sci. Nutr., 20, 249-273.

Masters, K., and Stoltze, A., 1973.
Agglomeration advances.
Fd. Eng., 45, 64-67.

Metaxas, A.C., and Meredith, R.J., 1983.
Industrial microwave heating.
IEE Power series 4.
Peter Peregrinus Ltd.

Mollan, M.J., and Celik, M., 1993.
Characterization of directly compressible maltodextrins manufactured by three different processes.
Drug Dev. Ind. Pharm., 19, 2335-2358.

Mollan, M.J., and Celik, M., 1995.
The effects of humidity and storage time on the behaviour of maltodextrins for direct compression.
Int. J. Pharm., 114, 23-32.

Morita, M., Nakai, Y., Fukuoka, E., and Nakajima, S., 1984.
Physicochemical properties of crystalline lactose. II. Effect of crystallinity on mechanical and structural properties.
Chem. Pharm. Bull., 32, 4076-4083.

Nyqvist, H., 1983.
Saturated salt solutions for maintaining specified relative humidities.
Int. J. Pharm. Tech. & Prod. Mfr., 4, 47-48.

Oksanen, C.A., and Zografi, G., 1990.
The relationship between the glass transition temperature and water vapour absorption by poly(vinylpyrrolidone).
Pharm. Res., 7, 654-657.

Oksanen, C.A., and Zografi, G., 1993.
Molecular mobility in mixtures of absorbed water and solid Poly(vinylpyrrolidone).
Pharm. Res., 10, 791-799.

Olano, A., Corzo, N., and Martinez-Castro, I., 1983.
Studies on β-lactose crystallization.
Milchwissenschaft, 38, 471-474.

Orford, P.D., Parker, R., Ring, S.G., and Smith, A.C., 1989.
Effect of water as a diluent on the glass transition behaviour of malto-oligosaccharides, amylose and amylopectin.
Int. J. Biol. Macromol., 11, 91-96.

Otsuka, M., and Kaneniwa, N., 1990.
Effect of grinding on the crystallinity and chemical stability in the solid state of cephalothin sodium.
Int. J. Pharm., 62, 65-73.

Otsuka, M., Ohtani, H., Kaneniwa, N., and Higuchi, S., 1991.
Isomerization of lactose in solid-state by mechanical stress during grinding.
J. Pharm. Pharmacol., 43, 148-153.

Otsuka, M., Ohtani, H., Otsuka, K., and Kaneniwa, N., 1993.
Effect of humidity on solid-state isomerization of various kinds of lactose during grinding.
J. Pharm. Pharmacol., 45, 2-5.

Papadimitriou, E., Efentakis, M., and Choulis, N.H., 1992.
Evaluation of maltodextrins as excipients for direct compression tablets and their influence on the rate of dissolution.
Int. J. Pharm., 86, 131-136.

Peleg, M., 1977.
Flowability of food powders and methods for its evaluation – a review.
J. Fd. Proc. Eng., 1, 303-328.

Peleg, M., 1983.
Chapter 10: Physical characteristics of food powders.
In *Physical properties of foods.*
Edited by Peleg, M. and Bagley, E.B.,
AVI Publishing Co., INC.

Peleg, M., and Mannheim, C.H., 1977.
The mechanism of caking of powdered onion.
J. Food. Process. Preserv., 1, 3-11.

Pikal, M.J., Lukes, A.L., Lang, J.E., and Gaines, K., 1978.
Quantitative crystallinity determinations for β-lactam antibiotics by solution calorimetry: Correlations with stability.
J. Pharm. Sci., 67, 767-773.

Pudipeddi, M., Sokoloski, T.D., Duddu, S.P., and Carstensen, J.T., 1996.
Quantitative characterization of adsorption isotherms using isothermal microcalorimetry.
J. Pharm. Sci., 85, 381-386.

Rankell, A.S., Lieberman, H.A., and Schiffmann, R.F., 1986.
Chapter 3: Drying.
In *The theory and practice of industrial pharmacy.*
Edited by Lachman, L., Lieberman, H.A., and Kanig, J.L.
Lea & Febiger, Philadelphia, USA.

Roos, Y., 1993a.
Melting and glass transitions of low molecular weight carbohydrates.
Carbohydr. Res., 238, 39-48.

Roos, Y.H., 1993b.
Water activity and physical state effects on amorphous food stability.
J. Food Process. Preserv., 16, 433-447.

Roos, Y., 1995.
Phase transitions in foods.
Academic Press, INC.

Roos, Y. and Karel, M., 1991a.
Phase transitions of mixtures of amorphous polysaccharides and sugars.
Biotechnol. Prog., 7, 49-53.

Roos,Y., and Karel, M., 1991b.
Plasticizing effect of water on thermal behaviour and crystallization of amorphous models.
J. Fd. Sci., 56, 38-43.

Roos, Y., and Karel, M., 1991c.
Water and molecular weight effects on glass transitions in amorphous carbohydrates and carbohydrate solutions.
J. Fd. Sci., 56, 1676-1681.

Saleki-Gerhardt, A., Ahlneck, C., and Zografi, G., 1994.
Assessment of disorder in crystalline solids.
Int. J. Pharm., 101, 237-247.

Saleki-Gerhardt, A., and Zografi, G., 1994.
Non-isothermal and isothermal crystallisation of sucrose from the amorphous state.
Pharm. Res., 11, 1166-1173.

Salvetti, G., Tognoni, E., Tombari, E., and Johari, G.P., 1996.
Excess energy of polymorphic states or glass over the crystal state by heat of solution measurement.
Therm. Acta., 285, 243-252.

Sebhatu, T., Angberg, M., and Ahlneck, C., 1994a.
Assessment of the degree of disorder in crystalline solids by isothermal microcalorimetry.
Int. J. Pharm., 104, 135-144.

Sebhatu, T., Elamin, A.A., and Ahlneck, C., 1994b.
Effect of moisture sorption on tabletting characteristics of spray dried (15% amorphous) lactose.
Pharm. Res., 11, 1233-1237.

Shalaev, E.Y., and Zografi, G., 1996.
How does residual water affect the solid-state degradation of drugs in the amorphous state.
J. Pharm. Sci., 85, 1137-1141.

Shamblin, S.L., Tang, X., Chang, L., Hancock, B.C., and Pikal, M.J., 1999.
Characterization of the time scales of molecular motion in pharmaceutically important glasses.
J. Phys. Chem., 103, 4113-4121.

Sheridan, P.L., Buckton, G. and Storey, D.E., 1995.
Development of a flow microcalorimetry method for the assessment of surface properties of powders.
Pharm. Res., 12, 1025-1030.

Slade, L., and Levine, H., 1991.
Beyond water activity: Recent advances based on an alternative approach to the assessment of food quality and safety.
Crit. Rev. Fd. Sci. Nutrit., 30, 115-360.

Slayter, E.M., and Slayter, H.S., 1992.
Light and electron microscopy.
Cambridge University Press.

Sluchly, S.S., and Stuchly, M.A., 1983.
Microwave drying: Potential and limitations.
In *Advances in Drying.*
Hemisphere Publishing Corporation, NY.

To, E.C., and Flink, J.M., 1978a.
'Collapse', a structural transition in freeze dried carbohydrates I. Evaluation of analytical methods.
J. Fd. Technol., 13, 551-565.

To, E.C., and Flink, J.M., 1978b.
'Collapse', a structural transition in freeze dried carbohydrates II. Effect of solute composition.
J. Fd. Technol., 13, 567-581.

To, E.C., and Flink, J.M., 1978c.
'Collapse', a structural transition in freeze dried carbohydrates III Prerequisite of recrystallisation.
J. Fd. Technol., 13, 583-594.

Tsourouflis, S., Flink, J.M. and Karel, M., 1976.
Loss of structure in freeze-dried carbohydrates solutions: Effect of temperature, moisture content and composition.
J. Sci. Fd Agric., 27, 509-519

Van den Berg, C., Kaper, F.S., Weldring, J.A.G., and Wolters, I., 1975.
Water binding by potato starch.
J. Fd. Technol., 10, 589-602.

Van Scoik, K.G., and Carstensen, J.T., 1990.
Nucleation phenomena in amorphous sucrose systems.
Int. J. Pharm., 58, 185-196.

Vorwerg, W., Schierbaum, F.R., Reuther, F., and Kettlitz, B., 1988.
Chapter 8: Formation of thermally reversible networks from starch polysaccharides.
In *Biological and synthetic polymeric networks.*
Edited by Kramer, O.
Elsevier Applied Science, London.

Wallack, D.A., and Judson King, C., 1988.
Sticking and agglomeration of hygroscopic, amorphous carbohydrate and food powders.
Biotech. Prog., 4, 31-35.

Waltersson, J., and Lundgren, P., 1985.
The effect of mechanical comminution on drug stability.
Acta Pharm. Suec., 22, 291-300.

Ward, G.H., and Schultz, R.K., 1995.
Process-induced crystallinity changes in albuterol sulfate and its effects on powder physical stability.
Pharm. Res., 12, 773-779.

Wells, J.I., and Aulton, M.E., 1988.
Chapter 13: Preformulation.
In *Pharmaceutics: The science of dosage form design.*
Edited by Aulton, M.E.
Churchill Livingstone, Edinburgh.

White, G.W., and Cakebread, S.H., 1966.
The glassy state in certain sugar-containing food products.
J. Fd. Technol., 1, 73-82.

Williams, M.L., Landel, R.F., and Ferry, J.D., 1955.
The temperature dependence of relaxation mechanisms in amorphous polymers and other glass-forming liquids.
J. Am. Chem. Soc., 77, 3701-3707.

Wurster, D.E., Peck, G.E., and Kildsig, D.O., 1984.
A thermodynamic study of the starch-water surface interaction.
Starch, 36, 294-299.

Yonemochi, E., Inoue, Y., Buckton, G., Moffat, A., Oguchi, T., and Yamamoto, K., 1999.
Differences in crystallisation behaviour between quenched and ground amorphous ursodeoxycholic acid.
Pharm. Res., 16, 835-840.

Yoshioka, M., Hancock, B.C., and Zografi, G., 1994
Crystallisation of indomethacin from the amorphous state below and above its glass transition temperature.
J. Pharm. Sci., 83, 1700-1705.

Zografi, G., 1988.
States of water associated with solids.
Drug Dev. Ind. Pharm., 14, 1905-1926.

Zografi, G., and Kontny, M.J., 1986.
The interactions of water with cellulose- and starch-derived pharmaceutical excipients.
Pharm. Res., 3, 187-194.

Zografi, G., and Hancock, B., 1993.
Chapter 28: Water-solid state interactions in pharmaceutical systems.
In *Topics in pharmaceutical sciences.*
Edited by Crommelin, D.J.A., Midha, K.K., and Nagai, T.,
Medpharm scientific publishers.

Zeleznak, K.J., and Hoseney, R.C., 1987.
The glass transition in starch.
Cereal Chem., 64, 121-124.